Geologica Acta, Vol. 13, Nº 1, March 2015, 25-43
DOI: 10.1344/GeologicaActa2015.13.1.2

The spatial and compositional evolution of the Late Jurassic Ghorveh-Dehgolan plutons of the Zagros Orogen, Iran: SHRIMP zircon U-Pb and Sr and Nd isotope evidence

S. YAJAM[1,2] P. MONTERO[3] J.H. SCARROW[3] J. GHALAMGHASH[4] S.M.H. RAZAVI[1] F. BEA[3]

[1]**Department of Geology, Faculty of Earth Sciences, Kharazmi University**
49 Mofatteh Av., Tehran 15614, Iran. Yajam E-mail: std_Yajam@khu.ac.ir Razavi E-mail: Razavi@khu.ac.ir

[2]**Payam Nppr University of Manjil**
Isargaran Av., Manjil, Iran

[3]**Departamento de Mineralogía y Petrología, Facultad de Ciencias, Universidad de Granada**
Av/ Fuentenueva, s/n, 18002, Granada, Spain.
Montero E-mail: pmontero@ugr.es Scarrow email: jscarrow@ugr.es Bea E-mail: fbea@ugr.es

[4]**Geological Survey of Iran, Research Institute for Earth Sciences**
PO Box 13185-1494, Tehran, Iran. Ghalamghash E-mail: Ghalamghash@gsi.ir

ABSTRACT

The Ghorveh-Dehgolan plutons of the northern Sanandaj-Sirjan Zone, Zagros Orogen, comprise seven composite intrusive bodies that were generated during northeastward subduction of Neotethys beneath the Iranian sector of the Eurasian plate. Zircon U-Pb SHRIMP dating reveals that the magmatic activity spanned from ~160 to ~140Ma. It started with intrusion of arc-related calc-alkaline mafic to intermediate rocks closely followed by felsic I-type granitoids. This magmatism was post-dated by felsic alkaline A-type granites. In addition to compositional changes over time, the plutons forming the arc young towards the southwest: the north Ghorveh batholith (161±4Ma) and Shanevareh (160±2Ma); Qalaylan (159±3Ma); then central Ghorveh, Galali and Saranjianeh (151±0.2Ma to 148±1Ma); and, lastly, the south Ghorveh batholith (147±3Ma) and Bolbanabad-Havarpan (144±1Ma). Whatever the process driving the changes, be it arc- or ridge-collision with the subducting system, slab roll-back, slab break-off, subduction initiation transference, etc., the progression from I-type to A-type magmatism appears to mark a significant change from a collisional to an extensional setting in the region in the Late Jurassic. Geochemical and isotopic characteristics of the Ghorveh-Dehgolan plutons indicate that Arabian-Nubian-like crust was an important component of the magmatic sources.

KEYWORDS **U-Pb SHRIMP dating. Sanandaj-Sirjan Zone. Neoproterozoic Arabian-Nubian crust. Neotethys. A-type granites.**

INTRODUCTION

The Zagros orogen of the Alpine-Himalayan belt records the collision between the Iranian sector of the Eurasian plate, Laurasia, and the Arabian plate, Gondwana, as Neotethys closed. The orogen consists of three main northwest-southeast elongated sub-parallel zones i) the Zagros Fold-Thrust Belt to the southwest, north of the

Persian Gulf, ii) the Sanandaj-Sirjan Zone (SSZ) in the middle, iii) and the Urumieh-Dokhtar Magmatic Arc to the northeast, bordering central Iran (Alavi 1994, 2004) (Fig. 1 inset). Various authors have attributed plutonism in the SSZ to northeastward subduction of Neotethys during the Mesozoic (Berberian and Berberian, 1981; Ghalamghash, 2002; Ahamdi Khalaji *et al.*, 2007). That said, more recent studies have shown that the SSZ had a longer and more complex magmatic history that resulted in intrusion of a large variety of diachronic I-, S- and, apparently anorogenic, A-type granitoids from the Carboniferous to the Eocene (Arvin *et al.*, 2007; Ghalamghash *et al.*, 2009; Mazhari *et al.*, 2009; Bea *et al.*, 2011). Furthermore, many massifs show field and compositional evidence for mixing between mafic and felsic components. The age and petrogenesis of the magmatism in the SSZ is, however, still relatively poorly defined (Mazhari *et al.*, 2009).

The ages of SSZ granitoids are potentially the 'critical missing link' in understanding along strike changes in formation of the collision-related rocks. The northern and central part of the SSZ host the extensive Jurassic Ghorveh–Aligoodarz Plutonic Belt (Mohajjel and Fergusson, 2014). The northern border of this belt is a 100km long northwest-southeast magmatic lineament, formed of the Ghorveh-Dehgolan plutons (Fig. 1), which are the target of this geochronological study. The seven Ghorveh-Dehgolan plutons are composed of a variety of rock types, from gabbros to granites, the age and geodynamic interpretation of which are controversial. The first geochronological data were published by Bellon and Braud (1975), who reported K-Ar ages around 38–40Ma. Letterrier (1985) dated the Ghorveh batholith with the Rb-Sr method and obtained an age of 119±3Ma. Nevertheless, this value was reported but discarded by the author because, in a regional context, the pluton was thought to be Miocene. Mahmoudi *et al.* (2011) reported ID-TIMS

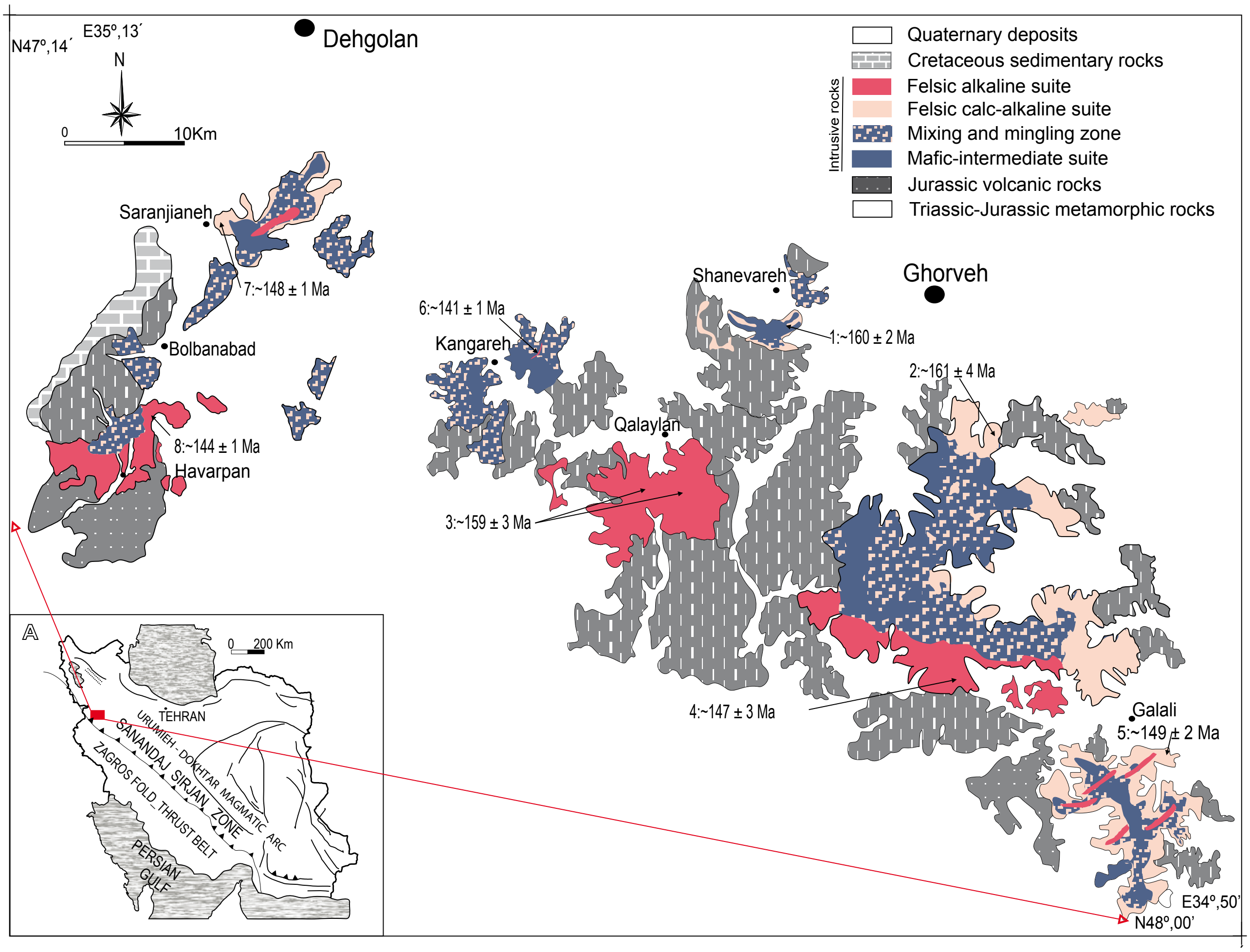

FIGURE 1. Simplified geological sketch of the Ghorveh-Dehgolan plutons showing the location of study samples: 1) sample SH177; 2) sample BA190; 3) sample QA153, 158; 4) sample BA19; 5) sample GA134; 6) sample KA113; 7) sample SA80; 8) sample B-H88. The inset highlights the position of the Ghorveh-Dehgolan plutons (after Eshraghi *et al.*, 1996; Hosseiny *et al.*, 1999; Sartibi *et al.*, 2005) within the Zagros orogen (rectangle) and main structural zones of Iran (Alavi, 2004). Boundaries between units are drawn as black lines where they can be observed. Inferred and transitional contacts are represented as a change in colour and pattern.

ages of 157Ma to 149Ma for the same pluton, and suggested an origin by partial melting of the lower crust in a back-arc environment. Notably, Torkian *et al.* (2008) had previously suggested a supra-subduction setting for the magmatism. Azizi *et al.* (2011) and Azizi and Asahara (2013) dated two other plutons, Saranjianeh and Bolbanabad-Havarpan (Fig. 1), by WR Rb-Sr and Sm-Nd. They proposed the existence of one mafic magmatic pulse at 185±45Ma, related to an island arc setting, which was followed by several other felsic pulses at 149±2Ma, 144±3Ma and 131±27Ma related to the collision of an island arc with the western part of the SSZ.

The large variety of published ages and conflicting geodynamic interpretations for this area are difficult to reconcile in a single geodynamic model. In our opinion, these discrepancies arise because of the lack of a precise geochronological framework for the whole arc. Furthermore, the aforementioned studies were focused on dating isolated plutons without considering other related magmatic bodies, the precise ages and geochemistry of which were unknown. Recently, Chui *et al.* (2013) presented a summary of zircon LA-ICPMS U-Pb and other age data to constrain the Zagros Orogeny magmatic evolution related to Neotethyan subduction. They identified a regional northeastward migration of arc-related magmatism through the Mesozoic and Cenozoic in the Sanandaj-Sirjan and younger Urumieh-Dokhtar arc magmatism. Within this general trend they noted that the first stage of magmatism mainly occurred in the SSZ during the Middle and Late Jurassic (176–144Ma), with a peak of activity at ~165Ma. In this context we decided to undertake a geochemical and geochronological study of the northern SSZ Ghorveh-Dehgolan plutons.

Here we present the field relationships, petrography, major and trace element and Sr-Nd isotope whole-rock compositions and zircon U-Pb SHRIMP ages for seven SSZ plutons. Our data reveal a spatial and temporal compositional evolution that sheds light on the tectonomagmatic history of the northern part of Zagros Orogen during the Jurassic.

GEOLOGICAL SETTING, FIELD RELATIONS AND PETROGRAPHY

The Ghorveh-Dehgolan plutons are located about 400km west of Tehran, in the northern part of the Sanandaj-Sirjan Zone, Kurdistan province, between E 34º 50', E 35º 13' and N 47º 14', N 48º 00' (Fig. 1). Seven plutons have exposures ranging from 150km^2 to 9km^2. They are intruded into Triassic and Early Jurassic volcanic and sedimentary rocks which show contact metamorphic aureoles (Hosseiny *et al.*, 1999).

All seven Ghorveh-Dehgolan plutons are composite bodies that include variable proportions of three different rock suites: i) a mafic-intermediate suite (MIS), mostly composed of gabbros, diorites and monzodiorites, ii) a felsic calc-alkaline suite (FCAS), composed of tonalites, granodiorites and granites, iii) a felsic alkaline suite (FAS), mostly composed of leucocratic alkali-feldspar granites and syenogranites with minor monzogranites and granodiorites. Extensive mingling and mixing between the first two suites indicates that they were emplaced simultaneously (Fig. 2). The felsic alkaline granites, on the other hand, always show sharp intrusive contacts with the other two suites, indicating that they represent the youngest intrusive facies (Fig. 2). These plutons are described below.

Representative mineral chemistry data are presented in Table I Electronic Appendix, available at www.geologica-acta.com.

Ghorveh

The Ghorveh batholith (previously called the Kharsareh batholith by Letterrier, 1985) crops out to the south of

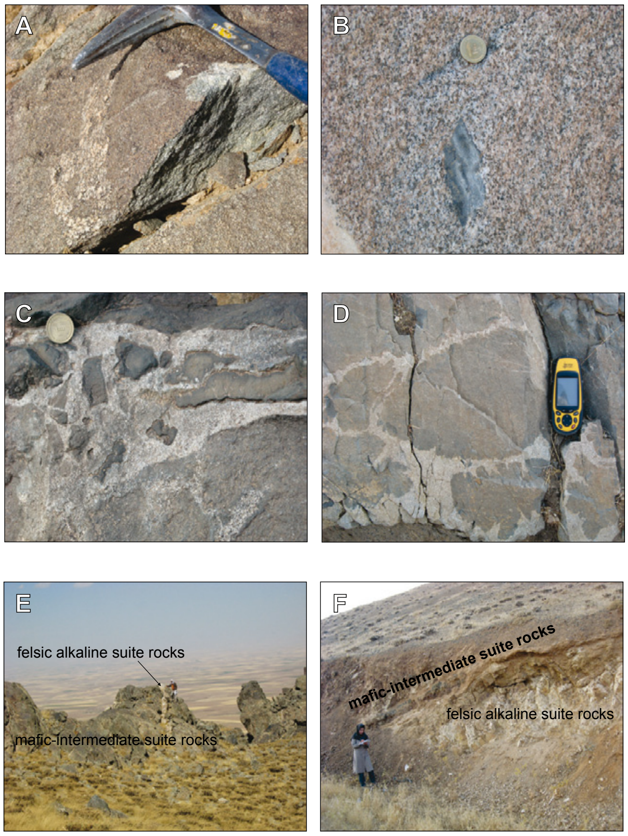

FIGURE 2. Field relations of the different suites of the Ghorveh-Dehgolan plutons. A) close up of the mafic-intermediate suite rocks. B) close up of the felsic calc-alkaline suite rocks. C and D) mixing and mingling between the mafic-intermediate rocks and felsic I-type calc-alkaline rocks indicates contemporaneous emplacement of the mafic and felsic suites-fragmented diorite and net-veining granite (C) and pillows with quenched margin and diffusion of granite veinlets into dioritic pillows (D). E and F) felsic alkaline suite field relationship with mafic-intermediate suite rocks.

TABLE 1. Sr and Nd isotope compositions of selected samples from the Ghorveh-Dehgolan plutons. Nd model dates were calculated for a depleted mantle with Ndt = 0.25t2 –3t + 8.5, where t is the age in Ga (DePaolo,1981)

sample id	BA20	BH92	KA102	SA168	SA84	BH98	BA59	KA106	QA153	GA140	BA38	SH202
rock suites	mafic-intermediate suite											
Rb (ppm)	85,126	63,19	8,91	71,812	29,801	62,317	69,993	15,511	109,506	141,984	43,391	57,894
Sr (ppm)	292,502	350,1	879,361	188,31	293,385	153,805	229,298	586,9	916,88	260,282	280,062	710,514
$^{87}Rb/^{86}Sr$	0,8419412	0,522093	0,0293054	1,103245	0,2937892	1,17226	0,8830012	0,0764465	0,3454578	1,578067	0,4481738	0,23567
$^{87}Sr/^{86}Sr$	0,706843	0,705509	0,704227	0,706848	0,70436	0,707777	0,705869	0,705275	0,704989	0,706419	0,705728	0,704371
$^{87}Sr7^{86}Sr_{(150\ Ma)}$	0,705048	0,704396	0,704165	0,704496	0,703734	0,705277	0,703986	0,705112	0,704252	0,703054	0,704772	0,703868
Nd (ppm)	35,319	28,264	34,66	29,703	24,691	39,132	24,405	5,351	40,527	34,468	25,67	44,293
Sm (ppm)	7,441	6,116	6,841	6,383	5,802	8,672	5,356	1,517	6,984	6,967	5,512	7,987
$^{147}Sm/^{144}Nd$	0,127	0,131	0,119	0,13	0,142	0,134	0,133	0,171	0,104	0,122	0,13	0,109
$^{143}Nd/^{144}Nd$	0,512648	0,512706	0,512587	0,512668	0,51296	0,512794	0,512795	0,512787	0,512581	0,512609	0,512649	0,512744
$^{143}Nd/^{144}Nd_{(150\ Ma)}$	0,512523	0,512578	0,51247	0,512541	0,512821	0,512663	0,512665	0,512619	0,512479	0,512489	0,512522	0,512637
€$Nd_{(150\ Ma)}$	1,52	2,59	0,49	1,86	7,33	4,25	4,29	3,39	0,66	0,86	1,5	3,75
T_{DM} (Ma)	710	637	747	696	224	501	492	930	655	734	728	456
sample id	BA191	SA172	BA193	BA196	SH181		QA158	BH90	GA145	BA19		
rock suites	felsic calc-alkaline suite						felsic alkaline suite					
Rb (ppm)	119,189	122,266	108,68	5,576	95,759		60,152	172,164	150,014	137,925		
Sr (ppm)	152,707	209,236	175,284	458,716	381,267		1074,37	59,436	153,167	79,163		
$^{87}Rb/^{86}Sr$	2,258535	1,690773	1,794027	0,035159	0,726658		0,1619433	8,393143	2,834506	5,044369		
$^{87}Sr/^{86}Sr$	0,709227	0,708434	0,708566	0,70457	0,707581		0,704924	0,722941	0,710665	0,714796		
$^{87}Sr7^{86}Sr_{(150\ Ma)}$	0,704411	0,704829	0,704741	0,704495	0,706032		0,704579	0,705045	0,704621	0,70404		
Nd (ppm)	33,177	11,866	29,651	37,617	19,353		24,16	17,898	30,641	25,183		
Sm (ppm)	6,495	2,34	5,629	6,69	2,894		4,076	3,711	6,271	5,063		
$^{147}Sm/^{144}Nd$	0,118	0,119	0,115	0,108	0,09		0,102	0,125	0,124	0,122		
$^{143}Nd/^{144}Nd$	0,512747	0,51261	0,512597	0,512754	0,51252		0,512577	0,512666	0,512671	0,512688		
$^{143}Nd/^{144}Nd_{(150\ Ma)}$	0,512631	0,512493	0,512484	0,512649	0,512431		0,512477	0,512543	0,51255	0,512569		
€$Nd_{(150\ Ma)}$	3,63	0,94	0,77	3,97	-0,27		0,62	1,91	2,04	2,42		
T_{DM} (Ma)	494	710	699	437	657		648	665	645	604		

Ghorveh city. With an area of 150km^2 it is the largest body of the seven Ghoreh–Dehgolan plutons (Fig. 1). It is composed of dominant gabbrodiorites and subordinate granodiorites to granites with a broad mingling zone which, in the south, is cut by the alkaline leucogranites. In the south the rocks are undeformed. In the north, however, the rocks are markedly deformed by a planar N 45º E to N 55º E subvertical foliation (Hosseiny *et al.*, 1999).

The gabbrodiorites are formed of zoned plagioclase (cores: An_{69-52}; rims: An_{45-32}), augite (Wo_{43-49} Fs_{11-27} En_{28-39}), magnesian hypersthene (Wo_{1-3} Fs_{38-46} En_{51-58}), and magnesio-hastingsitic or edenitic amphibole. They have subordinate Mg-rich biotite, epidote and rare K-feldspar. Accessory minerals include titanite, apatite, ilmenite (commonly mantled by titanite) magnetite, pyrite, allanite and zircon.

The felsic calc-alkaline granitoids comprise granodiorites to granites. Their modal composition comprises zoned andesine-oligoclase (cores: An_{37-25}; rims: An_{21-9}) locally with albitic rims, K-feldspar, quartz, biotite, hastingsitic amphibole, and epidote, with zircon, thorite, allanite, titanite, magnetite, ilmenite and apatite as accessories. These granites are extensively mixed and mingled with the gabbrodiorites, thus forming hybrid intermediate rocks that consist of meter-sized dioritic or quartz-dioritic enclaves cemented by a light-coloured, more granitic, material (Fig. 2).

The felsic alkaline granites are undeformed pink rocks composed of oligoclase-albite (cores: An_{26-15}; rims: An_{17-8}), K-feldspar, quartz, biotite, magnesio-hornblende and epidote with accessory zircon, titanite, magnetite, apatite, and ilmenite. This suite only crops out in the southernmost part of the batholith, where they cross-cut the gabbrodiorites. The alkaline granites commonly include angular xenoliths of mafic rocks.

Shanevareh

The Shanevareh stock crops out over 9km^2 to the west of Ghorveh city (Fig. 1). It is composed of dominant I-type leucogranites and subordinate mafic rocks. Both rock types are coeval and show extensive mixing and mingling as described by Sheikhzakariai and Ghafari (2008).

The mafic rocks are medium- to coarse-grained gabbrodiorites and quartz-monzodiorites formed of labradorite-andesine (cores: An_{65-56}; rims: An_{34-31}), magnesio-hornblende, biotite, epidote, mesoperthitic orthoclase. Rare quartz with titanite, magnetite, ilmenite, apatite and rare zircon are accessories.

The granites are medium-to coarse-grained myrmekite-bearing I-type syenogranites composed of microcline, oligoclase (An_{20-12}), interstitial quartz, biotite and epidote, with magnetite, ilmenite, titanite, apatite and zircon as accessories. They are locally deformed and often contain abundant elongated microgranular enclaves.

Qalaylan

The Qalaylan pluton crops out over 28km^2 to the south of Qalaylan village, southwest of Ghorveh (Fig. 1). It is composed of quartz-monzonites and quartz-monzodiorites cut by younger porphyritic micro-monzogranites and subvolcanic porphyritic quartz-micro-monzodiorites.

The quartz-monzonites and quartz-monzodiorites consist of variable proportions of andesine-oligoclase (cores: An_{49-32}; rims An_{21-18}), augitic clinopyroxene (Wo_{48} Fs_{14} En_{38}, especially abundant in the less silicic facies), magnesio-hornblende, biotite, K-feldspar, and interstitial quartz. Micrographic quartz-alkali feldspar intergrowths forming granophyric textures are common in the most silicic rocks. The accessories are allanite, magnetite, titanite, apatite and zircon, with rare ilmenite.

The late micro-monzogranites are porphyritic, with small (1–5mm) phenocrysts of mesoperthitic K-feldspar, albite (An_{6-4}), quartz and glomeroporphyric epidote within a microcrystalline groundmass of quartz, K-feldspar, epidote and rare biotite. Accessory minerals are zircon, thorite, allanite (mostly included in epidote), titanite and apatite.

Kangareh

The Kangareh pluton crops out over 30km^2 around Kangareh village southwest of Ghorveh (Fig. 1). It is mainly composed of gabbrodiorites with enclaves of ultramafic mantle peridotites. Felsic rocks are scarcely represented; just a few outcrops of I-type granodiorites in the south and a few north-south to northeast-southwest dyke swarms of A-type leucogranites.

The gabbrodiorites form two main facies, one marginal and the other central. The marginal facies consists of quartz-normative (CIPW) fine-grained foliated monzonitic rocks composed of plagioclase (An_{52-43}), augitic clinopyroxene (Wo_{45-47} Fs_{21-27} En_{26-31}) and non-perthitic K-feldspar as major minerals (with little or no hornblende or biotite) and apatite, magnetite, Mn-ilmenite and titanite as accessories. The central facies comprises olivine-normative (CIPW) gabbros formed of labradorite-andesine (cores: An_{59-52}; rims: An_{48-42}), magnesian pargasite, subordinate augite (Wo_{45-46} En_{35-40} Fs_{13-16}), biotite and epidote. Accessory minerals are ilmenite, magnetite, pyrite, apatite, and titanite.

Galali

Galali is the easternmost pluton. It crops out over 42km^2 to the south of the famous Galali iron mine (Eshraghi, 1996) (Fig. 1). The pluton is mainly composed of I-type biotite-epidote granitoids with minor coeval gabbrodiorites that form small continuous outcrops, broad enclave swarms or syn-plutonic dykes (Fig. 2). Both granites and gabbrodiorites are cut by abundant northeast-southwest dykes of pink alkaline syenogranites and alkali-feldspar granites.

The calc-alkaline granitoids are composed of untwinned plagioclase (An_{14-9}), orthoclase, quartz, magnesio-hornblende, biotite and epidote as major minerals, and allanite, zircon, thorite, ilmenite, titanite and apatite as accessories. Mafic rocks are gabbrodiorites to monzo-gabbrodiorites composed of plagioclase (cores: An_{66-52}; rims: An_{34-22}), augite (Wo_{41-44} Fs_{11-17} En_{39-46}), biotite, epidote, perthitic K-feldspar, and scarce hornblende. Magnetite, ilmenite, titanite, pyrite, apatite and zircon are the accessories. Mafic rocks and felsic calc-alkaline granitoids are extensively mingled in wide interaction zones. These two rock types are post-dated by dykes of alkaline leucogranites composed of mesoperthite, albite (An_{6-4}) rimmed by anhedral perthitic K-feldspar, quartz, biotite and epidote, with accessory ilmenite, magnetite, titanite, zircon and apatite. The A-type granites are locally agpaitic and show textural evidence of changing from hypersolvus to subsolvus conditions.

Saranjianeh

The Saranjianeh pluton is exposed over an area of 50km^2 (Fig. 1). The pluton is composed of mafic to intermediate rocks and minor volumes of coeval I-type monzogranites. It is cut, in particular to the north, by abundant northeast-southwest and north-south trending dykes of alkaline syenogranites and alkali-feldspar granites.

The mafic to intermediate rocks are gabbrodiorites, monzodiorites, monzonites, and quartz-monzonites formed of plagioclase (An_{55-51} to An_{48-30}, in the gabbrodiorites; An_{45-36} to An_{28-17}, in the others), magnesio-hornblende, clinopyroxene (Wo_{44-49} Fs_{7-23} En_{35-44}), ferro-hypersthene (Wo_{2-6} Fs_{50-55} En_{42-44}) and K-feldspar, with subordinate biotite, epidote and interstitial quartz. The accessory association is composed of titanite, apatite, ilmenite, magnetite and zircon.

The felsic calc-alkaline granitoids are monzogranites that form small discontinuous outcrops in the southernmost part of the pluton. Their modal composition is oligoclase (An_{28-15}), untwinned K-feldspar orthoclase, quartz, magnesio-hornblende, biotite and epidote, with magnetite, ilmenite, titanite, apatite and zircon as accessories.

The alkaline granites are composed of albite that locally may have cores of sodian oligoclase, highly perthitic K-feldspar, quartz, ferro-edenitic amphibole, Fe-rich biotite and epidote, with titanite, apatite, magnetite, ilmenite and zircon as accessories.

Bolbanabad-Havarpan

The Bolbanabad-Havarpan (previously called the Sufi Abad pluton by Azizi *et al.*, 2011) is the westernmost pluton (Fig. 1). It has a semi-oval exposure 8.5km long and 4km wide. The inner part of the pluton consists of I-type diorites, quartz-diorites and quartz-monzonites formed of plagioclase ($An_{33\text{-}29}$), magnesio-hornblende locally with relicts of clinopyroxene ($Wo_{45\text{-}47}$ $Fs_{12\text{-}17}$ $En_{37\text{-}39}$), K-feldspar, biotite and epidote, with titanite, apatite, ilmenite, pyrite, zircon and magnetite as accessories. The outer part of the pluton is formed of A-type granophyric granites intruding the diorites and quartz-diorites. These granites consist of small phenocrysts of microcline, quartz and albitic plagioclase ($An_{14\text{-}2}$) in a granophyric groundmass of quartz, K-feldspar and plagioclase, with a few scattered grains of epidote and biotite.

SAMPLES AND METHODS

For this survey of the age of the Ghorveh-Dehgolan plutons, some 200 samples were collected from different magmatic suites, enclaves and dykes. All the samples were studied by optical microscope. Thirty two polished thin sections were selected for electron microscopy and microprobe analysis. One hundred and twenty two samples were analyzed for major and trace elements, and a subset of twenty one were also analyzed for Sr and Nd isotopes. Zircons for SHRIMP U-Th-Pb analysis were separated from nine samples, two from each of the Ghorveh, and Qalaylan plutons and one from each of the other plutons: Kangareh, Galali, Shanevareh, Saranjianeh and Bolbanabad-Havarpan. All samples were taken from the main facies of each body.

Major element analyses of minerals were obtained with a four-spectrometer JEOL JXA-8200 electron probe at the University of Huelva (Spain) operated with an accelerating voltage of 15kV and a probe current of 15nA. Silicate standards were jadeite for Na, wollastonite for Ca, alkali feldspar for K and Al, enstatite for Mg, fayalite for Fe and Mn and apatite for P. Precision at 1 sigma level was within ±2 and ±5rel.% for major and minor elements, respectively.

Whole-rock major, trace and isotope analyses were carried out at the CIC, University of Granada. Major-element determinations were performed by X-ray fluorescence after fusion with lithium tetraborate. Typical precision was better than ±1.5% for an analyte concentration of 10wt.%. Trace-element determinations were done by ICP-mass spectrometry (ICP-MS) with a Perkin Elmer Elan-8000 spectrometer using Rh as internal standard. Precision was better than ±2% and ±5% for analyte concentrations of 50 and 5ppm respectively. Samples for Sr and Nd isotope analyses were digested in a clean room using ultra-clean reagents and analysed by thermal ionization mass spectrometry (TIMS) in a Finnigan Mat 262 spectrometer after chromatographic separation with ion-exchange resins. Normalization values were $^{86}Sr/^{88}Sr=0.1194$ and $^{146}Nd/^{144}Nd=0.7219$. Blanks were 0.6 and 0.09 nanograms for Sr and Nd respectively. The external precision (2σ), estimated from the results of the last 10 replicates of the standard WS–E (Govindaraju *et al.*, 1994), which is routinely analysed each 10 unknown samples, was better than 0.003% for $^{87}Sr/^{86}Sr$, and 0.0015% for $^{143}Nd/^{144}Nd$. Both $^{87}Rb/^{86}Sr$ and $^{147}Sm/^{144}Nd$ were directly determined by ICP-MS (Montero and Bea, 1998), with a precision, estimated by analyzing 10 replicates of the standard WS–E, better than 1.2% and 0.9% (2σ) respectively.

Zircon was separated using panning, first in water and then in ethanol, followed by magnetic extraction of Fe-rich minerals and, finally, hand picking under the binocular microscope. Zircons were analyzed in the SHRIMP IIe/mc instrument of the IBERSIMS laboratory, University of Granada, following the method described by Williams and Claesson (1987). Each spot was rastered with the primary beam for 120s prior to analysis, and then analyzed for 6 scans following the isotope peak sequence $^{196}Zr_2O$, ^{204}Pb, $^{204.1}$background, ^{206}Pb, ^{207}Pb, ^{208}Pb, ^{238}U, ^{248}ThO, ^{254}UO. Every peak of every scan was measured sequentially 10 times with the following total counting times per scan: 2s for mass 196; 5s for masses 238, 248, and 254; 15s for masses 204, 206, and 208; and 20s for mass 207. The primary beam, composed of $^{16}O^{16}O^+$, was set to an intensity of about 5nA, with a 120 microns Kohler aperture, which generated 17 20 micron elliptical spots on the target. The secondary beam exit slit was fixed at 80 microns, achieving a resolution of about 5000 at 1% peak height. All calibration procedures were performed on the standards included on the same mount. Mass calibration was done using the REG zircon (*ca.* 2.5Ga, very high U, Th and common lead content). The analytical session started measuring the SL13 zircon (Claoué-Long *et al.*, 1995), which was used as a concentration standard (238ppm U). The TEMORA zircon (416.8±1.1Ma; Black *et al.*, 2003), used as isotope ratios standard, was then measured every 4 unknowns. Data reduction was done with the SHRIMPTOOLS software (available from www.ugr.es/~fbea), which is a new implementation of the original PRAWN software developed for the SHRIMP. Errors are reported at one sigma. The error for $^{206}Pb/^{238}U$ includes the error on the mean of the normalization standard. These, calculated on the 40 replicates of the TEMORA standard measured during the analytical session, were ±0.37% for $^{206}Pb/^{238}U$ and ±0.91% for $^{207}Pb/^{206}Pb$. Errors for the pluton ages are reported at two sigmas.

SHRIMP U-PB RESULTS

We analyzed a total of 200 spots in 186 zircons for U-Th-Pb (Table II Electronic Appendix). The results are summarized below:

Ghorveh

The Ghorveh pluton was studied by Mahmoudi *et al.* (2011), they determined ID-TIMS U-Pb zircon ages of ~149Ma and ~151Ma in the central part of the body. Here we dated two samples, one from the deformed northern granitoids, and the other from the southern undeformed granites. The first sample (BA190: FCAS) is a mylonitic syenogranite that contains amber-coloured, small-sized (up to 150×100µm) prismatic euhedral to subhedral zircon crystals with short, poorly developed pyramidal terminations. Cathodoluminescence images show that most crystals present oscillatory zoning of probable magmatic origin. Overgrowths and small irregular inclusions are common (Fig. 3). Ten of eleven zircon grains yielded concordant ages with mean $^{206}Pb/^{238}U$=160.7±2.8Ma (MSWD=0.68), $^{207}Pb/^{235}U$=162±3.9Ma (MSWD=0.82) and a 207-corrected $^{206}Pb/^{238}U$ age of 160.6±3.8Ma (MSWD=0.64) (Fig. 4). One pre-magmatic zircon yielded an imprecise subconcordant Permo-Triassic age of 257±28Ma.

The second sample (BA19: FAS) is an undeformed monzogranite that contains pale amber anhedral to subhedral short crystal zircons with a mean size of 100×50µm. Under the cathodoluminescence microscope, these zircons are whitish with a poorly defined oscillatory zoning and low cathodoluminescent cores (Fig. 3). Sixteen grains out of 34 grains yielded concordant to subconcordant (discordance <5%) determinations with negligible common lead and the following averages: $^{206}Pb/^{238}U$=147.5±2.6Ma (MSWD=0.63), $^{207}Pb/^{235}U$=150±2.8Ma (MSWD=0.71) and a 207-corrected $^{206}Pb/^{238}U$ age of 147.3±2.7Ma (MSWD =0.60) (Fig. 4). Other ages are discordant due to Pb-loss and common lead, they were not considered in the age calculation.

We conclude, therefore, that the crystallization age of the undeformed Ghorveh granitoids is 147±3Ma, in excellent agreement with the data from Mahmoudi *et al.* (2011), but the northern mylonitic facies is clearly older, 161±4Ma.

Shanevareh

One sample of the Shanevareh quartz-monzodiorites (SH177: MIS) contained translucent pale brown to pinkish, euhedral to subhedral, small prismatic zircons with an average size of 200×100µm. Under the cathodoluminescence microscope they are often dark grey and show oscillatory zoning (Fig. 3). Fourteen analyses of 12 zircon grains yielded 204-corrected concordant to subconcordant results with mean $^{206}Pb/^{238}U$=160.1±1.7Ma (MSWD=0.32), $^{207}Pb/^{235}U$=158.7±2.9Ma (MSWD=0.81) and 207-corrected $^{206}Pb/^{238}U$ age of 160.2±1.7Ma (MSWD=0.3) (Fig. 4C). Therefore, we consider that 160±2Ma is the best estimate of the crystallization age.

Qalaylan

We separated zircon grains from two samples; one granular quartz-monzonite (QA153) and a porphyritic monzogranite (QA158). The quartz-monzonite (QA153) contained amber coloured, euhedral to subhedral and short prismatic zircons with a mean size around 100×50µm (Fig. 3). The monzogranite (QA158) contains amber to pale brown zircons, euhedral to subhedral, short and rarely needle-like prismatic, with a mean size of around 100–200µm long and 50–100µm wide and mostly well defined pyramidal terminations (Fig. 3). Under the cathodoluminescence microscope zircons from the two samples often show discordant cores with narrow, often less than 20μm, rims.

SHRIMP analyses of the cores yielded inherited ages ranging from 230 to 2700Ma (Fig. 4E). These ages are among the oldest ever recorded in the SSZ (Chiu, 2013). We also obtained the crystallization age of the thin rims. Nine rims out of 52 analyzed grains yielded 204-corrected mean ages of $^{206}Pb/^{238}U$=159.6±2.8Ma (MSWD=0.31), $^{207}Pb/^{235}U$=168.1±4.9Ma (MSWD=0.68) and a 207-corrected $^{206}Pb/^{238}U$ age of 159.2±2.8Ma (MSWD=0.28) (Fig. 4E). We therefore assume that the crystallization age of the body is 159±3Ma. The 230–2700Ma ages, hence, are inherited.

Kangareh

We were unable to obtain zircons from the Kangareh gabbros and diorites. Therefore, we studied one sample of granite from a felsic A-type leucogranite vein (KA113: FAS) that yielded enough grains for SHRIMP dating. Zircons are translucent, brownish, short, euhedral to subhedral prismatic crystals with well developed pyramidal terminations and a mean size around 100–150µm long and 100–50µm wide. Under the cathodoluminescence microscope some grains are dark, others are whitish, with a clear oscillatory zoning (Fig. 3). We analyzed 19 grains, all of them concordant and with no detectable amount of common lead. Eighteen of these grains yielded the same uncorrected common-lead age of $^{206}Pb/^{238}U$=141.5±2Ma (MSWD=0.37), $^{207}Pb/^{235}U$ of 142.8±2Ma (MSWD=0.36) and a 207-corrected $^{206}Pb/^{238}U$ age of 141.3±1.9Ma (MSWD=0.38), so that we assume 141±2Ma as the crystallization age of the youngest phase

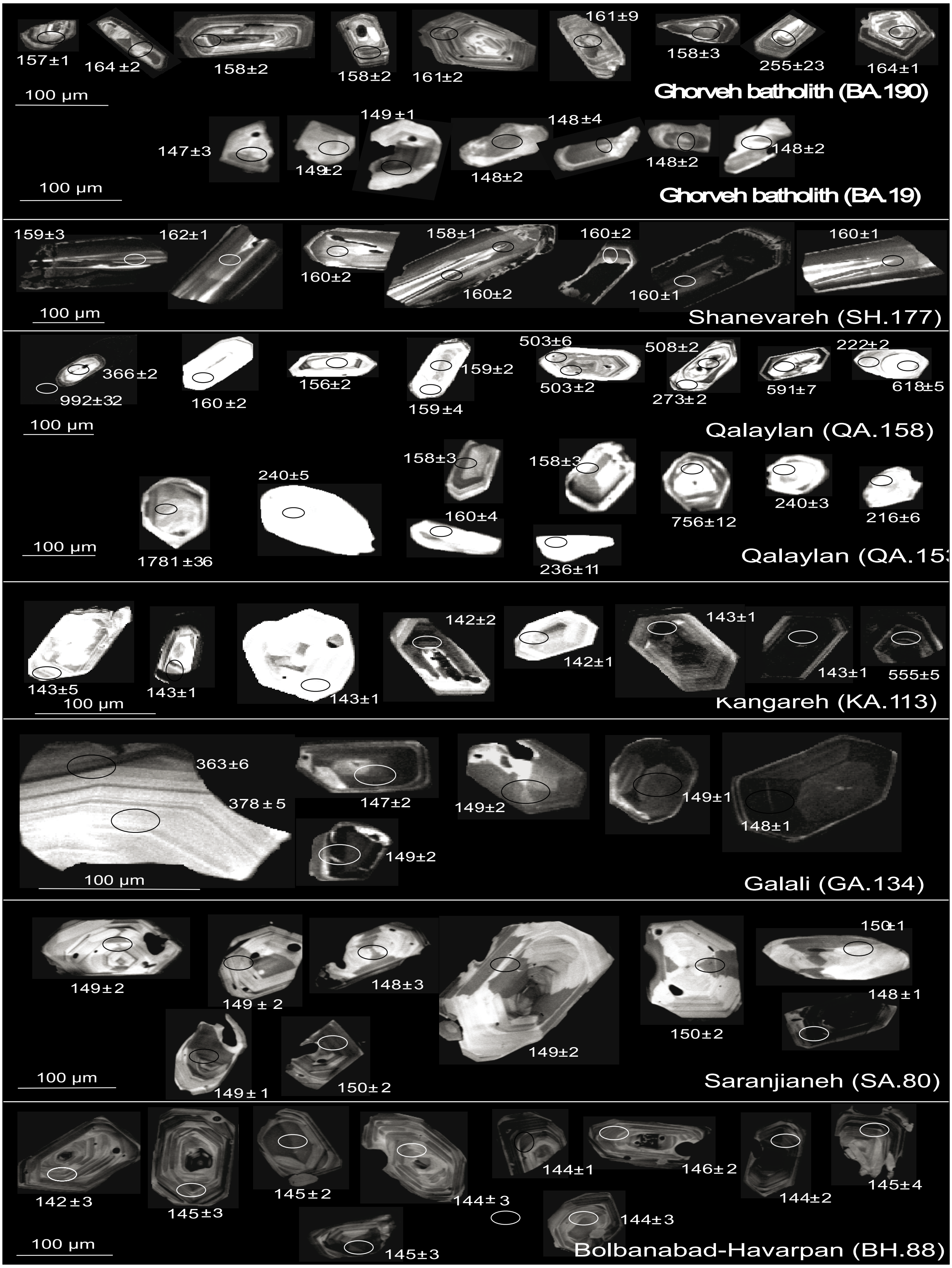

FIGURE 3. Cathodoluminescence images and ages of some of the analyzed zircons. The numbers indicate the age in Ma.

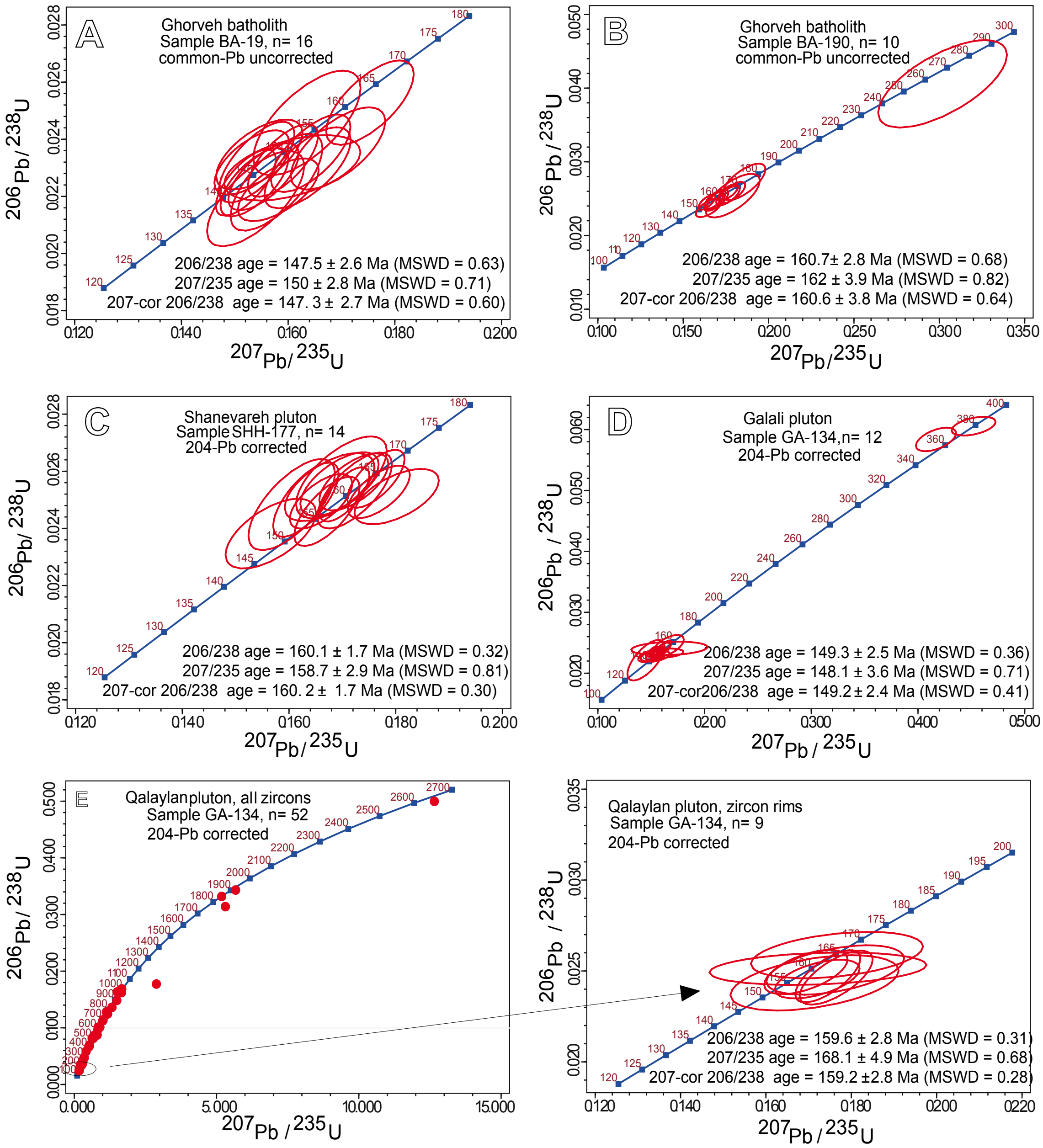

FIGURE 4. Wetherill concordia plots of the zircon SHRIMP data. A) South Ghorveh batholith, B) north Ghorveh batholith, C) Shanevareh pluton, D) Galali pluton, E) Qalaylan pluton (note the presence of premagmatic inherited cores with ages ranging from 230 to 2700Ma). Data (Electronic appendix Table II) were not corrected for common lead.

of the body (Fig. 5A). Additionally, one grain yielded a 204-corrected concordant age of 550±9Ma, so revealing a limited inheritance of Late Ediacaran material (Fig. 5A). This 141±1Ma age cannot thus be considered the crystallization age of the main facies of the Kangareh pluton, but rather its youngest age limit.

Galali

In Galali, we extracted zircons from one syenogranite (GA134: FCAS). Zircon crystals are amber to pale brown, euhedral to subhedral, rarely embayed, small grains up to 100×50µm. Most grains have low cathodoluminescence, showing oscillatory zoning and a few irregular inclusions (Fig. 3). Eight of ten grains studied with the SHRIMP yielded concordant 204-corrected U-Pb ages with mean $^{206}Pb/^{238}U$=149.3±2.5Ma (MSWD=0.36), $^{207}Pb/^{235}U$=148.1±3.6Ma (MSWD=0.71) and a 207-corrected $^{206}Pb/^{238}U$ age of 149.2±2.4Ma (MSWD=0.41) (Fig. 4D). Two other grains yielded inherited Pre-Variscan/Variscan ages of 366±10Ma and 379±8Ma (Fig. 4D). We assume, therefore that the crystallization age of Galali is 149±2Ma.

Saranjianeh

We dated one syenogranite (SA80: FAS) from Saranjianeh. Zircon grains are colourless to pale amber, euhedral to subhedral, small crystals with a mean size around 200×100µm. Under the cathodoluminescence microscope most of the grains are whitish, often displaying a well-developed oscillatory zoning with common euhedral inclusions of other minerals (Fig. 3). No pre-magmatic cores were found. Sixteen grains contained negligible common lead and yielded concordant ages of $^{206}Pb/^{238}U$=148.2±0.9Ma (MSWD=0.10), $^{207}Pb/^{235}U$=150.6±1.7Ma (MSWD=0.25) and a 207-corrected $^{206}Pb/^{238}U$ age of 148±1.1Ma (MSWD=0.10) (Fig. 5B), this last age is considered to be the crystallization age.

Bolbanabad-Havarpan

As is the case for most rocks in this area, zircon is not abundant in the Bolbanabad-Havarpan pluton. After failing to separate zircon from three samples, one alkali-feldspar granite, one quartz-monzodiorite and one quartz-monzonite, we were able to obtain enough zircon grains, with a size >30μm appropriate for SHRIMP dating, from one alkali-feldspar granite (BH88: FAS). Zircons are pale yellow to brownish, euhedral to subhedral, prismatic, short crystals with bipyramidal terminations. Under the cathodoluminescence microscope they are grey to black, with a well defined oscillatory zoning and abundant inclusions (Fig. 3).

Once corrected for common lead, twenty one grains yielded concordant ages with mean $^{206}Pb/^{238}U$=144.3±0.8Ma (MSWD=0.13), $^{207}Pb/^{235}U$=143.4±3Ma (MSWD=0.69) and a 207-corrected $^{206}Pb/^{238}U$ age of 144.3±0.9Ma (MSWD=0.11) (Fig. 5C), which indicate a crystallization age of 144±1Ma. These values are identical, within error, to the laser ablation inductively coupled plasma mass spectrometry (LA-ICP-MS) U-Pb age of 144±2Ma obtained by Azizi *et al.* (2011), but significantly younger than that of Mahmoudi *et al.* (2011), 156±1Ma.

WHOLE-ROCK GEOCHEMISTRY

Major and trace element geochemistry

All the plutons have similar geochemical features. Considered together they show a roughly bimodal distribution of SiO_2, with two maxima, one at about 50 to 55wt.%, and the other around at 72wt.% with a gap between 64 and 66wt.% (Fig. 6). The samples with SiO_2<64wt.% comprise the aforementioned mafic-intermediate suite mentioned in the field relations section. The samples with SiO_2>65wt.% correspond to the felsic calc-alkaline and alkaline suites (Table I Electronic Appendix). No

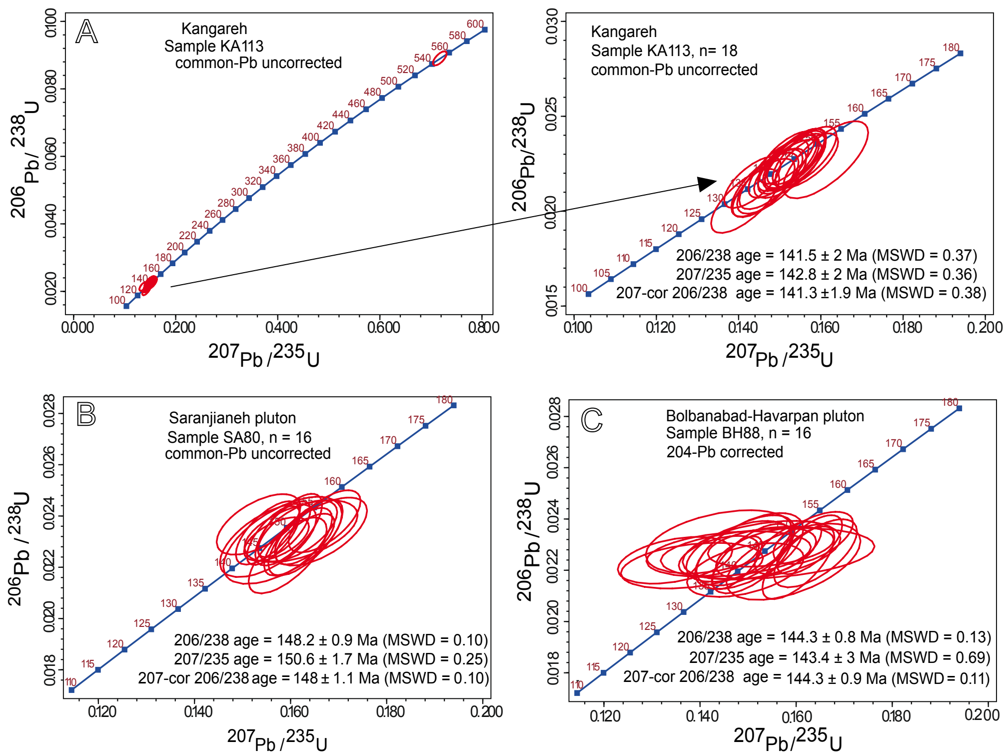

FIGURE 5. Wetherill concordia plots of the zircon SHRIMP data. A) The youngest phase of Kangareh pluton (note the limited inheritance of 555±5Ma (Late Ediacaran)), B) Saranjianeh pluton, C) Bolbanabad-Havarpan pluton. Data were not corrected for common lead (Electronic appendix Table II).

significant compositional differences were found between the three suites in the seven plutons (Table I Electronic Appendix). They differ mostly in the proportions of the three rock suites that they contain. For this reason, in the following paragraphs and figures we shall describe the composition of the rocks grouped in suites, referring to particular features of each pluton where relevant.

The major element composition of the mafic-intermediate suite is calc-alkaline, albeit with some peculiarities. The least silicic rocks are magnesian, calcic, medium-K calc-alkaline (Fig. 6). As SiO_2 increases the bulk-chemistry of the series quickly changes to ferroan and high-K calc-alkaline (Fig. 6) so that the most silicic members of the mafic-intermediate suite (SiO_2≈60wt.%–64wt.%) are in fact A-type granitoids (Fig. 7). Nevertheless, there are some differences with typical subduction-related magmas such as smaller Nb negative anomaly, lower Sr contents, and considerably flatter chondrite-normalized REE profiles (Fig. 8A).

The samples with SiO_2>65wt.% form two chemically distinct groups with little overlap between them: a high alkali group (Na_2O+K_2O=9.2±0.5wt.%) with an average calc-alkaline index (CAI=$CaO/(Na_2O+K_2O)$) of 0.29±0.12 and a (relatively) low alkali group (Na_2O+K_2O=8±0.8wt.%) with CAI=0.38±11 (Fig. 6). These two geochemical groups correspond to the felsic alkaline and felsic calc-alkaline suites defined from petrographic characteristics.

Most of the granitoids in the felsic alkaline suite are ferroan (Fig. 6) and correspond to A-type granites (Fig. 7). Many granitoids of the felsic calc-alkaline suite are magnesian (Fig. 6) and correspond to I-type granites, but a few are ferroan A-type granites that overlap with the alkaline suite. Accepting that the boundary between A-type and I-type granites is mol. FeO/(FeO+MgO)=0.8, in the Eby (1992) diagram to discriminate between A1 and A2 subtypes (Fig. 7C), all A-type granites from the felsic calc-alkaline series plot in the A2 field. This field contains crustally contaminated A1 type magmas or those derived from continental crust, or underplated crust that has been through a cycle of continent-continent collision or arc magmatism. By contrast, the granites from the mafic and felsic alkaline suites mostly plot ambiguously at the A1–A2 boundary. For this reason, we used the recently published A-type granite discrimination diagrams of Moreno *et al.* (2014) to reveal that the felsic alkaline suite also has an A2 type affinity (Fig. 7D). The only exception is the felsic alkaline suite from Qalaylan that has a true A1 type affinity representative of differentiates of magmas derived from OIB sources but emplaced in continental rifts or during intraplate magmatism.

The two types of felsic granitoids show similar trace element patterns, characterized by strong depletion in Ti, enrichment in Zr and, especially, Th and U (Fig. 8). The felsic alkaline granitoids tend to be richer in REE than the calc-alkaline granitoids but the chondrite-normalized patterns (Fig. 8) are almost parallel. In contrast with most subduction-related granites, the felsic alkaline granitoids show a small LREE/HREE fractionation and are almost flat from Ga to Lu. The alkaline granites always show a moderate Eu negative anomaly, this is absent in some felsic calc-alkaline granites.

Sr and Nd isotopes

The Sr and Nd composition of the twenty one analyzed samples is notably primitive (Table 1). All but one felsic calc-alkaline granitoid have positive $\varepsilon Nd_{(150Ma)}$. In the $\varepsilon Nd_{(t)}$ vs $^{87}Sr/^{86}Sr_{(t)}$ diagram (Fig. 9A) most samples plot either in the mantle array or are slightly displaced to higher $^{87}Sr/^{86}Sr_{(t)}$ as often is observed in arc-magmas. Remarkably, the three geochemically and petrographically distinct rock series have no discernible differences in their isotope composition.

Another significant feature is the elevated Nd model ages of the analyzed samples. Using the DePaolo (1981) expression, the Nd model ages in the neighbouring Arabian-Nubian Shield closely reflects the age of crust formation (Stern, 2002). The Nd model ages of all our studied samples spread from T_{DM}=220Ma to about 960Ma, and define a large cluster between 550Ma and 750Ma (Fig. 9B). The youngest T found so far is 220Ma, which is still older than the zircon crystallization ages. As discussed in the next section, Nd model ages indicate that the main source component of the Ghorveh-Dehgolan plutons was not juvenile mantle-derived subduction magmas. The presence of inherited grains supports this idea.

DISCUSSION

Our new SHRIMP data for the seven Ghorveh-Dehgolan plutons confirm that they are Late Jurassic and reveal that the magmatic activity occurred over a time span of 20 million years, from ~160 to ~140Ma. The activity started in the northeast with the intrusion of the syenogranites of the northern Ghorveh batholith at 161±4Ma and the gabbrodiorites of Shanevareh at 160±2Ma and Qalaylan at 159±3Ma. Magmatism then shifted to the central part of the Ghorveh batholith (around 151Ma to 149Ma; Mahmoudi, 2011) and following that to the Galali and Saranjianeh plutons (149±3Ma and 148±1Ma). Still younger ages are found in the west of the arc, corresponding to the alkaline granites of the southernmost Ghorveh batholith (147±3Ma) and the peraluminous granites of the Bolbanabad-Havarpan pluton (144±1Ma). The only exception is Kangareh, but it should be taken into account that the main rock facies of this gabbroic body does not contain zircons; therefore,

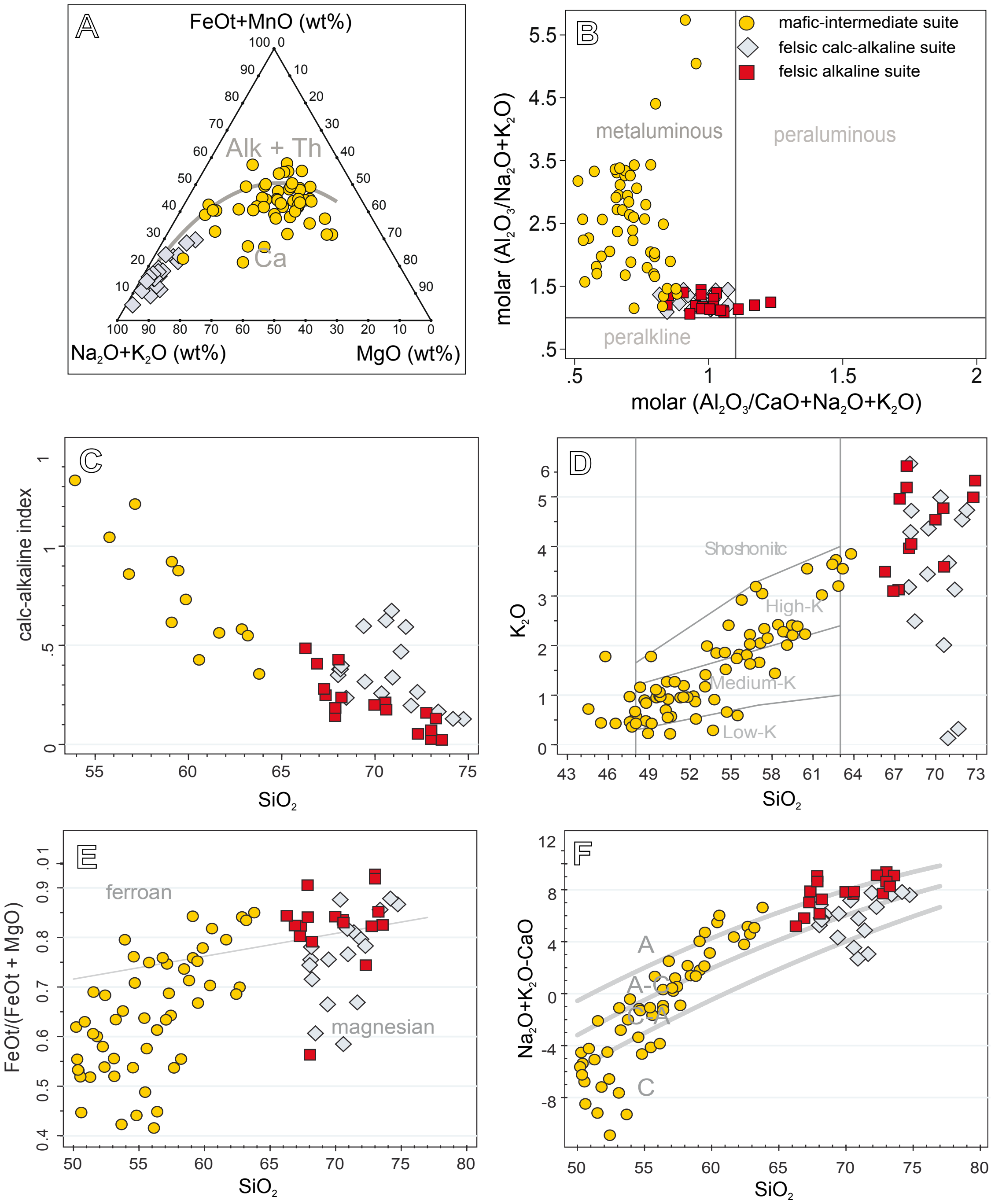

FIGURE 6. Major element relations in the Ghorveh-Dehgolan plutons. A) AFM (Na_2O+K_2O–FeO–MgO) diagram. Alk- alkaline; Th- tholeiite; Ca- calc-alkaline B) Al_2O_3/Na_2O+K_2O and $Al_2O_3/CaO+Na_2O+K_2O$ diagram, note the metaluminous to slightly peraluminous characteristics of felsic rocks (Shand, 1943). C) calc-alkaline index versus SiO_2. D) K_2O vs. SiO_2; most mafic rocks have a medium content of K, most of felsic rocks are high K. E). $FeO_t/(FeO_t+MgO)$ vs SiO_2 plot of Frost *et al.* (2001); note that most of the felsic alkaline suite rocks are ferroan. F) MALI (modified alkali-lime index) vs SiO_2 plot (Frost *et al.*, 2001).

we studied a felsic A-type leucogranite vein that has the youngest age (141±3Ma) found so far in the complex and which might not be representative of the whole pluton.

The Ghorveh-Dehgolan granitoids share many geochemical features with subduction-related rocks, but they also show significant differences, such as: the marked compositional bimodality (Fig. 6); the abundance of A-type granites; the low LREE/HREE fractionation (Fig. 8); and the small Nb negative anomaly. The presence of inherited zircons in several bodies, especially in Qalaylan, suggests that the magmatic sources contained older crustal components. This idea finds support from the elevated Nd model ages, which range from T_{DM}=220Ma to 930Ma (Fig 9B). The youngest Nd model ages are relatively close to the magmatic zircon crystallization ages, but most are Pan-African, especially the large cluster between 550Ma and 750Ma. These Nd model ages might reflect either the age of a crust formation event or mixing of materials with different Nd isotopic compositions.

The presence of inherited zircons is consistent with the mixing hypothesis. Esna-Ashari *et al.* (2012) dated the Aligoodarz granitoid complex to the southeast of the Ghorveh-Dehgolan plutons by in situ LA-ICP-MS U–Pb on zircon. In agreement with our findings they measured a crystallization age of ~165Ma and detected inherited grains spanning in age from ~180Ma up to 2027Ma, which they attributed to country rock assimilation. Inherited zircons are not abundant and their ages, mostly Lower Paleozoic to Neoproterozoic, may be seriously perturbed by diffusive effects (*e.g.* Bea and Montero, 2013), so they cannot necessarily be used to reliably estimate the age of the magmatic sources.

The positive $\varepsilon Nd_{(t)}$ and low $^{87}Sr/^{86}Sr_{(150Ma)}$ of the mafic-intermediate suite reflects that these rocks had a mantle source. Notably, the felsic calc-alkaline suite also has the same primitive Sr-Nd isotopic signatures but geochemical data, old Nd model ages and the presence of inherited zircons are not consistent with a mantle source origin. The only way to reconcile these mantle-like primitive isotopic features with the older-than-crystallization T_{DM} ages is to assume that the crustal components had a very primitive isotopic signature. This is the case for most of the crust of the Arabian-Nubian Shield which, with the exception of the Afif terrane, has a T_{DM}=0.85±0.18Ga (Stern, 2002) (Fig. 9B).

If the basement of the SSZ was compositionally comparable to that of the Arabian-Nubian Shield (Hassanzadeh *et al.*, 2008) and melted during generation of the Ghorveh-Dehgolan plutons, this would explain: the zircon inheritance; the Sr and Nd isotope features; and, the abundance of A-type, anorogenic, granitoids. Given that the composition of the Arabian-Nubian Shield crust is markedly heterogeneous, with abundant mafic rocks and A-type granites, its involvement in the felsic magmatic sources could also explain the peculiar composition of the granitoids (Fig. 9).

The mafic-intermediate suite rocks have a sub-alkaline, calc-alkaline metaluminous composition (Fig. 6). They most likely originated in a supra-subduction zone mantle source.

The felsic calc-alkaline suite granites are predominantly sub-alkaline, calc-alkaline, metaluminous although a few samples are alkaline with an A2 type, arc-like, character (Figs. 6 and 7). Field relations and our new SHRIMP data indicate that the mafic-intermediate suite was contemporaneous with the felsic calc-alkaline suite. We suggest that heat from mafic, mantle-derived, magma provoked crustal melting resulting in this suite incorporating a significant component of Arabian-Nubian Shield. This model is supported by field relations that show extensive mingling (Fig. 2).

Alkaline granites contemporaneous with the mafic-intermediate and felsic calc-alkaline suites, the Qalaylan pluton, are compositionally quite distinct from the younger alkaline granites. The former, have a metaluminous A1 type character whereas the latter are predominantly metaluminous A2 type although tending to peraluminous (Fig. 6 and 7). A key feature of the older alkaline granites is the abundance of premagmatic zircons. Localized fast melting of fertile, subduction fluid-metasomatized, Arabian-Nubian Shield crust followed by rapid crystallization could have preserved preexisting zircons. A similar process was invoked for the premagmatic zircon-rich Ordovician Ollo de Sapo orthogneisses in central Spain (*cf.*, Bea *et al.*, 2007).

The 15–20 million year younger felsic alkaline suite are alkaline, predominantly metaluminous A2, granites (Figs. 6 and 7). It appears that this suite was derived from partial melting of Arabian-Nubian Shield previously fertilized by alkaline mantle- or slab-derived fluids. The compositions of these felsic alkaline granites are comparable to typical post-collisional A-type granite suites (*cf.* Eby, 1992).

The Zagros Orogen formed related to a northeastward subducting system (Berberian and King, 1981; Sengör, 1990; Vernant, *et al.*, 2004; Doglioni *et al.*, 2009; Agard *et al.*, 2011); accordingly, one would expect the ages of the related magmatic rocks to become progressively younger to the northeast. This is not, however, the situation revealed by our SHRIMP data for the Ghorveh-Dehgolan plutons.

The tectonic scenarios proposed for the Zagros orogen are as varied as they are complex. The story begins in the late Permian as the Cimmerian plate, including Iran, broke away from northern Gondwana to form Neotethys. As early as the 1970s Stöcklin (1974) proposed that Neotethys was not a single ocean but rather a collection of several branch troughs, the formation of these led, temporarily, he suggested, to the isolation of a Central-and-East Iranian Microcontinent in the late Mesozoic. The idea of a second ocean, 'Neotethys II', that opened between the SSZ and central Iran in the middle Cretaceous is now quite well established (*e.g.* Ghasemi and Talbot, 2006; Richards *et al.*, 2006; Shafiei *et al.*, 2009; Darabi-Golestan *et al.*, 2012). Richards *et al.* (2006) suggested that this easterly ocean,

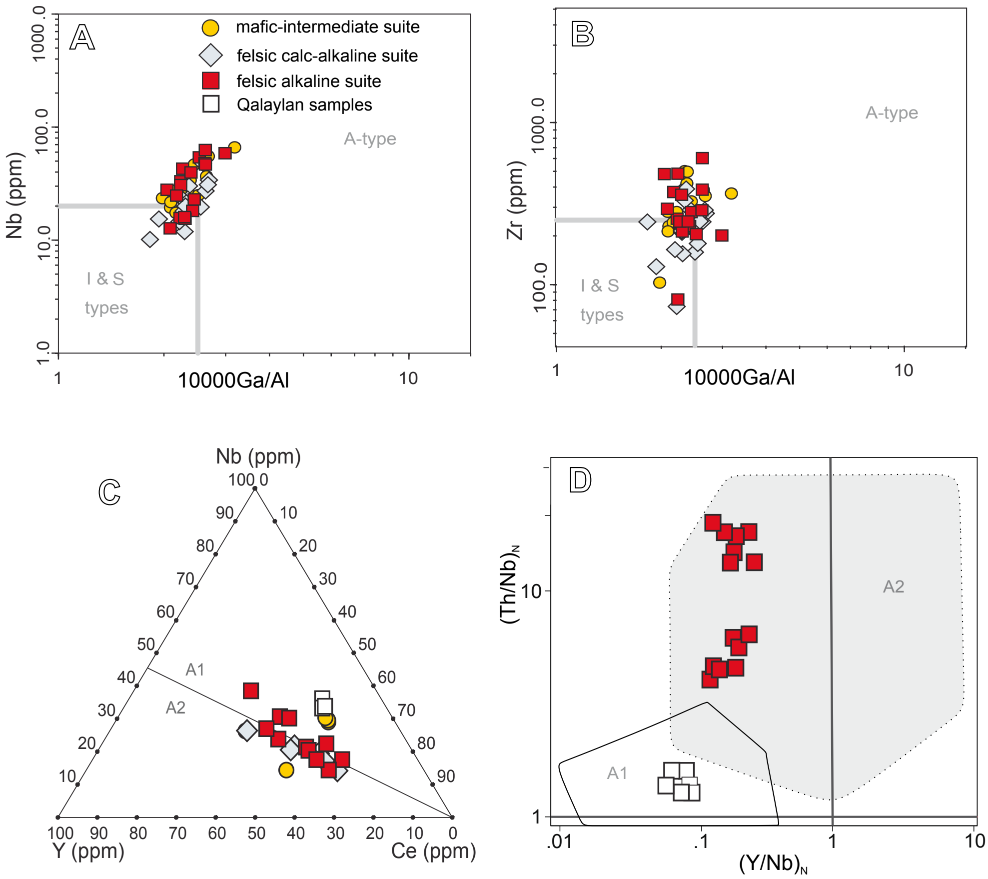

FIGURE 7. Whalen *et al.* (1987) plots of Ghorveh-Dehgolan plutonic rocks. A and B) reveal that most of the felsic alkaline suite are A-type granites. C) Discrimination diagram for A-type granites (Eby, 1992). All A-type granites from the felsic calc-alkaline series plot in the A2 field whereas the mafic and the felsic alkaline suites are A1 type. D) Discrimination of A1 and A2 granitoids based on the relationships of Y/Nb with Th/Nb, for felsic alkaline suite rocks. (Compositional fields from Moreno *et al.*, 2014 and references therein). Values normalized to Silicate Earth (McDonough and Sun, 1995).

Neotethys II, began to subduct in the Eocene. The data compilation of Chui *et al.* (2013) showed that, at least in the south, subduction began earlier, in the Late Cretaceous. In agreement with the two-ocean model, Zagros ophiolites can be divided into 'Inner Zagros' and 'Outer Zagros' supra-subduction zone ophiolitic belts that are separated by the SSZ (Shafaii Moghadan and Stern, 2011).

Turning out attention to the context of the Ghorveh-Dehgolan plutons, Chui *et al.* (2013) noted that the Sanandaj-Sirjan Jurassic magmatism was followed by a protracted magmatic quiescence. The latest Jurassic–Early Cretaceous gap in magmatism is coincident with an unconformity at the base of the SSZ Cretaceous succession (*cf.* Mohajjel and Fergusson, 2014). These authors conclude that uplift and erosion occurred at this time, although as the plutons are not overlain by the unconformity they remained at depth. On a regional scale, they attributed the cessation of magmatism to a reduction in slab dip. Consistent with this, when magmatism reinitiated it did so well inboard of the trench. Following the quiescence, in the Late Cretaceous subduction-related magmatism shifted ~300km inland to the Urumieh–Dokhtar magmatic arc. Azizi and Asahara (2013) attributed the temporal cessation and spatial shift in magmatism to a Jurassic arc-continent collision. These authors suggested that the intra-oceanic forearc is no longer present because it was removed by subsequent tectonic erosion during Cenozoic subduction, continental collision and strike-slip faulting (Mohajjel and Fergusson, 2014). A collisional context fits with the syn-magmatic foliations developed in the mafic-intermediate and felsic calc-alkaline plutons dated in this work. Simple transfer of subduction initiation is an alternative possible explanation for the change in magmatic focus (*cf.* Stern, 2004; Gerya, 2011). Our new geochronological data indicate a northeast to southwest migration of the magmatic focus. Accordingly, Mohajjel and Fergusson (2014) concluded that the Middle Jurassic to Early Cretaceous paleogeography of the northwest SSZ is consistent with localized trenchward advance of the arc.

In a landmark work Eby (1990) noted that A-type granites are typically generated in a non-orogenic setting either within-plate or along plate margins during the

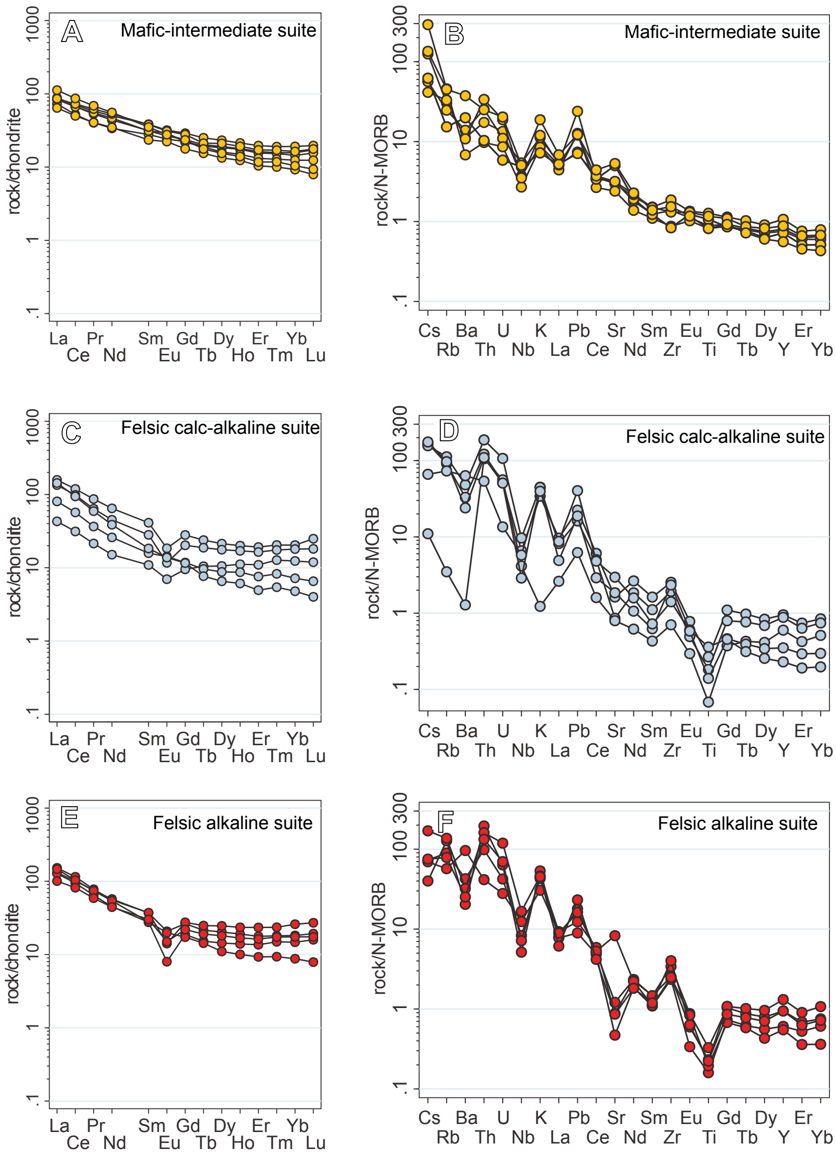

FIGURE 8. N-MORB normalized trace element plots (normalization values from Hofmann (1988)) and chondrite-normalized REE plots (normalization values from McDonough and Sun (1995)), of the mafic-intermediate suite (A, B), the felsic calc-alkaline suite (C, D), and the felsic alkaline suite (E, F).

waning stages of subduction-zone-related magmatism. Furthermore, in 2011 he concluded that a universal feature of A-type granites is that they are emplaced in an extensional context and as such do not show any tectonic fabric. Moreover, an I-type to A-type transition in a collisional to post-collisional extensional setting is quite well established in the literature (*e.g.* Mancuso *et al.*, 1996; Kerr, 1997; Chena *et al.*, 2000; Leite *et al.*, 2007).

Dall'Agnol *et al.* (2012) observed that A-type magmatism is an expected consequence of rapid ascent of asthenospheric material. They concluded that it may result from either foundering of the lithospheric mantle (delamination) or detachment of the subcontinental lithosphere from the surface slab (slab break-off) following continental collision. They went as far as to say that post-collisional processes involving delamination/slab break-off may explain most of the Phanerozoic A-type associations studied in the framework of IGCP-510.

Considering the above we suggest that the calc-alkaline I-type to alkaline A-type transition in the SSZ was the result of a change from compressional subduction and arc collision to extensional rifting. As mentioned above Azizi and Asahara (2013) suggested that an island arc collided with the SSZ in the Late Jurassic. This could have led to a blocking of the subducting plate leading to subduction stopping and, as a result, slab-gap formation. Whatever

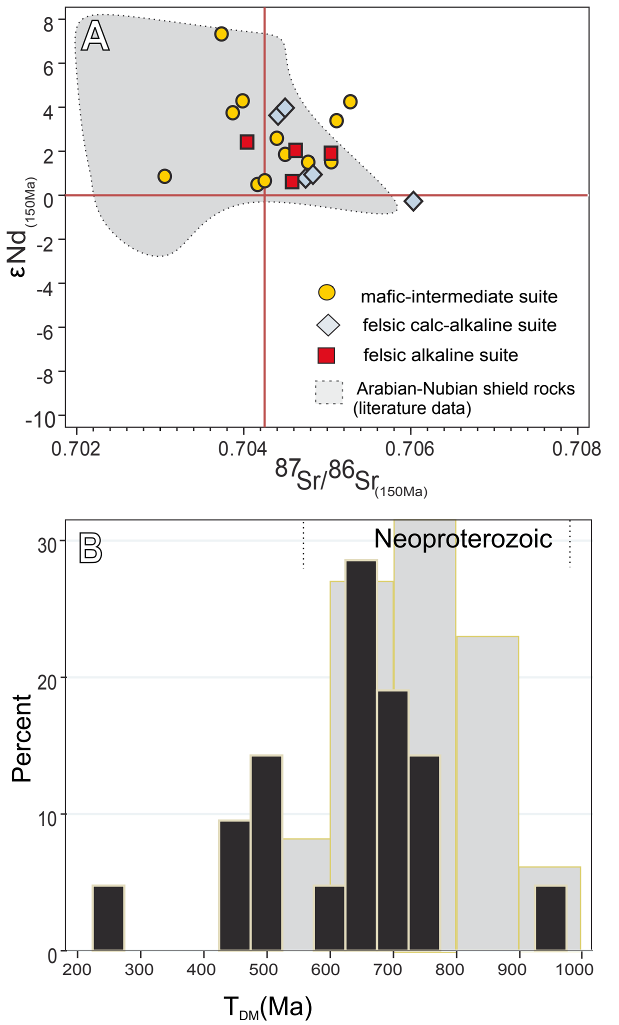

FIGURE 9. Nd-Sr isotopic characteristics of the Ghorveh-Dehgolan rocks. A) $\varepsilon Nd_{(t)}$ vs $^{87}Sr/^{86}Sr_{(t)}$. $\varepsilon Nd_{(t)}$ is calculated for t=150Ma. The shaded field: Isotopic composition of the Arabian–Nubian shield rocks for comparison (literature data from Liégeois and Stern, 2010; Stein, 2003; Stern, and Johnson, 2010 and references therein). Note the primitive and homogenous isotopic composition of the three rock suites and similarities to Arabian-Nubian shield rocks. See Table 3 for analytical data and text for explanation. B) Frequency of Nd model age of all studied samples. Note the remarkable cluster of Neoproterozoic ages and the similarity of inherited zircon ages of Arabian-Nubian Shield (grey field). Literature data from (Hargrove *et al.*, 2006; Liégeois *et al.*, 2010; Stein, 2003; Stern, 2002; Stern and Johnson, 2010 and references therein).

the complexities of the process, the Late Jurassic I-type to A-type transition clearly reflects a perturbation of the northeastward subduction of Neotethys beneath the Iranian sector of Eurasia, Laurasia. During this period magmatism in the region waned. Cessation of subduction, as reflected by the SSZ late Jurassic-Early Cretaceous gap in magmatism, would potential have permitted a more significant contribution of crustal melts to the magmatism.

The last manifestations of the continental magmatic arc were the Middle-Late Jurassic mafic-intermediate and felsic calc-alkaline suites. By contrast, the latest Jurassic to earliest Cretaceous magmatism comprises the felsic alkaline suite, A2 type, rocks (Fig. 7). The latter was apparently produced during initiation of extension, perhaps related to an ocean-opening event (Ghasemi and Talbot, 2006; Richards *et al.*, 2006; Shafiei *et al.*, 2009; Darabi-Golestan *et al.*, 2012). In agreement with this, our geochemical and geochronological data suggest involvement of Arabian-Nubian-like crust in the magmatic system related to extension, as revealed by the late-stage A2 type granites.

Extensive rifting would have resulted in the aforementioned ocean opening, potentially both to the west and to the east of the SSZ. Gaps in the magmatic record may reflect these periods of extension and formation of ocean crust, evidence for which would only be evident once convergence began once more and subduction was well established. The western ocean apparently subducted northeastward under the Sanandaj-Sirjan zone (Urumieh-Dokhtar arc) and the eastern ocean seemingly under Central Iran. Accordingly, Shafaii Moghadan and Stern (2011) concluded that subduction initiated on the northern side of Neotethys during the Cretaceous. The scenario is then that the Neotethys subduction beneath the western SSZ ceased temporarily in the Jurassic producing the A2 type alkaline granitoids. Subduction then began once more in the middle Cretaceous (see geochronology data compilation in Chui *et al.*, 2013) before closing again, definitively, in the Eocene (Mazhari *et al.*, 2009).

Agard *et al.* (2011) demonstrated that Cretaceous and younger magmatism in this area was subduction-related. They mentioned that more evidence was needed to prove earlier subduction. Our new SHRIMP zircon U-Pb data provide that evidence, revealing that subduction was active since, at least, 160Ma.

CONCLUSIONS

The Ghorveh-Dehgolan plutons, exposed in the northern part of the Sanandaj-Sirjan Zone, comprise seven composite intrusive bodies with a wide range of compositions from basic to acid. Most rocks have a calc-alkaline, arc-related, composition. Field relations show that the oldest rocks in each body are calc-alkaline mafic-intermediate rocks coeval with felsic calc-alkaline rocks, with extensive interaction between them. Both the mafic and felsic calc-alkaline rocks are intruded by younger alkaline, often A-type, locally hypersolvus, granites. New SHRIMP dating of the seven bodies reveals that the magmatic activity spanned 20 million years. It started in the northeastern plutons, the northern Ghorveh batholith (161±4Ma), Shanevareh (160±2Ma), and Qalaylan

(159±3Ma) then progressively migrated to the southwest: probably first to Kangareh, then to the central Ghorveh batholith, Galali and Saranjianeh (151±0.2Ma to 148±1Ma) and lastly to the southern Ghorveh batholith (147±3Ma) and Bolbanabad-Havarpan (144±1Ma).

We propose that the spatial-temporal pattern of the late Jurassic Ghorveh-Dehgolan plutons in the north part of the Sanandaj-Sirjan Zone was generated in a continental arc-related extensional environment. Considering the geochemical and isotopic characteristics of the Ghorveh-Dehgolan plutons, the Arabian-Nubian crust with a heterogeneous composition and similar T_{DM} ages could be an important magmatic source.

ACKNOWLEDGMENTS

Antonio García Casco and Mehraj Aghazadeh are thanked for their detailed revisions of our work. We are grateful to Antonio Castro for his editorial handling and constructive comments. The first author acknowledges the members of the University of Granada for their hospitality and preparing the analytical facilities during her stay in Granada, Spain, which was funded by the Iranian Ministry of Science and Technology. S. Yajam is also grateful to H. Fatemi for help with fieldwork and spiritual support. J.F. Molina is warmly thanked for useful advice. All research expenses were covered by the Spanish grant CGL2008-02864. This is the IBERSIMS publication nº 26.

REFERENCES

Agard, P., Omrani, J., Jolivet, L., Whitechurch, H., Vrielynck, B., Spakman, W., Monié, P., Meyer, B. Wortel, R., 2011. Zagros Orogeny: a subduction-dominated process. Geological Magazine, 148, 692-725. DOI: 10.1017/S001675681100046X.

Ahmadi-Khalaji, A., Esmaeily, D., Valizadeh, M.V., Rahimpour-Bonab, H., 2007. Petrology and geochemistry of the granitoid complex of Boroujerd, Sanandaj-Sirjan Zone, Western Iran. Journal of Asian Earth Sciences, 29, 859-877.

Alavi, M., 1994. Tectonics of the Zagros Orogenic belt of Iran. New data and interpretations. Tectonophysics, 229, 211-238.

Alavi, M., 2004. Regional stratigraphy of the Zagros fold-thrust belt of Iran and its proforeland evolution. American Journal of Science, 304, 1-20.

Arvin, M., Pan, Y., Dargahi, S., Malekizadeh, A., Babaei, A., 2007. Petrochemistry of the Siah-Kuh granitoid stock southwest of Kerman, Iran: Implications for initiation of Neotethys subduction. Journal of Asian Earth Sciences, 30, 474-489.

Azizi, H., Asahara, Y., 2013. Juvenile granite in the Sanandaj-Sirjan Zone, NW Iran: Late Jurassic–Early Cretaceous arc–continent collision. International Geology Review, 55, 1523-1540.

Azizi, H., Asahara, Y., Mehrabi, B., Chung, S.L., 2011. Geochronological and geochemical constraints on the petrogenesis of high-K granite from the Suffi abad area, Sanandaj-Sirjan Zone, NW Iran. Chemie der Erde, 71, 363-376.

Bea, F., Montero, P., 2013. Diffusion-induced disturbances of the U-Pb isotope system in pre-magmatic zircon and their influence on SIMS dating. A numerical study. Chemical Geology. 340-350: 1-17

Bea, F., Montero, P,. Gonzalez-Lodeiro, F., Talavera, C., 2007. Zircon Inheritance Reveals Exceptionally Fast Crustal Magma Generation Processes in Central Iberia during the Cambro-Ordovician. Journal of petrology, 48, 2327-2339.

Bea, F., Mazhari, A., Montero, P., Amini, S., Ghalamghash, J., 2011. Zircon dating, Sr and Nd isotopes, and element geochemistry of the Khalifan pluton, NW Iran: Evidence for Variscan magmatism in a supposedly Cimmerian superterrane. Journal of Asian Earth Sciences, 40, 172-179. DOI:10.1016/j.jseaes.2010.08.005.

Bellon, H., Braud, J., 1975. Donnes nouvelles sur le domaine metamorphique du Zagros (zone de Sanandaj-Sirjan) au niveau de Kermanshah-Hamadan (Iran): nature, age et interpretation des series metamorphiques et des intrusions Evolution structurale, Faculte des Sciences, Orsay, Paris, p. 14.

Berberian, F., Berberian, M., 1981. Tectono-plutonic episodes in Iran. In: Delany, F.M, Gupta, H.K., (eds.). Himalaya geodynamic evolution. Zagros, Hindukush. American Geophysical Union Geodynamic Series, 3, 5-33.

Berberian, M., King, G.C.P., 1981. Toward a paleogeography and tectonic evolution of Iran. Canadian Journal of Earth Sciences, 18, 210-265.

Black, L.P., Kamo, S.L., Allen, C.M., Aleinikoff, J.A., Davis, D.W., Korsch, J.R., Foudolis, C., 2003. TEMORA 1: a new zircon standard for Phanerozoic U-Pb geochonology. Chemical Geology, 200, 155-170.

Chena, C., Lina, W., Lua, H., Leea, C., Tiena, J., Laia, Y., 2000. Cretaceous fractionated I-type granitoids and metaluminous A-type granites in SE China: the Late Yanshanian post-orogenic magmatism. Fourth Hutton Symposium: The Origin of Granites and Related Rocks, Clermont-Ferrand, France. Transactions of the Royal Society of Edinburgh: Earth Sciences, 91(1-2), 195-205.

Chiu H.-Y., Chung S.-L., Zarrinkoub, M.H., Mohammadi, S.S., Khatib, M.M., Iizuka, Y., 2013. Zircon U–Pb age constraints from Iran on the magmatic evolution related to Neotethyan subduction and Zagros orogeny. Lithos, 162-163, 70-87.

Claoue-Long, J.C., Compston, W., Roberts, J., Fanning, C.M., 1995. Two Carboniferous ages: a comparison of SHRIMP zircon dating with conventional zircon ages and 40Ar/39Ar analysis. In: Aubry, M.P., Berggren, W.A., Hardenbol, J. , Kent, D.V. (eds.). Geochronology Time Scales and Global Stratigraphic Correlation. SEPM (Society for Sedimentary Geology), Special Publication, 4, 3-21.

Dall'Agnol, R., Frost, C.D., Rämö, O.T., 2012. Editorial, IGCP Project 510 A-type Granites and Related Rocks through Time:

Project vita, results, and contribution to granite research. Lithos, 151, 1-16.

Darabi-Golestan, F., Ghavami-Riabi, R., Khalokakaie, R., Asadi-Haroni, H., Seyedrahimi-Nyaragh, M., 2012. Interpretation of lithogeochemical and geophysical data to identify the buried mineralized area in Cu-Au porphyry of Dalli-Northern Hill. Arabian Journal of Geosciences, 6, 4499-4509.

DePaolo, D.J., 1981. Neodymium isotopes in the Colorado Front Range and implications for crust formation and Mantle evolution in the Proterozoic. Nature, 291, 193-197.

Doglioni, C., Tonarini, S., Innocenti, F., 2009. Mantle wedge asymmetries and geochemical signatures along W- and E-NE-directed subduction zones. Lithos, 113, 179-189. DOI:10.1016/j.lithos.2009.01.012.

Eby, G.N., 1990. The A-type granitoids: a review of their occurrence and chemical characteristics and speculations on their petrogenesis. Lithos, 26, 115-134.

Eby, G.N., 1992. Chemical subdivision of A-type granitoids: petrogenetic and tectonic implications. Geology, 20, 641-644.

Eby, G.N., 2011. A-type granites: magma sources and their contribution to the growth of the continental crust. Seventh Hutton Symposium on granites and related rocks, abstract volume, 50-51.

Eshraghi, S.A., Jafarian, M.B., Eghlimi, B., 1996. 1:100.000 Geological Map of Gorveh. Geological Survey of Iran.

Esna-Ashari, A., Tiepolo, M., Valizadeh, M.V., Hassanzadeh, J., Sepahi, A.A., 2012. Geochemistry and zircon U-Pb geochronology of Aligoodarz granitoid complex, Sanandaj-Sirjan Zone, Iran. Journal of Asian Earth Sciences, 43, 11-22.

Frost, B.R., Barnes, C.G., Collins, W.J., Arculus, R.J., Ellis, D.J., Frost, C.D., 2001. A geochemical classification for granitic rocks. Journal of Petrology, 42, 2033-2048.

Gerya, T., 2011. Transference initiation. Future directions in subduction modeling. Journal of Geodynamics, 52, 344-378.

Ghalamghash, J., 2002. Petrology and emplacement of Urumieh-Oshnavieh plutons. Doctoral Thesis. Shahid Beheshti University, 259pp (in Persian).

Ghalamghash, J., Nédélec, A., Bellon, H., Abedini, M.V., Bouchez, J.L., 2009. The Urumieh plutonic complex (NW Iran): A record of the geodynamic evolution of the Sanandaj-Sirjan Zone during Cretaceous times – Part I: Petrogenesis and K/Ar dating. Journal of Asian Earth Sciences, 35(5), 401-415.

Ghasemi, A., Talbot, C.J., 2006. A new tectonic scenario for the Sanandaj-Sirjan Zone (Iran). Journal of Asian Earth Sciences, 26, 683-693.

Govindaraju, K., Potts, P.J., Webb, P.C., Watson, J.S., 1994. 1994 Report on Whin Sill Dolerite WS-E from England and Pitscurrie micrograbbro PM-S from Scotland: assessment by one hundred and four international laboratories. Geostandards Newsletter, 18, 211-300.

Hargrove, U.S., Stern, R.J., Kimura, J.-I., Manton, W.I., Johnson, P.R., 2006. How juvenile is the Arabian-Nubian Shield? Evidence from Nd isotopes. Earth and Planetary Science Letters. 252, 308-326.

Hassanzadeh, J., Stockli, D.F., Horton, B.K., Axen, G.J., Stockli, L.D., Grove, M., Schmitt, A.K., Walker, J.D., 2008. U-Pb zircon geochronology of Late Neoproterozoic–Early Cambrian granitoids in Iran: Implications for paleogeography, magmatism, and exhumation history of Iranian basement. Tectonophysics, 451, 71-96

Hofmann, A.W., 1988. Chemical differentiation of the Earth: the relationship between mantle, continental crust, and oceanic crust. Earth and Planetary Science Letters, 90, 297-314.

Hosseiny, M., Mosawery, F., Karimynia, M., 1999. 1:100.000 Geological Map of Ghorveh. Geological Survey of Iran.

Irvine, T.N., Baragar, W.R.A., 1971. A guide to the chemical classification of the common volcanic rocks. Canadian Journal of Earth Sciences, 8, 523-548.

Kerr A. C., 1997. Space-time compositional relationships among Appalachian- cycle plutonic suites in Newfoundland. In The Nature of Magmatism in the Appalachian Orogen, In: Hogan, J.P., Sinha, A.K., Whalen, J.B. (eds.). Geological Society of America. Special Paper, 191, 429pp.

Leite, R.J., Heaman, L.M., de Assis Janasi, V., Martins, L., Crease, R.A., 2007. The late to postorogenic transition in the Neoproterozoic Agudos Grandes Granite Batholith (Apiaí Domain, SE Brazil): Constraints from geology, mineralogy, and U-Pb geochronology. Journal of South American Earth Sciences, 23(2), 193-212.

Letterrier, J., 1985. Mineralogical, geochemical and isotopic evolution of two Miocene mafic intrusions from the Zagros (Iran). Lithos, 18, 311-329.

Liégeois, J.P., Stern, R.J., 2010. Sr–Nd isotopes and geochemistry of granite-gneiss complexes from the Meatiq and Hafafit domes, Eastern Desert, Egypt: No evidence for pre-Neoproterozoic crust. Journal of African Earth Sciences, 57, 31-40.

Mahmoudi, S., Corfu, F., Masoudi, F., Mehrabi, B., Mohajjel, M., 2011. U-Pb dating and emplacement history of granitoid plutons in the northern Sanandaj-Sirjan Zone, Iran. Journal of Asian Earth Sciences, 41, 238-249.

Mancuso, I.C., Gates, A.E., Puffer, J.H., 1996. Geochemical and petrological evidence for Avalonian arc to rift transition from granitoids in southeastern Rhode Island. In: Nance, D., Thompson, M.D. (eds.). Avalonian and Related Peri-Gondwanan Terranes of the Circum-North Atlantic. Geological Society of America. Special Paper, 304, 390pp.

Mazhari, S.A., Bea, F., Amini, S., Ghalamghash, J., Molina, J.F., Montero, P., Scarrow, J.H., Williams, I.S., 2009. The Eocene bimodal Piranshahr massif of the Sanandaj-Sirjan Zone, NW Iran: a marker of the end of the collision in the Zagros Orogen. Journal of the Geological Society, 166, 53-69.

McDonough, W.F., Sun, S.-S., 1995. Composition of the Earth. Chemical Geology, 120, 223-253.

Mohajjel, M., Fergusson, C.L., 2014. Jurassic to Cenozoic tectonics of the Zagros Orogen in northwestern Iran. International Geology Review, 56(3), 263-287.

Montero, P., Bea, F., 1998. Accurate determination of $^{87}Rb/^{86}Sr$ and $^{147}Sm/^{144}Nd$ ratios by inductively-coupled-plasma mass spectrometry in isotope geoscience: an alternative to isotope dilution analysis. Analytica Chimica Acta, 358, 227-233.

Moreno, J.A., Molina, J.F., Montero, P., Abu Anbar, M., Scarrow, J.H., Cambeses, A., Bea, F., 2014. Unraveling sources of A-type magmas in juvenile continental crust: Constraints from compositionally diverse Ediacaran post-collisional granitoids in the Katerina Ring Complex, southern Sinai, Egypt. Lithos, 192-195, 56-85.

Richards, J.P., Wilkinson, D., Ullrich, T., 2006. Geology of the Sari Gunay Epithermal Gold Deposit, Northwest Iran. Economic Geology, 101, 1455-1496.

Sartibi, H., Haghfarshi, E., 2005. 1/100.000 Geological Map of Sanandaj. Geological Survey of Iran.

Sengör, A.M.C., 1990. A new model for the late Palaeozoic-Mesozoic tectonic evolution of Iran and implication for Oman. In: Ries, A.C., Robertson, A.H.F., Searle, M.P.,(eds.). The Geology and Tectonics of the Oman Region. London, Geological Society. Special Publication, 49, 797-831.

Shafaii Moghadam, H., Stern, R.J., 2011. Late Cretaceous forearc ophiolites of Iran. The Island Arc, 20, 1-4.

Shafiei, B., Haschke, M., Shahabpour, J., 2009. Recycling of orogenic arc crust triggers porphyry Cu mineralization in Kerman Cenozoic arc rocks, southeastern Iran. Mineralium Deposita, 44, 265-283.

Shand, S.J., 1943. The eruptive rocks: 2nd edition. New York, John Wiley, 444pp.

Sheikhzakariai, J., Ghafari Fakher, M., 2008. Types of Enclaves and Field-Microscopic Evidence of magma mingling in the South Ghorveh's Plutonic Granitoide bodies. Journal of sciences, Islamic, Azad Univesity, 18(69), 49-62.

Stein, M., 2003. Tracing the plume material in the Arabian-Nubian Shield. Precambrian Research. 123, 223-234.

Stern, R.J., 2002. Crustal evolution in the East African Orogen: a neodymium isotopic perspective. Journal of African Earth Sciences, 34, 109-117.

Stern, R.J., 2004. Subduction initiation: spontaneous and induced. Earth and Planetary Science Letters, 226, 275-292.

Stern, R.J., Johnson, P., 2010. Continental lithosphere of the Arabian Plate: A geologic, petrologic, and geophysical synthesis. Earth science reviews, 101, 29-67.

Stöcklin, J., 1974. Possible Ancient Continental Margins in Iran. In: Burk, C.A., Drake, C.L. (eds.). The Geology of Continental Margins. New York, Springer-Verlag, 873-887.

Torkian, A., Khalili, M., Sepahi, A.A., 2008. Petrology and geochemistry of the I-type calc-alkaline Qorveh Granitoid Complex, Sanandaj-Sirjan Zone, western Iran. Neues Jahrbuch für Mineralogie-Abhandlungen, 185, 131-142.

Vernant, P., Nilforoushan, F., Haztfeld, D., Abassi, M., Vigny, C., Masson, F., Nankali, H., Martinod, J., Ashtiany, A., Bayer, R., Tavakoli, F., Chéry, J., 2004. Present-day crustal deformation and plate kinematics in Middle East constrained by GPS measurement in Iran and northern Oman. Geophysical Journal International, 157, 381-398.

Whalen, J.B., Currie, K.L., Chappell, B.W., 1987. A-type granites: geochemical characteristics, discrimination and petrogenesis. Contributions Mineralogy and Petrology, 95, 407-419.

Williams, I. S., Claesson, S., 1987. Isotopic evidence for the Precambrian provenance and Caledonian metamorphism of high grade paragneisses from the Seve Nappes, Scandinavian Caledonides. II: Ion microprobe zircon U-Th-Pb. Contribution to Mineralogy and Petrology, 97, 205-217.

Manuscript received May 2014;
revision accepted October 2014;
published Online February 2015.

ELECTRONIC APPENDIX

TABLE I. Selected microprobe analyses and structural formulae of Ghorveh-Dehgolan pluton minerals. A) Feldspars. B) Pyroxenes (all data of mafic suite)

A) Feldspars																		
Plutone	Ghorveh batholith				Shanevareh		Qalaylan	Kangareh		Galali			Saranjianeh				Bolbanabad-Havarpan	
magmatic suite[a]	M		FCA	FA	M	FCA		M		M	FCA	FA	M		FCA	FA	M	
Rock type[b]	GB	GB	MG	GD	DI	SG	QM	MGB	GB	QM	MG	SG	MDI		QM	SG	MDI	
mineral[C]	Lab	Byt	And	Olg	Lab	Olg	And	And	Lab	Lab	Ab	Ab	Lab	And	Olg	Ab	Lab	And
SiO_2	53,77	48,21	58,27	64,58	53,74	63,42	56,32	56,53	54,44	51,51	66,67	66,87	54,62	60,14	62,26	68,02	54,84	58,29
TiO_2	0,06	b.d.l.	0,04	0,01	0,00	b.d.l.	b.d.l.	0,07	0,05	0,09	b.d.l.	0,01	0,05	0,06	0,11	0,02	0,07	0,08
Al_2O_3	29,73	32,50	25,72	22,81	29,63	23,13	27,42	27,51	29,09	31,05	20,40	20,84	29,10	25,08	22,99	20,10	28,21	26,26
FeO	0,09	0,27	0,49	0,13	0,11	0,02	0,34	0,24	0,12	0,38	0,01	0,03	0,22	0,29	0,20	b.d.l.	0,32	0,29
MnO	0,01	b.d.l.	0,01	b.d.l.	0,02	0,05	0,02	0,00	0,04	0,03	0,01	0,02	0,00	0,03		b.d.l.	b.d.l.	b.d.l.
MgO	0,01	0,01	0,03	0,01	b.d.l.	b.d.l.	0,01	0,01	0,01	0,01	0,01	0,00	b.d.l.	b.d.l.	b.d.l.	0,01	0,01	0,01
CaO	11,63	15,28	7,49	3,58	11,53	3,63	8,74	9,13	10,68	13,35	0,70	1,14	10,57	6,30	4,10	0,25	10,21	7,89
Na_2O	4,84	2,62	6,82	9,26	4,94	9,24	6,21	5,91	5,14	3,63	10,75	10,79	5,40	7,78	8,90	11,14	5,24	6,58
K_2O	0,07	0,10	0,41	0,19	0,07	0,08	0,16	0,21	0,12	0,20	0,11	0,08	0,15	0,24	0,16	0,04	0,33	0,19
BaO	0,06	b.d.l.	b.d.l.	0,07	0,04	0,05	0,07	b.d.l.	0,01	b.d.l.	0,00	b.d.l.	0,08	0,00	b.d.l.	b.d.l.	0,05	b.d.l.
Total	100,32	99,06	99,45	100,77	100,21	99,66	99,71	99,68	99,89	100,66	98,70	99,90	100,41	100,07	98,84	99,57	99,41	99,65
Numbers of ions on the basis of 6O																		
Si	2,42	2,23	2,63	2,83	2,43	2,81	2,55	2,55	2,46	2,34	2,95	2,93	2,46	2,68	2,79	2,98	2,49	2,61
Ti	0,00	0,00	0,00	0,00	0,00	0,00	0,00	0,00	0,00	0,00	0,00	0,00	0,00	0,00	0,00	0,00	0,00	0,00
Al	1,58	1,77	1,37	1,18	1,58	1,21	1,46	1,46	1,55	1,66	1,06	1,08	1,54	1,32	1,21	1,04	1,51	1,39
Fe_t	0,00	0,01	0,02	0,00	0,00	0,00	0,01	0,01	0,00	0,01	0,00	0,00	0,01	0,01	0,01	0,00	0,01	0,01
Mn	0,00	0,00	0,00	0,00	0,00	0,00	0,00	0,00	0,00	0,00	0,00	0,00	0,00	0,00	0,00	0,00	0,00	0,00
Mg	0,00	0,00	0,00	0,00	0,00	0,00	0,00	0,00	0,00	0,00	0,00	0,00	0,00	0,00	0,00	0,00	0,00	0,00
Ca	0,56	0,76	0,36	0,17	0,56	0,17	0,42	0,44	0,52	0,65	0,03	0,05	0,51	0,30	0,20	0,01	0,50	0,38
Na	0,42	0,23	0,60	0,79	0,43	0,79	0,54	0,52	0,45	0,32	0,92	0,92	0,47	0,67	0,77	0,95	0,46	0,57
K	0,00	0,01	0,02	0,01	0,00	0,00	0,01	0,01	0,01	0,01	0,01	0,00	0,01	0,01	0,01	0,00	0,02	0,01
Ba	0,00	0,00	0,00	0,00	0,00	0,00	0,00	0,00	0,00	0,00	0,00	0,00	0,00	0,00	0,00	0,00	0,00	0,00
x_{an}	0,57	0,76	0,37	0,17	0,56	0,18	0,43	0,45	0,53	0,66	0,03	0,05	0,52	0,30	0,20	0,01	0,51	0,39
x_{ab}	0,43	0,24	0,61	0,81	0,43	0,82	0,56	0,53	0,46	0,33	0,96	0,94	0,48	0,68	0,79	0,99	0,47	0,59
x_{or}	0,00	0,01	0,02	0,01	0,00	0,00	0,01	0,01	0,01	0,01	0,01	0,00	0,01	0,01	0,01	0,00	0,02	0,01

B) Pyroxenes (all data of mafic suite)																		
pluton	Ghorveh batholith					Qalaylan		Kangareh			Galali	Saranjianeh					Bolbanabad-Havarpan	
rock type[b]	GB		QMDI		DI	QM		MGB	GB	DI	QM	QM		MDI		MDI	QMDI	
mineral[c]	En	Di	Fs	Aug	Di	Aug (core)	Aug (rim)	Aug	Aug	Aug	Aug	Di	Aug	Aug	Fs	Di	Di (core)	Di (rim)
SiO_2	51,70	51,97	52,12	51,65	53,53	51,95	51,93	49,47	50,53	52,82	50,37	52,51	52,31	51,60	52,75	52,69	52,98	51,38
TiO_2	0,24	0,33	0,05	0,07	0,07	0,20	0,10	0,56	1,17	0,03	1,10	0,21	0,17	0,15	0,08	0,02	0,20	0,36
Al_2O_3	0,60	1,35	0,29	0,29	0,40	1,03	0,62	1,72	3,34	0,14	3,23	0,61	0,45	0,54	0,56	0,21	0,88	1,72
Cr_2O_3	0,05	0,06	b.d.l.	0,06	0,06	b.d.l.	0,04	0,02	0,08	0,02	0,07	0,02	0,09	0,04	0,03	b.d.l.	0,09	0,10
NiO	0,03	0,02	0,04	b.d.l.	0,04	0,05	b.d.l.	b.d.l.	0,02	0,01	0,01	0,01	0,05	0,05	0,03	b.d.l.	b.d.l.	0,05
FeO	28,45	10,32	30,62	16,57	7,40	9,10	9,47	16,54	8,71	8,93	8,49	10,73	10,94	14,52	29,35	9,56	8,07	10,32
MnO	0,83	0,37	1,23	0,42	0,29	1,32	1,88	0,47	0,28	0,27	0,24	0,54	0,40	0,55	0,96	0,21	0,47	0,52
MgO	17,95	13,28	11,88	9,74	14,10	12,61	12,95	9,02	13,71	12,78	15,51	12,96	13,36	11,42	12,55	12,72	13,94	12,68
CaO	0,91	21,89	1,06	21,17	24,42	22,31	21,65	21,58	21,47	24,80	20,03	21,79	21,72	20,50	1,04	24,29	23,26	21,20
Na_2O	0,01	0,29	0,06	0,15	0,29	0,66	0,44	0,29	0,44	0,10	0,32	0,34	0,36	0,31	0,15	0,22	0,20	0,39
K_2O	0,01	0,01	b.d.l.	0,01	b.d.l.	0,01	0,03	b.d.l.	b.d.l.	b.d.l.	0,01	0,01	b.d.l.	b.d.l.	0,01	b.d.l.	b.d.l.	0,08
Total	100,80	99,91	97,38	100,12	100,60	99,22	99,34	99,71	99,74	100,12	99,37	99,99	99,83	99,68	97,59	100,04	100,11	98,93
Numbers of ions on the basis of 4 cations/ 6O																		
Si	1,97	1,95	2,12	1,99	1,98	1,96	1,97	1,92	1,88	1,98	1,87	1,98	1,97	1,97	2,13	1,98	1,97	1,95
^{IV}Al	6,03	6,05	5,88	6,01	6,02	6,04	6,03	6,08	6,12	6,02	6,13	6,02	6,03	6,03	5,87	6,02	6,03	6,05
VIAl	-6,00	-5,99	-5,86	-6,00	-6,01	-6,00	-6,01	-6,01	-5,97	-6,01	-5,99	-6,00	-6,01	-6,00	-5,84	-6,01	-5,99	-5,97
Ti	0,01	0,01	0,00	0,00	0,00	0,01	0,00	0,02	0,03	0,00	0,03	0,01	0,00	0,00	0,00	0,00	0,01	0,01
Fe^{+3}	0,02	0,04	-0,26	0,01	0,04	0,15	0,16	0,08	0,05	0,03	0,07	0,03	0,06	0,04	-0,28	0,05	0,02	0,03
Fe^{+2}	0,89	0,28	1,30	0,52	0,18	0,37	0,38	0,46	0,22	0,25	0,19	0,31	0,28	0,42	1,27	0,25	0,23	0,30
Mn	0,03	0,01	0,04	0,01	0,01	0,04	0,06	0,02	0,01	0,01	0,01	0,02	0,01	0,02	0,03	0,01	0,01	0,02
Mg	1,02	0,74	0,72	0,56	0,78	0,71	0,73	0,52	0,76	0,72	0,86	0,73	0,75	0,65	0,76	0,71	0,77	0,72
Ca	0,04	0,88	0,05	0,87	0,97	0,90	0,88	0,90	0,86	1,00	0,80	0,88	0,87	0,84	0,04	0,98	0,93	0,86
Na	0,00	0,02	0,01	0,01	0,02	0,05	0,03	0,02	0,03	0,01	0,02	0,02	0,03	0,02	0,01	0,02	0,01	0,03
K	0,00	0,00	0,00	0,00	0,00	0,00	0,00	0,00	0,00	0,00	0,00	0,00	0,00	0,00	0,00	0,00	0,00	0,00
Cr	0,00	0,00	0,00	0,00	0,00	0,00	0,00	0,00	0,00	0,00	0,00	0,00	0,00	0,00	0,00	0,00	0,00	0,00
Ni	0,00	0,00	0,00	0,00	0,00	0,00	0,00	0,00	0,00	0,00	0,00	0,00	0,00	0,00	0,00	0,00	0,00	0,00
mg#	0,53	0,73	0,36	0,52	0,81	0,77	0,76	0,53	0,77	0,74	0,82	0,70	0,73	0,61	0,37	0,74	0,77	0,71

TABLE I. (Continued) Selected microprobe analyses and structural formulae of Ghorveh-Dehgolan pluton minerals. C) Amphiboles. D) Biotites

C) Amphiboles																		
pluton	Ghorveh batholith				Shanevareh	Qalaylan			Kangareh			Galali			Saranjianeh		Bolbanabad-Havarpan	
Magmatic suite[a]	M		FCA	FA	M	________			M		FCA	FA	M		FCA	FA	M	
rock type[b]	Gb		Mg	GD	DI	QM		GB		DI	MG	SG	M		QM	SG	QMDI	MDI
mineral[c]	Mg-Hs	Ed	Hs	Ed	Mg-Hbl	Mg-Hbl	Ed	Prg	Mg-Hbl	Mg-Hs	Mg-Hbl	Ed	Mg-Hbl	Ed	Ed	Fe2Ed	Mg-Hbl	Hs
SiO_2	47,87	44,25	39,57	50,26	46,16	49,47	47,87	42,24	52,51	42,68	51,53	48,75	47,61	46,15	46,18	44,69	47,96	41,24
TiO_2	1,04	1,88	0,60	1,09	0,87	0,41	0,98	3,83	0,39	2,77	0,46	1,23	1,54	2,11	1,62	1,23	1,32	0,59
Al_2O_3	5,45	10,48	11,84	4,28	8,20	4,80	6,28	11,95	3,63	10,48	2,52	5,12	6,09	7,15	6,46	5,91	6,08	9,66
Cr_2O_3	0,03	0,13	0,01	b.d.l.	0,08	0,09	0,02	0,11	0,04	0,04	0,07	b.d.l.	0,02	0,01	0,01	0,08	0,10	0,06
NiO	b.d.l.	b.d.l.	b.d.l.	0,03	0,08	0,04	0,01	0,05	b.d.l.	0,06	0,01	b.d.l.	b.d.l.	0,04	b.d.l.	b.d.l.	0,04	b.d.l.
FeO	20,52	14,85	26,24	11,00	16,14	11,00	12,71	12,70	13,56	14,64	13,18	13,03	16,47	16,24	19,01	23,98	15,87	24,42
MnO	0,45	0,21	0,61	0,42	0,51	1,42	1,41	0,17	0,22	0,21	0,23	0,34	0,35	0,26	0,30	0,54	0,40	0,26
MgO	9,77	11,36	4,14	16,82	12,11	16,22	14,63	12,26	15,10	11,70	15,67	14,99	12,37	11,97	11,28	7,60	12,70	6,22
CaO	10,68	11,91	11,16	10,97	12,21	11,59	11,45	11,48	11,49	11,27	11,38	11,32	11,06	11,30	10,69	10,49	11,49	11,41
Na_2O	0,93	1,35	1,37	1,50	1,10	1,18	1,47	2,13	0,43	1,98	0,84	1,48	1,20	1,39	1,63	2,13	0,95	1,53
K_2O	0,51	0,77	1,98	0,48	0,60	0,75	0,72	1,01	0,22	1,06	0,27	0,57	0,57	0,67	0,83	1,03	0,59	1,67
BaO	0,04	0,00	0,00	b.d.l.	0,00	b.d.l.	b.d.l.	b.d.l.	b.d.l.	0,04	b.d.l.	0,10	0,12	b.d.l.	b.d.l.	0,10	b.d.l.	b.d.l.
F	0,04	b.d.l.	0,24	0,95	0,04	1,30	1,21	b.d.l.	b.d.l.	0,38	0,33	0,22	0,06	0,23	0,60	1,14	0,12	0,06
Cl	b.d.l.	b.d.l.	b.d.l.	b.d.l.	b.d.l.	b.d.l.	b.d.l.	b.d.l.	b.d.l.	b.d.l.	b.d.l.	b.d.l.	b.d.l.	b.d.l.	b.d.l.	b.d.l.	b.d.l.	b.d.l.
Total	97,31	97,24	97,77	97,81	98,13	98,27	98,77	98,00	97,59	97,29	96,48	97,15	97,46	97,50	98,62	98,91	97,61	97,10
Numbers of ions on the basis of 23O																		
Si	7,14	6,56	6,23	7,20	6,77	7,14	6,94	6,21	7,49	6,37	7,49	7,10	7,00	6,83	6,82	6,88	7,02	6,46
^{IV}Al	0,86	1,44	1,77	0,80	1,23	0,86	1,06	1,79	0,51	1,63	0,51	0,90	1,00	1,17	1,18	1,12	0,98	1,54
^{VI}Al	0,09	0,39	0,42	-0,08	0,19	-0,05	0,01	0,28	0,10	0,22	-0,08	-0,02	0,05	0,08	-0,05	-0,05	0,07	0,24
Ti	0,12	0,21	0,07	0,12	0,10	0,04	0,11	0,42	0,04	0,31	0,05	0,14	0,17	0,23	0,18	0,14	0,15	0,07
Fe_t	2,56	1,84	3,45	1,32	1,98	1,33	1,54	1,56	1,62	1,83	1,60	1,59	2,02	2,01	2,35	3,09	1,94	3,20
Mn	0,06	0,03	0,08	0,05	0,06	0,17	0,17	0,02	0,03	0,03	0,03	0,04	0,04	0,03	0,04	0,07	0,05	0,03
Mg	2,17	2,51	0,97	3,59	2,65	3,49	3,16	2,69	3,21	2,60	3,39	3,26	2,71	2,64	2,48	1,74	2,77	1,45
Ca	1,71	1,89	1,88	1,68	1,92	1,79	1,78	1,81	1,76	1,80	1,77	1,77	1,74	1,79	1,69	1,73	1,80	1,91
Na	0,27	0,39	0,42	0,42	0,31	0,33	0,41	0,61	0,12	0,57	0,24	0,42	0,34	0,40	0,47	0,64	0,27	0,46
K	0,10	0,15	0,40	0,09	0,11	0,14	0,13	0,19	0,04	0,20	0,05	0,11	0,11	0,13	0,16	0,20	0,11	0,33
F	0,02	0,00	0,12	0,43	0,02	0,59	0,56	0,00	0,00	0,18	0,15	0,10	0,03	0,11	0,28	0,55	0,06	0,03
Cl	0,00	0,00	0,00	0,00	0,00	0,00	0,00	0,00	0,00	0,00	0,00	0,00	0,00	0,00	0,00	0,00	0,00	0,00
Cr	0,00	0,02	0,00	0,00	0,01	0,01	0,00	0,01	0,00	0,00	0,01	0,00	0,00	0,00	0,00	0,01	0,01	0,01
Ni	0,00	0,00	0,00	0,00	0,01	0,00	0,00	0,01	0,00	0,01	0,00	0,00	0,00	0,00	0,00	0,00	0,00	0,00
mg#	0,55	0,62	0,26	0,87	0,65	0,86	0,79	0,67	0,77	0,64	0,78	0,76	0,67	0,64	0,63	0,41	0,68	0,35

D) Biotites																		
pluton	Ghorveh batholith					Shanevareh		Qalaylan	Kangareh	Galali				Saranjianeh			Bolbanabad-Havarpan	
Magmatic suite[a]	M				FA	M	FCA	_____	M	M		FCA		FCA		M	M	
rock type[b]	GB	GB	QMDI	GB	GD	DI	SG	QM	DI	QM		MG		QM		MDI	QMDI	
SiO_2	36,16	36,57	36,02	36,35	34,76	37,11	46,33	37,16	36,48	38,28	38,49	37,13	37,80	36,40	36,66	36,16	36,50	36,56
TiO_2	2,34	4,40	3,61	5,21	2,07	2,47	0,10	3,33	5,70	2,60	3,28	2,60	1,72	4,50	4,30	4,89	4,34	4,71
Al_2O_3	16,45	15,08	15,08	13,96	15,72	16,17	30,30	13,87	14,48	13,45	13,33	13,86	14,92	13,71	13,15	13,40	13,91	14,05
Cr_2O_3	0,04	b.d.l.	0,06	0,09	0,03	b.d.l.	0,02	0,02	0,13	b.d.l.	0,09	0,02	0,02	0,14	0,00	0,06	0,10	0,09
NiO	0,07	0,02	0,01	0,02	0,03	0,02	b.d.l.	b.d.l.	b.d.l.	0,04	b.d.l.	b.d.l.	b.d.l.	b.d.l.	0,04	b.d.l.	0,06	b.d.l.
FeO	16,37	18,42	17,90	17,53	27,66	17,27	4,88	14,93	18,64	19,59	18,23	21,06	22,67	21,81	23,82	19,55	19,37	20,32
MnO	0,19	0,09	0,04	0,17	0,38	0,27	0,07	0,71	0,11	0,18	0,17	0,09	0,09	0,14	0,20	0,10	0,20	0,20
MgO	13,10	11,96	12,18	12,26	5,92	12,34	1,72	15,11	11,19	11,87	12,19	9,25	8,95	9,52	8,68	11,27	11,10	10,89
CaO	0,02	0,02	0,02	0,02	0,01	0,07	b.d.l.	b.d.l.	0,00	0,00	b.d.l.	0,01	b.d.l.	0,02	0,05	0,01	b.d.l.	0,03
Na_2O	0,12	0,17	0,18	0,05	0,05	0,15	0,24	0,09	0,14	0,03	0,06	0,08	0,07	0,09	0,11	0,12	0,09	0,16
K_2O	9,33	9,55	9,33	9,26	8,66	9,42	11,02	10,02	9,67	9,77	9,72	9,55	9,62	9,56	9,27	9,60	9,54	9,37
BaO	0,09	0,33	0,29	0,35	b.d.l.	0,22	0,10	0,18	0,28	0,11	0,08	0,17	0,10	0,09	0,03	0,10	0,11	0,10
F	0,03	b.d.l.	b.d.l.	0,28	b.d.l.	0,27	b.d.l.	2,21	b.d.l.	0,54	0,40	0,61	0,55	0,14	0,20	0,32	0,02	0,21
Cl	b.d.l.	b.d.l.	b.d.l.	b.d.l.	b.d.l.	b.d.l.	b.d.l.	b.d.l.	b.d.l.	b.d.l.	b.d.l.	b.d.l.	b.d.l.	b.d.l.	b.d.l.	b.d.l.	b.d.l.	b.d.l.
Total	94,30	96,59	94,72	95,53	95,28	95,77	94,78	97,62	96,82	96,46	96,03	94,44	96,52	96,11	96,51	95,56	95,35	96,68
Numbers of ions on the basis of 11O																		
Si	2,75	2,75	2,76	2,77	2,76	2,80	3,18	2,80	2,75	2,91	2,91	2,91	2,90	2,80	2,84	2,78	2,80	2,78
^{IV}Al	5,25	5,25	5,24	5,23	5,24	5,20	4,82	5,20	5,25	5,09	5,09	5,09	5,10	5,20	5,16	5,22	5,20	5,22
^{VI}Al	-3,77	-3,91	-3,88	-3,98	-3,76	-3,77	-2,37	-3,97	-3,97	-3,89	-3,90	-3,81	-3,75	-3,95	-3,96	-4,00	-3,94	-3,96
Ti	0,13	0,25	0,21	0,30	0,12	0,14	0,00	0,19	0,32	0,15	0,19	0,15	0,10	0,26	0,25	0,28	0,25	0,27
Fe_t	1,04	1,16	1,15	1,12	1,84	1,09	0,28	0,94	1,17	1,24	1,15	1,38	1,46	1,41	1,54	1,26	1,24	1,29
Mn	0,01	0,01	0,00	0,01	0,03	0,02	0,00	0,04	0,01	0,01	0,01	0,01	0,01	0,01	0,01	0,01	0,01	0,01
Mg	1,49	1,34	1,39	1,39	0,70	1,39	0,18	1,70	1,26	1,34	1,37	1,08	1,02	1,09	1,00	1,29	1,27	1,23
Ca	0,00	0,00	0,00	0,00	0,00	0,01	0,00	0,00	0,00	0,00	0,00	0,00	0,00	0,00	0,00	0,00	0,00	0,00
Na	0,02	0,02	0,03	0,01	0,01	0,02	0,03	0,01	0,02	0,00	0,01	0,01	0,01	0,01	0,02	0,02	0,01	0,02
K	0,91	0,92	0,91	0,90	0,88	0,91	0,96	0,96	0,93	0,95	0,94	0,95	0,94	0,94	0,91	0,94	0,93	0,91
F	0,01	0,00	0,00	0,07	0,00	0,06	0,00	0,53	0,00	0,13	0,10	0,15	0,13	0,03	0,05	0,08	0,00	0,05
Cl	0,00	0,00	0,00	0,00	0,00	0,00	0,00	0,00	0,00	0,00	0,00	0,00	0,00	0,00	0,00	0,00	0,00	0,00
Cr	0,00	0,00	0,00	0,01	0,00	0,00	0,00	0,00	0,01	0,00	0,01	0,00	0,00	0,01	0,00	0,00	0,01	0,01
Ni	0,00	0,00	0,00	0,00	0,00	0,00	0,00	0,00	0,00	0,00	0,00	0,00	0,00	0,00	0,00	0,00	0,00	0,00

[a] M: mafic sute; FCA: felsic calc- alkaline suite; FA: felsic alkaline suite

[b] GB: gabbro; MG: monzogranite; GD: granodiorite; DI: diorite; SG: syenogranite; QM: quartz monzonite; MGB: monzogabbro; MDI: monzodiorite; QMDI: quartz monzodiorite

[c] Mg-Hs: magnesiohastingsite; Hs: hastingsite; Mg-Hbl: magnesiohornblende; Ed: edenite; Fe2-Ed: Ferro-edenite; Prg: pargasite; Byt: bytownite; Lab:labradorite; And:andesine; Olg:oligoclase; Ab: albite; En: enstatite; Di: diopside; Fs: Ferrosilite; Aug: augite; Pgt: pigeonite

TABLE II. U-Pb SHRIMP data of analyzed zircon grains from the Ghorveh-Dehgolan plutons

spot	Concentrations (p.p.m)					common lead uncorrected Isotope ratios						Ages(Ma)								
	U	Th	^{206}Pb	$^{232}Th/^{235}U$	f206%*	$^{207}Pb/^{206}Pb$	±err	$^{206}Pb/^{238}U$	±err	$^{207}Pb/^{235}U$	±err	$^{207}Pb/^{206}Pb$	±err	$^{206}Pb/^{238}U$	±err	$^{207}Pb/^{235}U$	±err	d (%)**	$^{207}corr$	±err
sample BA190 (n=23). Ghorveh batholith. (N35° 05′47.11" E47° 50´18.34")																				
zr 1	952.8	247.9	26.0	0.27	20.2	0.22076	0.00279	0.03151	0.00121	0.95925	0.03895	2986.3	20.2	200.0	7.6	682.9	20.4	70.8	156.8	6.6
zr 2	1859.7	730.0	43.9	0.40	0.1	0.04932	0.00092	0.02726	0.00179	0.18542	0.01267	163.3	43.0	173.4	11.2	172.7	10.9	-0.4	173.4	11.4
zr 3	1079.4	537.6	23.7	0.51	0.1	0.05110	0.00136	0.02540	0.00214	0.17898	0.01585	245.5	60.2	161.7	13.5	167.2	13.8	3.2	161.3	13.8
zr 4	2541.4	779.8	57.0	0.31	4.2	0.08396	0.00038	0.02591	0.00080	0.29995	0.00939	1291.7	8.8	164.9	5.0	266.4	7.4	38.2	157.7	4.9
zr 5	1867.2	532.3	40.0	0.29	0.0	0.04927	0.00020	0.02475	0.00082	0.16811	0.00565	160.7	9.8	157.6	5.2	157.8	4.9	0.2	157.5	5.2
zr 6	1380.7	739.2	27.6	0.55	10.5	0.12205	0.00297	0.02309	0.00100	0.38858	0.01932	1986.3	42.8	147.2	6.3	333.3	14.2	55.8	133.6	6.3
zr 7	754.1	206.4	26.5	0.28	0.1	0.05396	0.00320	0.04058	0.00446	0.30188	0.03770	369.3	128.2	256.4	27.7	267.9	29.9	4.2	255.5	28.7
zr 8	1504.1	563.9	33.6	0.38	0.5	0.05017	0.00069	0.02581	0.00105	0.17857	0.00771	202.9	31.6	164.3	6.6	166.8	6.6	1.4	164.1	6.8
zr 9	845.4	298.2	34.1	0.36	11.5	0.14142	0.00134	0.04654	0.00077	0.90743	0.01753	2244.7	16.2	293.2	4.7	655.7	9.4	55.2	260.2	4.7
zr 10	1472.8	645.8	31.6	0.45	0.1	0.04954	0.00033	0.02478	0.00102	0.16925	0.00710	173.5	15.6	157.8	6.5	158.8	6.2	0.6	157.7	6.6
zr 11	886.5	601.2	19.8	0.70	0.2	0.04943	0.00055	0.02587	0.00079	0.17630	0.00576	168.3	25.6	164.6	4.9	164.9	5.0	0.2	164.5	5.0
zr 12	1942.2	554.9	41.2	0.29	0.0	0.04849	0.00018	0.02450	0.00073	0.16383	0.00495	123.3	8.6	156.1	4.6	154.0	4.3	-1.4	156.2	4.7
zr 13	4455.1	3050.5	131.3	0.70	27.3	0.23548	0.00159	0.03404	0.00097	1.10512	0.03258	3089.7	10.6	215.8	6.1	755.8	15.8	71.4	165.3	5.1
zr 14	2468.5	1574.6	68.4	0.65	19.9	0.20961	0.00342	0.03201	0.00106	0.92517	0.03425	2902.5	26.2	203.1	6.6	665.1	18.2	69.4	162.2	6.2
zr 15	631.7	499.5	14.2	0.81	1.3	0.05652	0.00148	0.02602	0.00145	0.20280	0.01254	473.1	57.0	165.6	9.1	187.5	10.7	11.6	164.1	9.5
zr 16	957.0	315.8	19.7	0.34	0.2	0.05036	0.00107	0.02375	0.00094	0.16492	0.00747	211.7	48.6	151.3	5.9	155.0	6.5	2.4	151.0	6.1
zr 17	2100.8	897.4	47.6	0.44	3.1	0.07090	0.00106	0.02619	0.00087	0.25599	0.00934	954.5	30.2	166.6	5.4	231.4	7.5	28.0	162.0	5.5
zr 18	1059.9	469.2	22.8	0.45	0.6	0.04913	0.00020	0.02489	0.00091	0.16863	0.00624	153.9	9.6	158.5	5.7	158.2	5.4	-0.2	158.5	5.8
zr 19	879.6	580.0	20.3	0.68	5.2	0.10096	0.00262	0.02666	0.00106	0.37112	0.01763	1641.7	47.6	169.6	6.6	320.5	13.2	47.0	158.5	6.7
zr 20	1210.7	392.4	26.6	0.33	-0.2	0.05031	0.00054	0.02540	0.00095	0.17620	0.00686	209.3	24.4	161.7	5.9	164.8	5.9	1.8	161.4	6.0
zr 21	2279.0	1843.6	71.6	0.83	21.1	0.22994	0.00803	0.03629	0.00229	1.15056	0.08309	3051.7	54.8	229.8	14.3	777.5	40.0	70.4	177.8	13.4
zr 22	1026.4	254.5	30.8	0.25	0.1	0.05407	0.00101	0.03468	0.00122	0.25858	0.01037	373.9	41.8	219.8	7.6	233.5	8.4	5.8	218.8	7.9
zr 23	227.5	99.4	12.1	0.45	53.2	0.51787	0.01768	0.06150	0.00230	4.39155	0.22296	4292.9	49.2	384.8	14.0	1710.8	42.9	77.6	158.2	14.2
sample BA19 (n=29). Ghorveh batholith. (N34° 59' 53.83" E47° 49' 27.63")																				
zr 1	309.3	256.8	6.4	0.85	0.8	0.04399	0.00108	0.02373	0.00099	0.14394	0.00696	-98.9	47.0	151.2	6.2	136.5	6.2	-10.8	152.1	6.4
zr 2	147.2	83.8	3.0	0.58	0.6	0.05233	0.00241	0.02328	0.00154	0.16796	0.01354	299.9	101.6	148.3	9.7	157.6	11.8	6.0	147.6	10.1
zr 3	136.6	93.7	2.7	0.70	-0.5	0.04968	0.00088	0.02269	0.00087	0.15539	0.00659	179.9	40.6	144.6	5.5	146.7	5.8	1.4	144.4	5.7
zr 4	272.4	217.8	5.5	0.82	1.5	0.05185	0.00123	0.02327	0.00131	0.16636	0.01020	278.9	53.6	148.3	8.3	156.3	9.0	5.2	147.7	8.5
zr 5	489.4	259.1	9.8	0.54	4.2	0.07605	0.00260	0.02324	0.00096	0.24373	0.01306	1096.5	66.8	148.1	6.0	221.5	10.7	33.2	143.0	6.3
zr 6	2041.1	729.0	44.7	0.37	0.2	0.05030	0.00091	0.02528	0.00109	0.17533	0.00820	208.9	41.2	160.9	6.8	164.0	7.1	1.8	160.6	7.0
zr 7 core	286.0	252.6	5.6	0.91	1.1	0.04906	0.00017	0.02248	0.00082	0.15207	0.00562	150.5	8.2	143.3	5.2	143.7	4.9	0.2	143.2	5.2
zr 7 core	210.6	164.2	4.2	0.80	0.6	0.04791	0.00123	0.02319	0.00087	0.15317	0.00699	94.9	59.8	147.8	5.5	144.7	6.2	-2.2	148.0	5.8
zr 8	223.0	159.1	4.3	0.73	0.6	0.05088	0.00044	0.02249	0.00121	0.15782	0.00861	235.5	19.8	143.4	7.6	148.8	7.6	3.6	143.0	7.7
zr 9 rim	158.0	109.4	3.1	0.71	1.9	0.05188	0.00055	0.02296	0.00085	0.16421	0.00638	280.1	24.0	146.3	5.4	154.4	5.6	5.2	145.7	5.5
zr 9 rim	215.8	173.6	4.4	0.83	0.6	0.05066	0.00081	0.02351	0.00099	0.16422	0.00745	225.5	36.6	149.8	6.3	154.4	6.5	3.0	149.4	6.4
zr 9 rim	133.7	83.8	2.8	0.64	-0.1	0.04828	0.00126	0.02457	0.00136	0.16352	0.01005	112.9	60.6	156.4	8.5	153.8	8.8	-1.6	156.5	8.8
zr 10	369.4	313.5	7.0	0.87	0.8	0.05093	0.00102	0.02192	0.00122	0.15391	0.00910	237.5	45.8	139.8	7.7	145.4	8.1	3.8	139.4	7.9
zr 11	339.0	365.6	6.8	1.11	0.0	0.04959	0.00057	0.02326	0.00092	0.15904	0.00657	176.1	26.6	148.2	5.8	149.9	5.8	1.2	148.0	5.9
zr 12	97.9	65.3	1.9	0.68	0.0	0.05070	0.00335	0.02300	0.00100	0.16078	0.01276	227.3	146.2	146.6	6.4	151.4	11.2	3.2	146.2	7.0
zr 13	160.0	125.6	3.2	0.81	-0.4	0.04779	0.00154	0.02346	0.00096	0.15460	0.00808	88.9	74.6	149.5	6.1	146.0	7.2	-2.4	149.7	6.4
zr 14 core	252.1	215.8	5.0	0.88	0.7	0.05324	0.00049	0.02270	0.00103	0.16663	0.00774	339.1	20.6	144.7	6.5	156.5	6.8	7.6	143.9	6.6
zr 14 core	285.3	230.1	6.1	0.83	6.4	0.07353	0.00321	0.02471	0.00097	0.25054	0.01472	1028.7	85.8	157.4	6.1	227.0	12.0	30.6	152.5	6.5
zr 15	145.0	100.3	2.9	0.71	1.6	0.05160	0.00099	0.02300	0.00104	0.16365	0.00809	267.9	43.2	146.6	6.6	153.9	7.1	4.8	146.1	6.8
zr 16	170.5	102.7	3.5	0.62	0.3	0.04616	0.00080	0.02403	0.00152	0.15290	0.01007	5.7	41.6	153.0	9.6	144.5	8.9	-5.8	153.5	9.8
zr 17	570.0	399.2	9.7	0.72	0.6	0.05142	0.00068	0.01971	0.00133	0.13974	0.00963	259.7	30.0	125.8	8.4	132.8	8.6	5.2	125.3	8.5
zr 18	1598.5	583.2	36.2	0.37	1.0	0.05379	0.00046	0.02618	0.00107	0.19421	0.00816	362.5	19.0	166.6	6.7	180.2	6.9	7.6	165.6	6.8
zr 19	238.6	159.6	4.6	0.69	0.5	0.05160	0.00145	0.02223	0.00086	0.15816	0.00756	267.7	63.2	141.7	5.4	149.1	6.7	5.0	141.2	5.7
zr 20	296.9	198.1	5.7	0.68	1.4	0.05472	0.00153	0.02233	0.00093	0.16849	0.00849	400.7	61.2	142.4	5.9	158.1	7.4	10.0	141.3	6.1
zr 21	1191.8	550.7	23.2	0.47	0.0	0.04955	0.00068	0.02250	0.00087	0.15368	0.00636	173.9	31.8	143.4	5.5	145.2	5.7	1.2	143.2	5.6
zr 22	185.6	149.6	3.7	0.83	1.1	0.04818	0.00061	0.02320	0.00102	0.15409	0.00708	108.1	29.4	147.8	6.4	145.5	6.2	-1.6	147.9	6.5
zr 23	216.2	188.3	5.4	0.89	22.2	0.25609	0.02877	0.02910	0.00251	1.02770	0.14559	3222.9	167.0	184.9	15.7	717.8	75.7	74.2	136.6	17.8
zr 24	226.8	180.9	4.8	0.82	7.9	0.10790	0.00057	0.02432	0.00102	0.36181	0.01537	1764.3	9.6	154.9	6.4	313.6	11.6	50.6	143.4	6.1
zr 25	196.0	141.8	3.9	0.74	2.9	0.05989	0.00168	0.02311	0.00107	0.19079	0.01032	599.5	59.6	147.2	6.7	177.3	8.8	17.0	145.1	6.9
zr 26	161.2	81.4	5.1	0.52	32.9	0.30622	0.02896	0.03632	0.00397	1.53364	0.22172	3501.9	139.0	230.0	24.7	944.0	93.0	75.6	155.7	24.4
zr 27	166.3	129.9	3.4	0.80	0.4	0.05187	0.00130	0.02368	0.00108	0.16935	0.00885	279.9	56.2	150.9	6.9	158.9	7.8	5.0	150.3	7.1
zr 28	218.7	75.0	4.1	0.35	1.4	0.05188	0.00022	0.02186	0.00081	0.15638	0.00587	280.3	9.8	139.4	5.1	147.5	5.1	5.4	138.8	5.1
zr 29 core	231.5	191.4	4.6	0.85	3.7	0.07700	0.00332	0.02303	0.00091	0.24455	0.01431	1121.1	83.8	146.8	5.7	222.1	11.7	34.0	141.6	6.2
zr 29 core	555.3	576.1	11.5	1.06	0.4	0.05377	0.00143	0.02388	0.00079	0.17705	0.00753	361.3	58.8	152.1	4.9	165.5	6.5	8.0	151.2	5.2
sample SH177 (n=12). Shanevareh pluton. (N35° 9' 2.23" E47° 42' 42.56")																				
zr 1	3594.9	4530.2	79.7	1.29	1.9	0.06748	0.00076	0.02561	0.00080	0.23827	0.00798	852.5	23.2	163.0	5.0	217.0	6.6	24.8	159.2	5.0
zr 2	1887.4	1930.8	40.8	1.05	0.2	0.05002	0.00050	0.02500	0.00074	0.17245	0.00539	195.9	23.0	159.2	4.6	161.5	4.6	1.4	159.0	4.7
zr 3	1232.5	1627.9	26.6	1.36	0.2	0.04883	0.00082	0.02489	0.00117	0.16760	0.00839	139.9	38.8	158.5	7.4	157.3	7.3	-0.8	158.5	7.6
zr 4 rim	1427.2	922.3	31.0	0.66	0.2	0.04915	0.00024	0.02506	0.00093	0.16980	0.00637	154.9	11.2	159.5	5.8	159.2	5.5	-0.2	159.5	5.9
zr 4 rim	1302.9	1361.1	27.7	1.07	0.0	0.04928	0.00042	0.02459	0.00087	0.16710	0.00612	161.1	19.8	156.6	5.5	156.9	5.3	0.2	156.5	5.6
zr 5	633.3	480.4	13.1	0.78	0.3	0.04992	0.00167	0.02388	0.00098	0.16439	0.00871	191.3	76.0	152.2	6.2	154.5	7.6	1.4	152.0	6.5
zr 6	2455.7	1255.0	54.4	0.52	0.6	0.05278	0.00048	0.02561	0.00096	0.18634	0.00720	319.3	20.4	163.0	6.0	173.5	6.2	6.0	162.2	6.1
zr 7	1319.1	1440.9	29.2	1.12	0.2	0.04988	0.00013	0.02561	0.00088	0.17613	0.00607	189.7	5.8	163.0	5.5	164.7	5.2	1.0	162.8	5.5
zr 8	1073.6	1636.3	23.5	1.56	0.0	0.05113	0.00079	0.02529	0.00070	0.17829	0.00570	246.9	35.2	161.0	4.4	166.6	4.9	3.4	160.6	4.6
zr 9 rim	6077.3	6628.1	132.6	1.12	0.1	0.04984	0.00003	0.02521	0.00068	0.17325	0.00470	187.3	1.4	160.5	4.2	162.2	4.0	1.0	160.3	4.2
zr 9 core	1795.3	2382.0	39.4	1.36	0.1	0.04985	0.00054	0.02534	0.00097	0.17418	0.00694	188.1	24.8	161.3	6.1	163.0	6.0	1.0	161.1	6.2
zr10	2500.4	3854.1	55.5	1.58	0.0	0.04895	0.00045	0.02563	0.00078	0.17302	0.00551	145.7	21.2	163.2	4.9	162.0	4.7	-0.8	163.2	5.0
zr11	3923.3	3328.7	87.4	0.87	0.0	0.04988	0.00033	0.02574	0.00074	0.17703	0.00525	189.3	15.2	163.8	4.6	165.5	4.5	1.0	163.6	4.6
zr12	927.6	1249.2	20.8	1.38	0.3	0.05041	0.00086	0.02587	0.00110	0.17981	0.00825	214.1	39.0	164.6	6.9	167.9	7.1	2.0	164.3	7.1
sample QA153 (n=9). Qalaylan pluton. (N35° 4' 43.19" E47° 37' 40.91")																				
zr 1	416.3	454.3	9.5	1.12	0.7	0.05313	0.00186	0.02641	0.00129	0.19347	0.01163	334.5	77.6	168.0	8.1	179.6	10.0	6.4	167.2	8.5
zr 2	41.7	41.1	1.3	1.01	0.0	0.05415	0.00152	0.03729	0.00244	0.27843	0.01982	377.3	61.8	236.0	15.1	249.4	15.9	5.4	235.0	15.6
zr 3	264.9	196.2	74.2	0.76	0.1	0.11904	0.00091	0.32345	0.00679	5.30902	0.12015	1941.9	13.6	1806.6	33.2	1870.3	19.5	3.4	1785.0	39.7
zr 4	295.6	204.4	6.3	0.71	0.0	0.05122	0.00060	0.02471	0.00104	0.17450	0.00761	250.7	26.6	157.3	6.5	163.3	6.6	3.6	156.8	6.6
zr 5	131.1	75.7	3.9	0.59	0.0	0.05098	0.00332	0.03406	0.00153	0.23944	0.01896	239.9	143.4	215.9	9.5	218.0	15.7	1.0	215.7	10.4
zr 6	240.3	224.4	5.4	0.96	0.4	0.05260	0.00050	0.02597	0.00118	0.18838	0.00877	311.7	21.6	165.3	7.4	175.2	7.5	5.6	164.6	7.5
zr 7	43.5	41.4	1.5	0.98	5.7	0.06647	0.00046	0.03870	0.00157	0.35470	0.01461	821.3	14.4	244.8	9.8	308.2	11.0	20.6	240.0	9.8
zr 8	202.4	102.3	21.9	0.52	0.3	0.06824	0.00122	0.12498	0.00253	1.17602	0.03201	875.9	36.6	759.2	14.5	789.5	15.1	3.8	755.6	16.0
zr 9	219.9	109.4	7.2	0.51	0.4	0.05231	0.00289	0.03791	0.00096	0.27342	0.01665	299.1	121.2	239.8	5.9	245.4	13.3	2.2	239.3	6.7
sample QA158 (n=50). Qalaylan pluton. (N35° 4' 35.98"E47° 37' 17.78")																				
zr 1	1164.8	2522.6	35.0	2.22	0.4	0.05802	0.00011	0.03475	0.00125	0.27799	0.01006	530.5	4.2	220.2	7.8	249.1	8.1	11.6	218.1	7.8
zr 2	235.8	82.7	17.7	0.36	0.0	0.05960	0.00086	0.08682	0.00158	0.71346	0.01677	589.1	31.0	536.7	9.4	546.8	10.0	1.8	535.7	10.1
zr 3	181.0	62.5	5.2	0.35	-0.2	0.05192	0.00175	0.03341	0.00147	0.23917	0.01328	281.9	75.4	211.9	9.2	217.7	10.9	2.6	211.4	9.6
zr 4	387.0	225.8	11.8	0.60	0.8	0.05223	0.00048	0.03533	0.00117	0.25443	0.00879	295.5	20.8	223.8	7.3	230.2	7.2	2.8	223.3	7.5
zr 5	131.1	34.5	14.1	0.27	0.0	0.06832	0.00087	0.12455	0.00263	1.17326	0.02924	878.3	26.2	756.7	15.1	788.2	13.8	4.0	753.0	16.3
zr 6	82.9	39.2	6.2	0.49	0.0	0.05994	0.00235	0.08698	0.00275	0.71885	0.03630	601.5	82.6	537.7	16.4	550.0	21.7	2.2	536.5	18.2
zr 7	765.5	455.7	110.3	0.61	0.1	0.07103	0.00022	0.16651	0.00144	1.63075	0.01609	958.3	6.4	992.9	8.0	982.1	6.2	-1.0	994.4	8.7
zr 8	115.8	110.5	16.9	0.98	0.0	0.07182	0.00077	0.16869	0.00179	1.67047	0.02591	980.9	21.6	1004.9	9.9	997.4	9.9	-0.8	1005.9	11.3
zr 9	448.5	269.7	14.0	0.62	0.5	0.05273	0.00084	0.03603	0.00150	0.26195	0.01171	317.3	35.8	228.2	9.4	236.2	9.4	3.4	227.6	9.7
zr 10	106.7	102.7	2.8	0.99	0.0	0.04842	0.00570	0.03054	0.00100	0.20389	0.02492	119.9	256.2	193.9	6.2	188.4	21.2	-3.0	194.2	7.6
zr 11	599.2	158.7	35.3	0.27	0.2	0.05735	0.00078	0.06808	0.00191	0.53834	0.01690	505.1	29.6	424.6	11.6	437.3	11.2	3.0	423.5	12.2
zr 12	1773.3	174.2	102.2	0.10	0.0	0.05608	0.00113	0.06659	0.00323	0.51490	0.02711	455.5	44.2	415.6	19.6	421.7	18.3	1.4	415.0	20.3
zr 13	1361.3	304.2	55.7	0.23	0.0	0.05415	0.00093	0.04725	0.00105	0.35278	0.00999	377.3	38.2	297.6	6.5	306.8	7.5	3.0	296.8	6.8
zr 14	334.2	164.3	24.0	0.50	0.0	0.06024	0.00069	0.08293	0.00147	0.68881	0.01475	612.3	24.4	513.6	8.8	532.1	8.9	3.4	511.8	9.3
zr 15	909.5	34.3	68.8	0.04	0.0	0.06724	0.00177	0.08733	0.00485	0.80965	0.04985	845.3	53.8	539.7	28.8	602.3	28.4	10.4	533.6	30.1
zr 16	83.4	52.6	1.6	0.65	0.0	0.04985	0.00338	0.02513	0.00085	0.17273	0.01310	188.1	150.6	160.0	5.4	161.8	11.4	1.2	159.8	6.0
zr 17	478.3	185.7	61.4	0.40	0.0	0.07318	0.00107	0.14833	0.00468	1.49667	0.05233	1018.9	29.4	891.6	26.3	929.0	21.5	4.0	886.6	28.3
zr 18 rim	725.9	12.2	22.0	0.02	-0.1	0.05151	0.00042	0.03505	0.00099	0.24893	0.00737	263.7	18.6	222.1	6.2	225.7	6.0	1.6	221.8	6.4
zr 18 core	147.0	132.2	12.8	0.92	-0.2	0.06288	0.00048	0.10095	0.00153	0.87523	0.01518	704.1	16.2	620.0	9.0	638.4	8.3	2.8	618.1	9.6
zr 19	262.5	111.7	25.5	0.44	0.0	0.06457	0.00148	0.11236	0.00159	1.00034	0.02719	760.3	47.6	686.4	9.2	704.0	13.9	2.4	684.4	10.6
zr 20	316.5	275.8	90.9	0.89	0.0	0.11338	0.00037	0.33191	0.00272	5.18873	0.04944	1854.3	5.8	1847.6	13.1	1850.8	8.2	0.2	1846.5	16.3
zr 21 rim	268.1	132.3	10.1	0.51	0.3	0.05437	0.00094	0.04344	0.00104	0.32565	0.00969	386.5	38.2	274.1	6.4	286.2	7.4	4.2	273.1	6.7
zr 21 core	1116.1	228.8	80.9	0.21	2.2	0.07340	0.00039	0.08372	0.00102	0.84729	0.01167	1025.1	10.6	518.3	6.1	623.2	6.5	16.8	508.0	6.3
zr 21 rim	361.1	56.2	11.7	0.16	-0.5	0.05342	0.00113	0.03746	0.00107	0.27592	0.00986	346.7	47.2	237.1	6.7	247.4	7.9	4.2	236.3	7.0
zr 22	563.3	559.2	66.4	1.02	0.1	0.07154	0.00071	0.13626	0.00266	1.34407	0.02983	972.9	20.2	823.5	15.1	865.0	13.0	4.8	818.3	16.3
zr 23	258.7	139.6	36.7	0.55	0.3	0.06964	0.00096	0.16392	0.00403	1.57397	0.04473	917.7	28.2	978.5	22.3	960.0	17.8	-2.0	981.1	24.5
zr 24	600.9	210.9	259.9	0.36	0.0	0.18368	0.00075	0.49969	0.00498	12.65514	0.14373	2686.3	6.8	2612.5	21.5	2654.3	10.7	1.6	2573.3	34.8
zr 25	174.9	110.8	19.4	0.65	0.2	0.06597	0.00064	0.12788	0.00275	1.16320	0.02776	805.5	20.2	775.8	15.8	783.5	13.2	1.0	774.8	16.8
zr 26	413.0	67.7	112.2	0.17	0.0	0.12272	0.00125	0.31391	0.00696	5.31159	0.13101	1996.1	18.0	1759.9	34.2	1870.7	21.3	6.0	1723.5	40.9
zr 27 rim	199.4	40.5	6.1	0.21	0.0	0.04946	0.00073	0.03554	0.00139	0.24237	0.01017	169.7	34.2	225.1	8.6	220.4	8.4	-2.2	225.4	8.9

**d (%)=100 (1–206/238 age/207/235 age); *f206%=(common 206Pb/total 206Pb)×100. Data are uncorrected for common lead. All errors are at the 95% confidence interval

TABLE II. (continuation)

spot	Concentrations (p.p.m)					Isotope ratios						Ages(Ma)								
	U	Th	^{206}Pb	^{232}Th/ ^{235}U	f206%*	^{207}Pb/ ^{206}Pb	±err	^{206}Pb/ ^{238}U	±err	^{207}Pb/ ^{235}U	±err	^{207}Pb/ ^{206}Pb	±err	^{206}Pb/ ^{238}U	±err	^{207}Pb/ ^{235}U	±err	d (%)**	^{207}corr	±err
zr 27 core	1999.1	44.5	64.6	0.02	0.0	0.05178	0.00057	0.03735	0.00086	0.26666	0.00687	275.7	25.0	236.4	5.4	240.0	5.5	1.6	236.1	5.6
zr 28 rim	111.2	67.9	2.5	0.63	0.5	0.05499	0.00394	0.02518	0.00121	0.19092	0.01649	411.9	152.6	160.3	7.6	177.4	14.1	9.6	159.1	8.3
zr 28 core	551.8	695.7	11.9	1.29	0.0	0.04925	0.00107	0.02494	0.00100	0.16936	0.00775	159.7	50.2	158.8	6.3	158.9	6.8	0.0	158.7	6.5
zr 29	354.4	161.0	31.0	0.47	0.0	0.06021	0.00033	0.10112	0.00155	0.83948	0.01400	611.1	11.8	621.0	9.1	618.9	7.8	-0.4	621.2	9.6
zr 30 rim	971.5	439.9	68.2	0.46	0.1	0.05754	0.00063	0.08110	0.00163	0.64342	0.01491	512.3	23.8	502.7	9.7	504.4	9.2	0.4	502.5	10.3
zr 30 core	932.1	382.7	65.7	0.42	0.1	0.05986	0.00060	0.08141	0.00092	0.67192	0.01043	598.5	21.6	504.5	5.5	521.9	6.4	3.4	502.9	6.0
zr 31 rim	7245.3	262.7	415.7	0.04	2.6	0.07317	0.00022	0.06000	0.00084	0.60532	0.00894	1018.7	6.0	375.6	5.1	480.6	5.7	21.8	366.5	5.1
zr 31 core	173.1	561.7	26.9	3.33	1.4	0.12868	0.00288	0.17966	0.00594	3.18762	0.12779	2080.1	38.8	1065.1	32.5	1454.2	31.5	26.8	992.0	35.5
zr 32	95.6	58.9	2.0	0.63	0.2	0.05282	0.00480	0.02440	0.00137	0.17770	0.01899	321.1	194.2	155.4	8.6	166.1	16.5	6.4	154.6	9.5
zr 33	77.4	56.5	10.9	0.75	0.0	0.07433	0.00148	0.16219	0.00182	1.66224	0.03846	1050.5	39.6	968.9	10.1	994.2	14.7	2.6	965.3	12.3
zr 34	249.8	225.7	5.3	0.93	0.2	0.05228	0.00123	0.02460	0.00090	0.17733	0.00774	297.7	52.8	156.7	5.7	165.8	6.7	5.4	156.0	5.9
zr 35	554.2	316.2	32.9	0.59	0.0	0.05696	0.00057	0.06854	0.00145	0.53829	0.01275	490.1	21.8	427.4	8.8	437.3	8.5	2.2	426.5	9.2
zr 36	68.1	33.0	20.2	0.50	0.0	0.11985	0.00291	0.34316	0.00101	5.67073	0.14019	1953.9	42.8	1901.9	4.9	1926.9	21.5	1.2	1892.6	13.5
zr 37	962.5	200.9	106.8	0.21	0.0	0.06453	0.00168	0.12823	0.00394	1.14092	0.04613	759.1	54.0	777.8	22.6	772.9	22.1	-0.6	778.3	24.9
zr 38	389.1	38.8	32.4	0.10	0.0	0.06223	0.00035	0.09633	0.00189	0.82654	0.01713	682.1	12.0	592.9	11.2	611.7	9.6	3.0	591.0	11.7
zr 39	440.0	381.1	17.6	0.89	-0.2	0.05208	0.00054	0.04610	0.00087	0.33104	0.00723	288.9	23.6	290.5	5.3	290.4	5.6	0.0	290.5	5.6
zr 40	200.6	69.4	12.0	0.36	0.0	0.05612	0.00017	0.06918	0.00115	0.53531	0.00925	457.1	6.8	431.2	6.9	435.3	6.1	1.0	430.8	7.1
zr 41	623.8	322.0	61.6	0.53	0.0	0.06455	0.00086	0.11415	0.00221	1.01596	0.02416	759.7	27.8	696.8	12.8	711.9	12.3	2.2	695.1	13.8
zr 42	1164.3	2533.5	34.1	2.23	0.4	0.05675	0.00035	0.03387	0.00157	0.26508	0.01242	482.1	13.6	214.8	9.8	238.8	10.1	10.0	213.0	9.8
zr 43	620.7	430.7	32.0	0.71	0.0	0.06584	0.00700	0.05958	0.04375	0.54085	0.40129	801.1	208.4	373.1	271.8	439.0	306.4	15.0	367.5	269.5
zr 44	1863.8	180.5	101.4	0.10	0.0	0.05609	0.00008	0.06285	0.00223	0.48604	0.01736	455.7	3.2	392.9	13.5	402.2	11.9	2.4	392.1	13.7
zr 45	275.2	150.9	33.4	0.56	0.2	0.07214	0.00029	0.14022	0.01723	1.39478	0.17151	990.1	8.2	845.9	98.1	886.7	75.4	4.6	840.6	100.6
zr 46	257.9	232.3	5.5	0.92	0.0	0.05195	0.00099	0.02463	0.00109	0.17645	0.00854	283.3	43.0	156.9	6.9	165.0	7.4	5.0	156.3	7.1
zr 47	394.8	39.5	33.2	0.10	0.0	0.06151	0.00025	0.09705	0.00204	0.82306	0.01788	656.9	8.6	597.1	12.0	609.8	10.1	2.0	595.8	12.4
zr 48	456.3	395.8	18.4	0.89	-0.2	0.05384	0.00051	0.04650	0.00121	0.34518	0.00960	364.3	21.0	293.0	7.4	301.1	7.3	2.6	292.3	7.6
zr 49	206.1	71.6	12.9	0.36	0.0	0.05711	0.00033	0.07208	0.00157	0.56758	0.01294	495.7	12.8	448.7	9.4	456.4	8.4	1.6	448.0	9.7
zr 50	631.9	324.5	63.2	0.53	0.0	0.06665	0.00038	0.11556	0.00200	1.06202	0.01972	826.9	11.8	705.0	11.6	734.8	9.7	4.0	701.6	12.1
sample KA113 (n=19). Kangareh pluton. (N35° 8' 7.12" E47° 33' 22.12")																				
zr 1	3406.0	2814.9	66.7	0.85	0.1	0.04884	0.00021	0.02223	0.00108	0.14971	0.00732	140.3	10.0	141.7	6.8	141.7	6.5	0.0	141.7	6.9
zr 2	2998.5	1305.0	58.9	0.45	0.1	0.04913	0.00013	0.02246	0.00110	0.15214	0.00746	154.3	6.0	143.2	7.0	143.8	6.6	0.4	143.1	7.0
zr 3	1140.5	828.1	22.3	0.74	0.2	0.04941	0.00035	0.02257	0.00108	0.15375	0.00744	167.3	16.2	143.9	6.8	145.2	6.6	0.8	143.8	6.9
zr 4	1328.4	758.2	26.2	0.59	0.1	0.04824	0.00048	0.02282	0.00099	0.15176	0.00676	110.9	23.2	145.4	6.2	143.5	6.0	-1.4	145.5	6.3
zr 5	665.0	480.9	12.8	0.74	0.0	0.04957	0.00093	0.02224	0.00113	0.15199	0.00823	175.1	43.4	141.8	7.1	143.7	7.3	1.4	141.6	7.3
zr 6	2115.8	1244.2	41.6	0.60	0.1	0.04904	0.00017	0.02272	0.00107	0.15365	0.00727	149.5	8.0	144.9	6.8	145.1	6.4	0.2	144.8	6.8
zr 7	751.0	373.3	13.8	0.51	0.1	0.04992	0.00021	0.02122	0.00109	0.14608	0.00756	191.3	9.6	135.4	6.9	138.4	6.7	2.2	135.1	6.9
zr 8	2062.3	1463.0	38.7	0.73	0.0	0.04948	0.00031	0.02168	0.00112	0.14788	0.00769	170.7	14.6	138.2	7.0	140.0	6.8	1.2	138.0	7.0
zr 9	757.6	529.5	13.5	0.72	-0.1	0.05000	0.00021	0.02054	0.00120	0.14160	0.00828	195.1	9.6	131.1	7.6	134.5	7.4	2.6	130.8	7.6
zr 10	5631.2	3839.3	111.2	0.70	0.1	0.04963	0.00005	0.02139	0.00119	0.14640	0.00818	177.7	2.2	136.5	7.6	138.7	7.2	1.6	136.3	7.6
zr 11	2136.0	1114.6	39.9	0.54	0.1	0.04975	0.00025	0.02158	0.00122	0.14805	0.00841	183.3	11.4	137.7	7.7	140.2	7.5	1.8	137.5	7.8
zr 12	1167.2	324.8	90.0	0.29	0.0	0.05858	0.00032	0.08907	0.00153	0.71934	0.01325	551.3	12.0	550.0	9.1	550.3	7.9	0.0	549.9	9.5
zr 13	541.3	345.7	10.1	0.66	0.3	0.04832	0.00070	0.02152	0.00098	0.14337	0.00687	115.1	34.0	137.2	6.1	136.0	6.1	-0.8	137.2	6.2
zr 14	583.1	371.1	11.5	0.65	0.4	0.05148	0.00035	0.02271	0.00144	0.16118	0.01032	262.5	15.6	144.7	9.1	151.7	9.0	4.6	144.2	9.2
zr 15	778.8	318.7	15.3	0.42	0.1	0.05011	0.00078	0.02266	0.00104	0.15657	0.00763	199.9	35.6	144.5	6.6	147.7	6.7	2.2	144.2	6.7
zr 16	1166.3	571.9	22.8	0.50	-0.1	0.04887	0.00032	0.02254	0.00106	0.15188	0.00722	141.5	15.4	143.7	6.7	143.6	6.4	0.0	143.7	6.8
zr 17	2391.1	1736.5	47.3	0.74	0.2	0.04951	0.00020	0.02286	0.00113	0.15604	0.00777	171.9	9.6	145.7	7.1	147.2	6.8	1.0	145.5	7.1
zr 18	4050.2	2318.4	82.3	0.59	0.0	0.04897	0.00016	0.02275	0.00114	0.15360	0.00770	146.3	8.0	145.0	7.1	145.1	6.8	0.0	144.9	7.2
zr 19	2074.6	924.0	41.1	0.46	0.0	0.04883	0.00013	0.02287	0.00104	0.15396	0.00706	139.7	6.2	145.8	6.6	145.4	6.2	-0.2	145.8	6.7
sample GA134 (n=13). Galali pluton. (N34° 57' 59.05" E47° 56' 1.89")																				
zr 1	3986.7	1844.5	83.5	0.47	0.1	0.04969	0.00034	0.02421	0.00084	0.16587	0.00590	180.3	16.0	154.2	5.3	155.8	5.1	1.0	154.0	5.3
zr 2	1807.6	1140.0	36.7	0.65	2.7	0.07091	0.00191	0.02347	0.00085	0.22950	0.01043	954.7	54.4	149.6	5.4	209.8	8.7	28.6	145.4	5.6
zr 3	2128.0	1340.5	43.6	0.65	0.6	0.05309	0.00011	0.02367	0.00074	0.17329	0.00545	332.7	4.8	150.8	4.6	162.3	4.8	7.0	150.0	4.6
zr 4	1780.7	1121.8	35.9	0.65	0.0	0.04740	0.00064	0.02326	0.00082	0.15204	0.00576	69.5	31.8	148.2	5.1	143.7	5.1	-3.2	148.4	5.2
zr 5	673.0	416.0	15.0	0.63	11.1	0.13762	0.00072	0.02573	0.00096	0.48829	0.01841	2197.5	9.0	163.8	6.0	403.7	12.6	59.4	145.5	5.5
zr 6	924.8	439.1	17.8	0.49	0.3	0.05010	0.00178	0.02221	0.00246	0.15338	0.01783	199.5	80.6	141.6	15.5	144.9	15.8	2.2	141.3	15.8
zr 7	1451.5	942.1	29.1	0.67	0.1	0.04933	0.00018	0.02313	0.00088	0.15731	0.00601	163.5	8.4	147.4	5.5	148.3	5.2	0.6	147.3	5.6
zr 8	2024.0	1466.1	42.2	0.74	0.1	0.04933	0.00036	0.02409	0.00075	0.16384	0.00528	163.7	16.6	153.4	4.7	154.1	4.7	0.4	153.3	4.8
zr 9	1950.1	1604.2	45.6	0.84	13.5	0.15993	0.00120	0.02702	0.00083	0.59576	0.01901	2454.9	12.6	171.9	5.3	474.5	12.1	63.8	147.9	4.9
zr 10	498.9	281.6	11.2	0.58	5.6	0.09442	0.00023	0.02600	0.00153	0.33856	0.01992	1516.5	4.6	165.5	9.6	296.1	15.2	44.2	156.0	9.1
zr 11	1484.6	817.3	30.1	0.56	0.0	0.04810	0.00067	0.02339	0.00077	0.15517	0.00555	104.5	32.6	149.1	4.8	146.5	4.9	-1.8	149.2	5.0
zr 12 rim	114.8	42.3	5.8	0.38	0.4	0.05502	0.00125	0.05861	0.00165	0.44465	0.01612	413.1	49.8	367.2	10.1	373.5	11.4	1.6	366.6	10.7
zr 12 core	70.2	26.5	3.7	0.39	0.1	0.05491	0.00207	0.06062	0.00138	0.45890	0.02030	408.5	82.2	379.4	8.4	383.5	14.2	1.0	379.0	9.4
zr 13	3384.3	3029.2	86.9	0.92	18.4	0.19972	0.00838	0.02966	0.00135	0.81673	0.05058	2823.9	66.8	188.4	8.4	606.2	28.6	69.0	152.7	8.8
sample SA80 (n=16). Saranjianeh pluton. (N35° 11' 54.73" E47° 21' 41.18")																				
zr 1	142.9	62.4	2.9	0.45	0.6	0.05025	0.00289	0.02340	0.00103	0.16217	0.01177	206.7	128.2	149.1	6.5	152.6	10.3	2.2	148.8	7.0
zr 2	94.5	51.0	1.9	0.55	0.3	0.05156	0.00187	0.02339	0.00105	0.16630	0.00961	266.1	81.0	149.1	6.7	156.2	8.4	4.6	148.6	7.1
zr 3	1010.7	980.8	20.3	1.00	0.2	0.04882	0.00010	0.02324	0.00081	0.15642	0.00552	139.1	4.8	148.1	5.1	147.6	4.9	-0.4	148.1	5.2
zr 4	444.8	347.0	8.9	0.80	0.0	0.05119	0.00093	0.02310	0.00075	0.16302	0.00610	249.3	41.4	147.2	4.7	153.3	5.3	4.0	146.7	4.8
zr 5	121.8	57.9	2.5	0.49	0.1	0.04933	0.00040	0.02346	0.00100	0.15961	0.00695	163.7	19.0	149.5	6.3	150.4	6.1	0.6	149.4	6.4
zr 6	180.6	91.6	3.6	0.52	0.1	0.04888	0.00203	0.02305	0.00114	0.15532	0.01004	142.1	94.8	146.9	7.2	146.6	8.9	-0.2	146.9	7.6
zr 7	170.1	97.2	3.5	0.59	0.1	0.04698	0.00186	0.02367	0.00096	0.15333	0.00871	48.3	91.8	150.8	6.0	144.8	7.7	-4.2	151.1	6.4
zr 8	164.1	91.7	3.3	0.57	0.2	0.05096	0.00066	0.02299	0.00096	0.16156	0.00708	239.1	29.6	146.5	6.0	152.1	6.2	3.6	146.1	6.1
zr 9	294.1	185.0	6.0	0.65	0.4	0.05001	0.00157	0.02341	0.00094	0.16145	0.00824	195.5	71.4	149.2	5.9	152.0	7.3	1.8	149.0	6.2
zr 10	133.3	70.2	2.7	0.54	0.1	0.05093	0.00114	0.02379	0.00092	0.16706	0.00748	237.7	50.8	151.6	5.8	156.9	6.6	3.4	151.2	6.0
zr 11	343.9	206.5	6.7	0.62	0.3	0.05147	0.00086	0.02246	0.00108	0.15939	0.00812	261.9	38.0	143.2	6.8	150.2	7.2	4.6	142.7	7.0
zr 12	135.2	78.0	2.7	0.59	0.3	0.04982	0.00253	0.02305	0.00136	0.15834	0.01233	186.5	114.4	146.9	8.5	149.2	10.8	1.6	146.7	9.1
zr 13	318.3	172.9	6.4	0.56	0.0	0.04824	0.00082	0.02334	0.00091	0.15524	0.00664	111.1	39.8	148.7	5.7	146.5	5.8	-1.6	148.8	5.9
zr 14	157.0	99.8	3.1	0.65	0.2	0.05109	0.00057	0.02316	0.00106	0.16311	0.00774	244.9	25.6	147.6	6.7	153.4	6.8	3.8	147.2	6.8
zr 15	260.3	132.2	5.2	0.52	0.0	0.04931	0.00151	0.02310	0.00070	0.15706	0.00676	162.9	69.8	147.2	4.4	148.1	5.9	0.6	147.1	4.7
zr 16	2250.9	1453.3	45.7	0.66	0.2	0.04900	0.00042	0.02348	0.00078	0.15862	0.00550	147.7	19.8	149.6	4.9	149.5	4.8	0.0	149.6	5.0
sample BH88 (n=21). Bolbanabad-Havarpan pluton. (N35° 6' 28.26" E47° 18' 48.13")																				
zr 1	318.2	191.3	6.4	0.62	0.7	0.05058	0.00087	0.02327	0.00112	0.16225	0.00834	221.7	39.0	148.3	7.1	152.7	7.3	2.8	148.0	7.3
zr 2	345.5	195.0	6.8	0.58	0.5	0.05172	0.00096	0.02286	0.00121	0.16302	0.00919	273.3	41.8	145.7	7.7	153.3	8.0	5.0	145.1	7.8
zr 3	468.5	239.6	9.2	0.52	0.3	0.05159	0.00132	0.02272	0.00086	0.16161	0.00739	267.3	57.6	144.8	5.4	152.1	6.5	4.8	144.3	5.7
zr 4	321.4	173.7	6.2	0.55	1.0	0.05299	0.00016	0.02240	0.00084	0.16364	0.00619	328.5	7.0	142.8	5.3	153.9	5.4	7.2	142.0	5.3
zr 5	546.0	354.1	10.7	0.67	0.7	0.04899	0.00065	0.02254	0.00084	0.15223	0.00606	147.1	31.0	143.7	5.3	143.9	5.4	0.2	143.6	5.4
zr 6	315.9	158.0	6.2	0.51	0.0	0.05249	0.00146	0.02266	0.00101	0.16401	0.00865	306.9	62.0	144.5	6.4	154.2	7.6	6.2	143.8	6.6
zr 7	374.2	164.6	7.4	0.45	0.2	0.05034	0.00096	0.02283	0.00105	0.15843	0.00791	210.5	43.8	145.5	6.6	149.3	6.9	2.6	145.2	6.8
zr 8	1388.9	1094.7	26.8	0.81	0.0	0.04830	0.00032	0.02230	0.00075	0.14849	0.00510	113.9	15.6	142.2	4.8	140.6	4.5	-1.2	142.3	4.9
zr 9	310.4	202.9	6.2	0.67	0.2	0.05056	0.00108	0.02297	0.00073	0.16012	0.00615	220.7	48.4	146.4	4.6	150.8	5.4	3.0	146.1	4.8
zr 10	299.8	158.2	5.9	0.54	0.2	0.05111	0.00111	0.02270	0.00094	0.15998	0.00750	245.7	49.0	144.7	5.9	150.7	6.6	4.0	144.3	6.1
zr 11	332.6	174.9	6.4	0.54	0.3	0.05130	0.00071	0.02207	0.00093	0.15610	0.00694	254.5	31.4	140.7	5.9	147.3	6.1	4.4	140.2	6.0
zr 12	420.1	221.5	8.5	0.54	0.0	0.05100	0.00182	0.02326	0.00083	0.16355	0.00830	240.9	80.4	148.2	5.2	153.8	7.3	3.6	147.8	5.7
zr 13	645.8	445.1	12.7	0.71	0.4	0.04968	0.00166	0.02271	0.00084	0.15559	0.00778	179.9	76.2	144.8	5.3	146.8	6.8	1.4	144.6	5.6
zr 14	752.7	495.5	14.7	0.68	0.3	0.05085	0.00045	0.02251	0.00104	0.15784	0.00745	234.1	20.2	143.5	6.6	148.8	6.5	3.6	143.1	6.7
zr 15	428.6	209.9	8.3	0.50	0.1	0.05298	0.00122	0.02236	0.00125	0.16336	0.00991	327.9	51.2	142.6	7.9	153.6	8.6	7.2	141.8	8.1
zr 16	630.8	401.9	12.5	0.65	0.4	0.05054	0.00142	0.02286	0.00112	0.15928	0.00901	220.1	63.6	145.7	7.1	150.1	8.0	3.0	145.4	7.4
zr 17	531.5	368.7	10.5	0.71	0.0	0.04999	0.00050	0.02287	0.00080	0.15763	0.00578	194.5	23.2	145.8	5.1	148.6	5.0	1.8	145.6	5.2
zr 18	801.0	498.7	15.7	0.64	0.6	0.05088	0.00037	0.02269	0.00070	0.15916	0.00505	235.5	16.8	144.6	4.4	150.0	4.5	3.6	144.2	4.5
zr 19	734.6	508.9	14.5	0.71	0.1	0.04835	0.00106	0.02277	0.00102	0.15177	0.00756	116.3	50.8	145.1	6.4	143.5	6.7	-1.2	145.2	6.7
zr 20	337.7	193.1	6.7	0.59	0.1	0.05236	0.00086	0.02303	0.00086	0.16626	0.00680	301.3	37.0	146.8	5.5	156.2	6.0	6.0	146.1	5.6
zr 21	272.2	157.7	5.3	0.59	0.0	0.05221	0.00051	0.02229	0.00102	0.16047	0.00750	294.7	22.0	142.1	6.4	151.1	6.6	6.0	141.5	6.5

**d (%)=100 (1–206/238 age/207/235 age); *f206%=(common 206Pb/total 206Pb)×100. Data are uncorrected for common lead. All errors are at the 95% confidence interval

TABLE II. (continuation)

spot	Concentrations (p.p.m)					common lead corrected Isotope ratios						Ages(Ma)						
	U	Th	^{206}Pb	^{232}Th/ ^{235}U	f206%*	^{207}Pb/^{206}Pb	±err	^{206}Pb/^{238}U	±err	^{207}Pb/^{235}U	±err	^{207}Pb/^{206}Pb	±err	^{206}Pb/^{238}U	±err	^{207}Pb/^{235}U	±err	d (%)**
sample BA190 (n=23). Ghorveh batholith. (N35° 05´47.11" E47° 50´18.34")																		
zr 1	952.8	247.9	26.0	0.27	20.2	0.05864	0.00595	0.02501	0.00097	0.20219	0.02198	553.7	207.4	159.2	6.1	187.0	18.8	14.8
zr 2	1859.7	730.0	43.9	0.40	0.1	0.04860	0.00096	0.02724	0.00179	0.18255	0.01253	128.7	45.8	173.3	11.3	170.3	10.9	-1.8
zr 3	1079.4	537.6	23.7	0.51	0.1	0.05011	0.00164	0.02537	0.00214	0.17527	0.01587	199.9	74.2	161.5	13.5	164.0	13.8	1.6
zr 4	2541.4	779.8	57.0	0.31	4.2	0.05009	0.00266	0.02480	0.00077	0.17131	0.01055	199.3	119.0	157.9	4.8	160.6	9.2	1.6
zr 5	1867.2	532.3	40.0	0.29	0.0	0.04935	0.00103	0.02475	0.00082	0.16839	0.00662	164.3	48.0	157.6	5.2	158.0	5.7	0.2
zr 6	1380.7	739.2	27.6	0.55	10.5	0.03535	0.01045	0.02061	0.00092	0.10045	0.03004	0.0	12.9	131.5	5.8	97.2	28.1	-35.2
zr 7	754.1	206.4	26.5	0.28	0.1	0.05313	0.00352	0.04053	0.00446	0.29695	0.03812	334.5	143.4	256.1	27.6	264.0	30.3	3.0
zr 8	1504.1	563.9	33.6	0.38	0.5	0.04591	0.00140	0.02568	0.00105	0.16253	0.00830	0.0	65.1	163.4	6.6	152.9	7.3	-6.8
zr 9	845.4	298.2	34.1	0.36	11.5	0.04744	0.00829	0.04110	0.00078	0.26883	0.04725	71.7	370.0	259.6	4.8	241.8	38.6	-7.4
zr 10	1472.8	645.8	31.6	0.45	0.1	0.04898	0.00116	0.02476	0.00102	0.16720	0.00799	146.7	54.8	157.7	6.5	157.0	7.0	-0.4
zr 11	886.5	601.2	19.8	0.70	0.2	0.04740	0.00134	0.02580	0.00079	0.16863	0.00705	69.5	66.0	164.2	4.9	158.2	6.1	-3.8
zr 12	1942.2	554.9	41.2	0.29	0.0	0.04871	0.00111	0.02451	0.00073	0.16461	0.00620	133.9	52.4	156.1	4.6	154.7	5.4	-1.0
zr 13	4455.1	3050.5	131.3	0.70	27.3	0.00051	0.03721	0.02455	0.00129	0.00172	0.12597	0.0	98.9	156.4	8.1	1.7	136.4	-9100.0
zr 14	2468.5	1574.6	68.4	0.65	19.9	0.04736	0.00575	0.02549	0.00085	0.16646	0.02098	67.3	266.4	162.3	5.4	156.3	18.4	-3.8
zr 15	631.7	499.5	14.2	0.81	1.3	0.04616	0.00308	0.02568	0.00144	0.16344	0.01425	5.7	153.4	163.5	9.1	153.7	12.5	-6.4
zr 16	957.0	315.8	19.7	0.34	0.2	0.04865	0.00187	0.02370	0.00094	0.15897	0.00882	130.9	88.0	151.0	5.9	149.8	7.8	-0.8
zr 17	2100.8	897.4	47.6	0.44	3.1	0.04520	0.00112	0.02535	0.00084	0.15797	0.00655	0.0	14.5	161.4	5.3	148.9	5.7	-8.4
zr 18	1059.9	469.2	22.8	0.45	0.6	0.04394	0.00050	0.02473	0.00091	0.14983	0.00577	0.0	86.7	157.5	5.7	141.8	5.1	-11.0
zr 19	879.6	580.0	20.3	0.68	5.2	0.05948	0.00855	0.02525	0.00103	0.20710	0.03096	584.9	284.8	160.8	6.5	191.1	26.4	15.8
zr 20	1210.7	392.4	26.6	0.33	-0.2	0.05169	0.00070	0.02545	0.00095	0.18134	0.00721	271.5	30.6	162.0	6.0	169.2	6.2	4.2
zr 21	2279.0	1843.6	71.6	0.83	21.1	0.06172	0.01355	0.02850	0.00182	0.24252	0.05548	664.3	411.4	181.2	11.5	220.5	46.4	17.8
zr 22	1026.4	254.5	30.8	0.25	0.1	0.05305	0.00117	0.03464	0.00122	0.25336	0.01058	330.9	49.4	219.5	7.6	229.3	8.6	4.2
zr 23	227.5	99.4	12.1	0.45	53.2	0.13014	0.04637	0.02815	0.00135	0.50520	0.18165	2099.9	520.4	179.0	8.5	415.2	130.6	56.8
sample BA19 (n=29). Ghorveh batholith. (N34° 59' 53.83" E47° 49' 27.63")																		
zr 1	309.3	256.8	6.4	0.85	0.8	0.03748	0.00162	0.02354	0.00098	0.12163	0.00732	0.0	98.9	150.0	6.2	116.5	6.6	-28.8
zr 2	147.2	83.8	3.0	0.58	0.6	0.04754	0.00638	0.02314	0.00154	0.15166	0.02271	76.5	291.2	147.5	9.7	143.4	20.2	-2.8
zr 3	136.6	93.7	2.7	0.70	-0.5	0.05409	0.01246	0.02281	0.00094	0.17013	0.03983	374.7	449.0	145.4	5.9	159.5	35.1	8.8
zr 4	272.4	217.8	5.5	0.82	1.5	0.03969	0.00234	0.02292	0.00129	0.12542	0.01025	0.0	98.9	146.1	8.2	120.0	9.3	-21.8
zr 5	489.4	259.1	9.8	0.54	4.2	0.04152	0.00492	0.02224	0.00092	0.12733	0.01599	0.0	20.5	141.8	5.8	121.7	14.5	-16.6
zr 6	2041.1	729.0	44.7	0.37	0.2	0.04902	0.00101	0.02524	0.00109	0.17058	0.00815	148.7	47.4	160.7	6.8	159.9	7.1	-0.6
zr 7 core	286.0	252.6	5.6	0.91	1.1	0.04032	0.00432	0.02224	0.00082	0.12364	0.01401	0.0	75.3	141.8	5.2	118.4	12.8	-19.8
zr 7 core	210.6	164.2	4.2	0.80	0.6	0.04339	0.00328	0.02306	0.00087	0.13795	0.01167	0.0	32.7	146.9	5.4	131.2	10.4	-12.0
zr 8	223.0	159.1	4.3	0.73	0.6	0.04594	0.00562	0.02236	0.00121	0.14160	0.01895	0.0	265.7	142.5	7.6	134.5	17.0	-6.0
zr 9 rim	158.0	109.4	3.1	0.71	1.9	0.03620	0.00282	0.02251	0.00084	0.11235	0.00972	0.0	98.9	143.5	5.3	108.1	8.9	-32.8
zr 9 rim	215.8	173.6	4.4	0.83	0.6	0.04615	0.00443	0.02338	0.00100	0.14876	0.01562	5.7	216.0	149.0	6.3	140.8	13.9	-5.8
zr 9 rim	133.7	83.8	2.8	0.64	-0.1	0.04928	0.00593	0.02460	0.00137	0.16714	0.02218	161.3	259.6	156.6	8.6	156.9	19.4	0.2
zr 10	369.4	313.5	7.0	0.87	0.8	0.04472	0.00289	0.02175	0.00121	0.13409	0.01143	0.0	79.7	138.7	7.6	127.8	10.3	-8.6
zr 11	339.0	365.6	6.8	1.11	0.0	0.04988	0.00342	0.02327	0.00092	0.16001	0.01269	189.5	152.0	148.3	5.9	150.7	11.2	1.6
zr 12	97.9	65.3	1.9	0.68	0.0	0.05070	0.00335	0.02300	0.00100	0.16078	0.01276	227.3	146.2	146.6	6.4	151.4	11.2	3.2
zr 13	160.0	125.6	3.2	0.81	-0.4	0.05102	0.00906	0.02356	0.00100	0.16572	0.03027	241.7	364.8	150.1	6.3	155.7	26.7	3.6
zr 14 core	252.1	215.8	5.0	0.88	0.7	0.04752	0.00645	0.02253	0.00104	0.14764	0.02117	75.3	294.4	143.7	6.6	139.8	18.9	-2.8
zr 14 core	285.3	230.1	6.1	0.83	6.4	0.02001	0.00346	0.02310	0.00091	0.06373	0.01131	0.0	98.9	147.2	5.7	62.7	10.8	-134.8
zr 15	145.0	100.3	2.9	0.71	1.6	0.03863	0.00806	0.02263	0.00105	0.12054	0.02577	0.0	33.7	144.3	6.7	115.6	23.7	-24.8
zr 16	170.5	102.7	3.5	0.62	0.3	0.04364	0.00372	0.02395	0.00152	0.14411	0.01533	0.0	67.3	152.6	9.6	136.7	13.7	-11.6
zr 17	570.0	399.2	9.7	0.72	0.6	0.04647	0.00220	0.01959	0.00132	0.12551	0.01036	22.3	109.8	125.0	8.3	120.1	9.4	-4.0
zr 18	1598.5	583.2	36.2	0.37	1.0	0.04604	0.00104	0.02593	0.00106	0.16461	0.00773	0.0	53.5	165.0	6.7	154.7	6.7	-6.6
zr 19	238.6	159.6	4.6	0.69	0.5	0.04719	0.00303	0.02211	0.00085	0.14385	0.01080	58.9	146.6	141.0	5.4	136.5	9.7	-3.2
zr 20	296.9	198.1	5.7	0.68	1.4	0.04296	0.00547	0.02200	0.00093	0.13034	0.01750	0.0	120.5	140.3	5.9	124.4	15.8	-12.8
zr 21	1191.8	550.7	23.2	0.47	0.0	0.04994	0.00070	0.02251	0.00087	0.15497	0.00642	192.1	32.4	143.5	5.5	146.3	5.7	2.0
zr 22	185.6	149.6	3.7	0.83	1.1	0.03882	0.00523	0.02293	0.00102	0.12272	0.01741	0.0	98.9	146.1	6.4	117.5	15.8	-24.4
zr 23	216.2	188.3	5.4	0.89	22.2	0.08325	0.04548	0.02248	0.00206	0.25803	0.14295	1275.1	805.6	143.3	13.0	233.1	122.5	38.6
zr 24	226.8	180.9	4.8	0.82	7.9	0.04352	0.00437	0.02236	0.00095	0.13419	0.01464	0.0	94.3	142.6	6.0	127.9	13.2	-11.4
zr 25	196.0	141.8	3.9	0.74	2.9	0.03625	0.00371	0.02243	0.00104	0.11211	0.01259	0.0	98.9	143.0	6.6	107.9	11.6	-32.6
zr 26	161.2	81.4	5.1	0.52	32.9	0.03338	0.07221	0.02409	0.00310	0.11087	0.24024	0.0	1724.5	153.4	19.5	106.8	247.5	-43.6
zr 27	166.3	129.9	3.4	0.80	0.4	0.04885	0.00748	0.02359	0.00110	0.15888	0.02543	140.9	324.6	150.3	6.9	149.7	22.5	-0.4
zr 28	218.7	75.0	4.1	0.35	1.4	0.04074	0.00653	0.02156	0.00082	0.12108	0.01995	0.0	62.7	137.5	5.2	116.0	18.2	-18.6
zr 29 core	231.5	191.4	4.6	0.85	3.7	0.04728	0.00445	0.02217	0.00088	0.14456	0.01476	63.5	210.0	141.4	5.5	137.1	13.2	-3.2
zr 29 core	555.3	576.1	11.5	1.06	0.4	0.05071	0.00182	0.02379	0.00079	0.16635	0.00813	227.7	80.8	151.6	5.0	156.2	7.1	3.0
sample SH177 (n=12). Shanevareh pluton. (N35° 9' 2.23" E47° 42' 42.56")																		
zr 1	3594.9	4530.2	79.7	1.29	1.9	0.05204	0.00158	0.02511	0.00079	0.18018	0.00789	287.1	68.0	159.9	5.0	168.2	6.8	5.0
zr 2	1887.4	1930.8	40.8	1.05	0.2	0.04826	0.00092	0.02495	0.00073	0.16600	0.00585	111.9	44.4	158.9	4.7	155.9	5.1	-2.0
zr 3	1232.5	1627.9	26.6	1.36	0.2	0.04688	0.00084	0.02483	0.00117	0.16050	0.00810	43.1	42.4	158.1	7.3	151.1	7.1	-4.6
zr 4 rim	1427.2	922.3	31.0	0.66	0.2	0.04733	0.00024	0.02500	0.00093	0.16316	0.00613	66.1	12.0	159.2	5.8	153.5	5.4	-3.8
zr 4 rim	1302.9	1361.1	27.7	1.07	0.0	0.04928	0.00042	0.02459	0.00087	0.16711	0.00612	161.1	19.8	156.6	5.5	156.9	5.3	0.2
zr 5	633.3	480.4	13.1	0.78	0.3	0.04768	0.00168	0.02382	0.00097	0.15658	0.00847	83.5	81.4	151.7	6.1	147.7	7.5	-2.8
zr 6	2455.7	1255.0	54.4	0.52	0.6	0.04777	0.00158	0.02544	0.00095	0.16761	0.00841	88.1	76.8	162.0	6.0	157.3	7.3	-3.0
zr 7	1319.1	1440.9	29.2	1.12	0.2	0.04810	0.00126	0.02555	0.00087	0.16946	0.00733	104.3	61.0	162.6	5.5	159.0	6.4	-2.2
zr 8	1073.6	1636.3	23.5	1.56	0.0	0.05075	0.00087	0.02528	0.00070	0.17685	0.00580	229.3	39.0	160.9	4.4	165.3	5.0	2.6
zr 9 rim	6077.3	6628.1	132.6	1.12	0.1	0.04907	0.00005	0.02519	0.00068	0.17043	0.00462	151.3	2.4	160.4	4.3	159.8	4.0	-0.4
zr 9 core	1795.3	2382.0	39.4	1.36	0.1	0.04934	0.00065	0.02532	0.00097	0.17230	0.00699	164.3	30.4	161.2	6.1	161.4	6.1	0.2
zr10	2500.4	3854.1	55.5	1.58	0.0	0.04872	0.00106	0.02563	0.00078	0.17215	0.00646	134.5	50.6	163.1	4.9	161.3	5.6	-1.2
zr11	3923.3	3328.7	87.4	0.87	0.0	0.04968	0.00047	0.02573	0.00074	0.17628	0.00537	180.1	22.0	163.8	4.6	164.9	4.7	0.6
zr12	927.6	1249.2	20.8	1.38	0.3	0.04777	0.00125	0.02578	0.00110	0.16982	0.00850	87.9	61.0	164.1	6.9	159.3	7.4	-3.0
sample QA153 (n=9). Qalaylan pluton. (N35° 4' 43.19" E47° 37' 40.91")																		
zr 1	416.3	454.3	9.5	1.12	0.7	0.04752	0.00508	0.02622	0.00129	0.17182	0.02021	75.5	236.2	166.9	8.1	161.0	17.7	-3.6
zr 2	41.7	41.1	1.3	1.01	0.0	0.05415	0.00152	0.03729	0.00244	0.27843	0.01982	377.3	61.8	236.0	15.1	249.4	15.9	5.4
zr 3	264.9	196.2	74.2	0.76	0.1	0.11827	0.00099	0.32317	0.00679	5.27000	0.12061	1930.3	14.8	1805.2	33.2	1864.0	19.7	3.2
zr 4	295.6	204.4	6.3	0.71	0.0	0.05122	0.00060	0.02471	0.00104	0.17450	0.00761	250.7	26.6	157.3	6.5	163.3	6.6	3.6
zr 5	131.1	75.7	3.9	0.59	0.0	0.05098	0.00332	0.03406	0.00153	0.23944	0.01896	239.9	143.4	215.9	9.5	218.0	15.7	1.0
zr 6	240.3	224.4	5.4	0.96	0.4	0.04952	0.00517	0.02587	0.00119	0.17663	0.02015	172.3	227.0	164.7	7.5	165.2	17.6	0.4
zr 7	43.5	41.4	1.5	0.98	5.7	0.01842	0.00059	0.03646	0.00148	0.09260	0.00479	0.0	98.9	230.9	9.2	89.9	4.4	-156.8
zr 8	202.4	102.3	21.9	0.52	0.3	0.06599	0.00137	0.12464	0.00252	1.13405	0.03310	806.1	42.6	757.2	14.4	769.7	15.9	1.6
zr 9	219.9	109.4	7.2	0.51	0.4	0.04869	0.00415	0.03774	0.00097	0.25336	0.02256	133.1	189.0	238.8	6.0	229.3	18.4	-4.2
sample QA158 (n=50). Qalaylan pluton. (N35° 4' 35.98"E47° 37' 17.78")																		
zr 1	1164.8	2522.6	35.0	2.22	0.4	0.05495	0.00126	0.03462	0.00125	0.26225	0.01125	410.1	50.6	219.4	7.8	236.5	9.1	7.2
zr 2	235.8	82.7	17.7	0.36	0.0	0.05960	0.00086	0.08682	0.00158	0.71346	0.01677	589.1	31.0	536.7	9.4	546.8	10.0	1.8
zr 3	181.0	62.5	5.2	0.35	-0.2	0.05324	0.00215	0.03347	0.00147	0.24566	0.01470	339.1	89.0	212.2	9.2	223.0	12.0	4.8
zr 4	387.0	225.8	11.8	0.60	0.8	0.04556	0.00257	0.03504	0.00116	0.22012	0.01445	0.0	106.1	222.0	7.3	202.0	12.1	-10.0
zr 5	131.1	34.5	14.1	0.27	0.0	0.06832	0.00087	0.12455	0.00263	1.17326	0.02924	878.3	26.2	756.7	15.1	788.2	13.8	4.0
zr 6	82.9	39.2	6.2	0.49	0.0	0.05994	0.00235	0.08698	0.00275	0.71885	0.03630	601.5	82.6	537.7	16.4	550.0	21.7	2.2
zr 7	765.5	455.7	110.3	0.61	0.1	0.07060	0.00038	0.16642	0.00144	1.62004	0.01754	945.9	11.0	992.4	8.0	978.0	6.8	-1.4
zr 8	115.8	110.5	16.9	0.98	0.0	0.07182	0.00077	0.16869	0.00179	1.67047	0.02591	980.9	21.6	1004.9	9.9	997.4	9.9	-0.8
zr 9	448.5	269.7	14.0	0.62	0.5	0.04845	0.00251	0.03584	0.00150	0.23941	0.01595	121.3	117.8	227.0	9.3	217.9	13.1	-4.2
zr 10	106.7	102.7	2.8	0.99	0.0	0.04827	0.00571	0.03053	0.00100	0.20323	0.02495	112.7	257.6	193.9	6.3	187.9	21.3	-3.2
zr 11	599.2	158.7	35.3	0.27	0.2	0.05545	0.00148	0.06792	0.00191	0.51927	0.02021	430.3	58.4	423.6	11.5	424.7	13.6	0.2
zr 12	1773.3	174.2	102.2	0.10	0.0	0.05608	0.00117	0.06659	0.00323	0.51490	0.02726	455.5	45.8	415.6	19.6	421.7	18.4	1.4
zr 13	1361.3	304.2	55.7	0.23	0.0	0.05415	0.00093	0.04725	0.00105	0.35278	0.00999	377.3	38.2	297.6	6.5	306.8	7.5	3.0
zr 14	334.2	164.3	24.0	0.50	0.0	0.06024	0.00069	0.08293	0.00147	0.68881	0.01475	612.3	24.4	513.6	8.8	532.1	8.9	3.4
zr 15	909.5	34.3	68.8	0.04	0.0	0.06695	0.00188	0.08730	0.00485	0.80589	0.05023	836.3	57.4	539.5	28.8	600.1	28.6	10.0
zr 16	83.4	52.6	1.6	0.65	0.0	0.04970	0.00713	0.02513	0.00087	0.17219	0.02541	181.1	303.8	160.0	5.5	161.3	22.2	0.8
zr 17	478.3	185.7	61.4	0.40	0.0	0.07318	0.00107	0.14833	0.00468	1.49667	0.05233	1018.9	29.4	891.6	26.3	929.0	21.5	4.0
zr 18 rim	725.9	12.2	22.0	0.02	-0.1	0.05268	0.00223	0.03510	0.00100	0.25499	0.01303	315.3	93.6	222.4	6.2	230.6	10.6	3.6
zr 18 core	147.0	132.2	12.8	0.92	-0.2	0.06462	0.00119	0.10117	0.00154	0.90130	0.02181	761.9	38.4	621.2	9.0	652.4	11.7	4.8
zr 19	262.5	111.7	25.5	0.44	0.0	0.06457	0.00148	0.11236	0.00159	1.00034	0.02719	760.3	47.6	686.4	9.2	704.0	13.9	2.4
zr 20	316.5	275.8	90.9	0.89	0.0	0.11324	0.00040	0.33186	0.00272	5.18173	0.04989	1852.1	6.4	1847.4	13.2	1849.6	8.2	0.2
zr 21 rim	268.1	132.3	10.1	0.51	0.3	0.05231	0.00269	0.04333	0.00105	0.31253	0.01776	299.1	113.2	273.4	6.4	276.1	13.8	1.0
zr 21 core	1116.1	228.8	80.9	0.21	2.2	0.05601	0.00180	0.08193	0.00101	0.63271	0.02195	452.7	70.0	507.6	6.0	497.8	13.8	-2.0
zr 21 rim	361.1	56.2	11.7	0.16	-0.5	0.05780	0.00246	0.03767	0.00108	0.30017	0.01543	522.1	90.6	238.4	6.8	266.5	12.1	10.6
zr 22	563.3	559.2	66.4	1.02	0.1	0.07068	0.00078	0.13612	0.00266	1.32651	0.03010	948.1	22.4	822.7	15.1	857.4	13.3	4.0
zr 23	258.7	139.6	36.7	0.55	0.3	0.06719	0.00134	0.16344	0.00402	1.51422	0.04833	843.7	41.2	975.9	22.3	936.1	19.7	-4.2
zr 24	600.9	210.9	259.9	0.36	0.0	0.18368	0.00075	0.49969	0.00498	12.65514	0.14373	2686.3	6.8	2612.5	21.5	2654.3	10.7	1.6
zr 25	174.9	110.8	19.4	0.65	0.0	0.06423	0.00155	0.12761	0.00275	1.13022	0.03678	749.3	50.2	774.2	15.7	767.9	17.7	-0.8
zr 26	413.0	67.7	112.2	0.17	0.0	0.12272	0.00125	0.31391	0.00696	5.31159	0.13101	1996.1	18.0	1759.9	34.2	1870.7	21.3	6.0
zr 27 rim	199.4	40.5	6.1	0.21	0.0	0.04946	0.00073	0.03554	0.00139	0.24237	0.01017	169.7	34.2	225.1	8.6	220.4	8.4	-2.2

**d (%)=100 (1–206/238 age/207/235 age); *f206%=(common 206Pb/total 206Pb)×100. Data are uncorrected for common lead. All errors are at the 95% confidence interval

TABLE II. (continuation)

spot	Concentrations (p.p.m)					common lead corrected Isotope ratios						Ages(Ma)						
	U	Th	^{206}Pb	^{232}Th/ ^{235}U	f206%*	^{207}Pb/^{206}Pb	±err	^{206}Pb/^{238}U	±err	^{207}Pb/^{235}U	±err	^{207}Pb/^{206}Pb	±err	^{206}Pb/^{238}U	±err	^{207}Pb/^{235}U	±err	d (%)**
zr 27 core	1999.1	44.5	64.6	0.02	0.0	0.05178	0.00057	0.03735	0.00086	0.26666	0.00687	275.7	25.0	236.4	5.4	240.0	5.5	1.6
zr 28 rim	111.2	67.9	2.5	0.63	0.5	0.05102	0.00396	0.02505	0.00120	0.17624	0.01611	241.7	169.8	159.5	7.6	164.8	14.0	3.2
zr 28 core	551.8	695.7	11.9	1.29	0.0	0.04925	0.00203	0.02494	0.00100	0.16936	0.00976	159.7	93.8	158.8	6.3	158.9	8.6	0.0
zr 29	354.4	161.0	31.0	0.47	0.0	0.06021	0.00033	0.10112	0.00155	0.83948	0.01400	611.1	11.8	621.0	9.1	618.9	7.8	-0.4
zr 30 rim	971.5	439.9	68.2	0.46	0.1	0.05652	0.00070	0.08100	0.00163	0.63119	0.01510	472.7	27.4	502.1	9.7	496.8	9.4	-1.0
zr 30 core	932.1	382.7	65.7	0.42	0.1	0.05942	0.00062	0.08137	0.00092	0.66666	0.01054	582.7	22.4	504.3	5.5	518.7	6.5	2.8
zr 31 rim	7245.3	262.7	415.7	0.04	2.6	0.05186	0.00053	0.05842	0.00082	0.41774	0.00741	279.5	23.4	366.0	5.0	354.4	5.3	-3.2
zr 31 core	173.1	561.7	26.9	3.33	1.4	0.11813	0.00367	0.17728	0.00588	2.88749	0.13157	1928.1	54.6	1052.1	32.3	1378.6	34.9	23.6
zr 32	95.6	58.9	2.0	0.63	0.2	0.05105	0.00511	0.02435	0.00137	0.17138	0.01969	243.3	215.6	155.1	8.7	160.6	17.2	3.4
zr 33	77.4	56.5	10.9	0.75	0.0	0.07433	0.00148	0.16219	0.00182	1.66224	0.03846	1050.5	39.6	968.9	10.1	994.2	14.7	2.6
zr 34	249.8	225.7	5.3	0.93	0.2	0.05081	0.00225	0.02455	0.00090	0.17202	0.00992	232.1	99.4	156.4	5.7	161.2	8.7	3.0
zr 35	554.2	316.2	32.9	0.59	0.0	0.05696	0.00057	0.06854	0.00145	0.53829	0.01275	490.1	21.8	427.4	8.8	437.3	8.5	2.2
zr 36	68.1	33.0	20.2	0.50	0.0	0.11985	0.00291	0.34316	0.00101	5.67073	0.14019	1953.9	42.8	1901.9	4.9	1926.9	21.5	1.2
zr 37	962.5	200.9	106.8	0.21	0.0	0.06453	0.00168	0.12823	0.00394	1.14092	0.04613	759.1	54.0	777.8	22.6	772.9	22.1	-0.6
zr 38	389.1	38.8	32.4	0.10	0.0	0.06223	0.00035	0.09633	0.00189	0.82654	0.01713	682.1	12.0	592.9	11.2	611.7	9.6	3.0
zr 39	440.0	381.1	17.6	0.89	-0.2	0.05369	0.00122	0.04619	0.00087	0.34198	0.01019	358.1	50.6	291.1	5.4	298.7	7.8	2.6
zr 40	200.6	69.4	12.0	0.36	0.0	0.05612	0.00017	0.06918	0.00115	0.53531	0.00925	457.1	6.8	431.2	6.9	435.3	6.1	1.0
zr 41	623.8	322.0	61.6	0.53	0.0	0.06455	0.00086	0.11415	0.00221	1.01596	0.02416	759.7	27.8	696.8	12.8	711.9	12.3	2.2
zr 42	1164.3	2533.5	34.1	2.23	0.4	0.05347	0.00111	0.03373	0.00156	0.24871	0.01265	348.9	46.0	213.9	9.8	225.5	10.3	5.2
zr 43	620.7	430.7	32.0	0.71	0.0	0.06584	0.00700	0.05958	0.04375	0.54085	0.40129	801.1	208.4	373.1	271.8	439.0	306.4	15.0
zr 44	1863.8	180.5	101.4	0.10	0.0	0.05595	0.00023	0.06284	0.00223	0.48475	0.01741	450.3	9.0	392.9	13.6	401.3	12.0	2.0
zr 45	275.2	150.9	33.4	0.56	0.2	0.07039	0.00052	0.13992	0.01719	1.35803	0.16720	939.9	14.8	844.2	97.9	871.0	74.7	3.0
zr 46	257.9	232.3	5.5	0.92	0.0	0.05195	0.00099	0.02463	0.00109	0.17645	0.00854	283.3	43.0	156.9	6.9	165.0	7.4	5.0
zr 47	394.8	39.5	33.2	0.10	0.0	0.06151	0.00025	0.09705	0.00204	0.82306	0.01788	656.9	8.6	597.1	12.0	609.8	10.1	2.0
zr 48	456.3	395.8	18.4	0.89	-0.2	0.05510	0.00078	0.04657	0.00121	0.35381	0.01052	416.3	31.2	293.5	7.5	307.6	7.9	4.6
zr 49	206.1	71.6	12.9	0.36	0.0	0.05711	0.00033	0.07208	0.00157	0.56758	0.01294	495.7	12.8	448.7	9.4	456.4	8.4	1.6
zr 50	631.9	324.5	63.2	0.53	0.0	0.06632	0.00044	0.11551	0.00200	1.05625	0.01996	816.5	13.8	704.7	11.6	732.0	9.9	3.8
sample KA113 (n=19). Kangareh pluton. (N35° 8' 7.12" E47° 33' 22.12")																		
zr 1	3406.0	2814.9	66.7	0.85	0.1	0.04822	0.00043	0.02221	0.00108	0.14768	0.00731	110.1	20.8	141.6	6.8	139.9	6.5	-1.2
zr 2	2998.5	1305.0	58.9	0.45	0.1	0.04817	0.00030	0.02243	0.00110	0.14897	0.00736	107.5	14.8	143.0	6.9	141.0	6.5	-1.4
zr 3	1140.5	828.1	22.3	0.74	0.2	0.04761	0.00096	0.02252	0.00108	0.14783	0.00768	80.1	47.4	143.6	6.8	140.0	6.8	-2.6
zr 4	1328.4	758.2	26.2	0.59	0.1	0.04770	0.00060	0.02280	0.00099	0.14996	0.00679	84.3	29.8	145.3	6.2	141.9	6.0	-2.4
zr 5	665.0	480.9	12.8	0.74	0.0	0.04983	0.00125	0.02224	0.00113	0.15281	0.00866	187.1	57.4	141.8	7.1	144.4	7.7	1.8
zr 6	2115.8	1244.2	41.6	0.60	0.1	0.04846	0.00059	0.02271	0.00107	0.15172	0.00740	121.7	28.4	144.7	6.7	143.4	6.5	-1.0
zr 7	751.0	373.3	13.8	0.51	0.1	0.04949	0.00119	0.02121	0.00109	0.14475	0.00824	171.1	55.4	135.3	6.9	137.3	7.4	1.4
zr 8	2062.3	1463.0	38.7	0.73	0.0	0.04949	0.00070	0.02168	0.00112	0.14790	0.00792	171.1	32.6	138.2	7.0	140.1	7.1	1.4
zr 9	757.6	529.5	13.5	0.72	-0.1	0.05051	0.00057	0.02055	0.00120	0.14312	0.00850	218.5	25.8	131.1	7.5	135.8	7.6	3.4
zr 10	5631.2	3839.3	111.2	0.70	0.1	0.04909	0.00017	0.02138	0.00119	0.14470	0.00810	151.9	8.0	136.4	7.6	137.2	7.2	0.6
zr 11	2136.0	1114.6	39.9	0.54	0.1	0.04930	0.00034	0.02157	0.00122	0.14664	0.00836	162.3	16.0	137.6	7.7	138.9	7.4	1.0
zr 12	1167.2	324.8	90.0	0.29	0.0	0.05843	0.00036	0.08905	0.00153	0.71739	0.01339	545.9	13.4	549.9	9.1	549.1	7.9	-0.2
zr 13	541.3	345.7	10.1	0.66	0.3	0.04609	0.00131	0.02146	0.00098	0.13636	0.00733	2.3	67.0	136.9	6.2	129.8	6.6	-5.4
zr 14	583.1	371.1	11.5	0.65	0.4	0.04803	0.00187	0.02261	0.00144	0.14973	0.01118	100.9	89.8	144.1	9.1	141.7	9.9	-1.6
zr 15	778.8	318.7	15.3	0.42	0.1	0.04905	0.00175	0.02263	0.00104	0.15308	0.00894	150.3	81.6	144.3	6.6	144.6	7.9	0.2
zr 16	1166.3	571.9	22.8	0.50	-0.1	0.04999	0.00063	0.02257	0.00106	0.15558	0.00759	194.5	29.2	143.9	6.7	146.8	6.7	2.0
zr 17	2391.1	1736.5	47.3	0.74	0.2	0.04802	0.00069	0.02282	0.00113	0.15106	0.00781	100.3	33.8	145.4	7.1	142.8	6.9	-1.8
zr 18	4050.2	2318.4	82.3	0.59	0.0	0.04921	0.00023	0.02276	0.00114	0.15439	0.00776	157.7	10.8	145.1	7.2	145.8	6.9	0.4
zr 19	2074.6	924.0	41.1	0.46	0.0	0.04883	0.00013	0.02287	0.00104	0.15396	0.00706	139.7	6.2	145.8	6.6	145.4	6.2	-0.2
sample GA134 (n=13). Galali pluton. (N34° 57' 59.05" E47° 56' 1.89")																		
zr 1	3986.7	1844.5	83.5	0.47	0.1	0.04882	0.00056	0.02419	0.00084	0.16280	0.00597	139.3	26.4	154.1	5.3	153.2	5.3	-0.6
zr 2	1807.6	1140.0	36.7	0.65	2.7	0.04884	0.00395	0.02282	0.00084	0.15368	0.01366	140.3	179.6	145.5	5.3	145.2	12.1	-0.2
zr 3	2128.0	1340.5	43.6	0.65	0.6	0.04812	0.00182	0.02353	0.00074	0.15610	0.00769	105.5	87.0	149.9	4.6	147.3	6.8	-1.8
zr 4	1780.7	1121.8	35.9	0.65	0.0	0.04705	0.00067	0.02325	0.00082	0.15084	0.00576	51.7	34.0	148.2	5.2	142.7	5.1	-3.8
zr 5	673.0	416.0	15.0	0.63	11.1	0.04703	0.00266	0.02280	0.00085	0.14788	0.01004	50.9	130.0	145.3	5.3	140.0	8.9	-3.8
zr 6	924.8	439.1	17.8	0.49	0.3	0.04754	0.00217	0.02213	0.00245	0.14508	0.01737	76.3	105.2	141.1	15.4	137.6	15.6	-2.6
zr 7	1451.5	942.1	29.1	0.67	0.1	0.04880	0.00021	0.02311	0.00088	0.15549	0.00595	138.1	9.8	147.3	5.5	146.8	5.3	-0.4
zr 8	2024.0	1466.1	42.2	0.74	0.1	0.04852	0.00120	0.02406	0.00075	0.16100	0.00644	124.9	57.0	153.3	4.8	151.6	5.7	-1.2
zr 9	1950.1	1604.2	45.6	0.84	13.5	0.05056	0.00531	0.02329	0.00073	0.16234	0.01780	220.7	226.4	148.4	4.6	152.8	15.7	2.8
zr 10	498.9	281.6	11.2	0.58	5.6	0.04918	0.00304	0.02452	0.00144	0.16629	0.01419	156.5	138.4	156.2	9.1	156.2	12.4	0.0
zr 11	1484.6	817.3	30.1	0.56	0.0	0.04810	0.00067	0.02339	0.00077	0.15517	0.00555	104.5	32.6	149.1	4.8	146.5	4.9	-1.8
zr 12 rim	114.8	42.3	5.8	0.38	0.4	0.05179	0.00181	0.05838	0.00164	0.41685	0.01877	276.1	78.2	365.7	10.0	353.8	13.5	-3.4
zr 12 core	70.2	26.5	3.7	0.39	0.1	0.05414	0.00212	0.06056	0.00138	0.45209	0.02052	376.9	85.8	379.0	8.4	378.7	14.4	0.0
zr 13	3384.3	3029.2	86.9	0.92	18.4	0.05033	0.01050	0.02407	0.00109	0.16704	0.03568	210.1	423.2	153.3	6.9	156.8	31.5	2.2
sample SA80 (n=16). Saranjianeh pluton. (N35° 11' 54.73" E47° 21' 41.18")																		
zr 1	142.9	62.4	2.9	0.45	0.6	0.04559	0.00296	0.02327	0.00103	0.14626	0.01151	0.0	126.3	148.3	6.5	138.6	10.2	-7.0
zr 2	94.5	51.0	1.9	0.55	0.3	0.04878	0.00188	0.02331	0.00105	0.15677	0.00930	137.1	88.4	148.5	6.6	147.9	8.2	-0.4
zr 3	1010.7	980.8	20.3	1.00	0.2	0.04723	0.00129	0.02319	0.00081	0.15102	0.00673	60.7	63.6	147.8	5.1	142.8	5.9	-3.6
zr 4	444.8	347.0	8.9	0.80	0.0	0.05087	0.00249	0.02309	0.00075	0.16195	0.00955	235.1	109.4	147.1	4.7	152.4	8.4	3.4
zr 5	121.8	57.9	2.5	0.49	0.1	0.04875	0.00063	0.02345	0.00100	0.15759	0.00704	135.7	29.8	149.4	6.3	148.6	6.2	-0.6
zr 6	180.6	91.6	3.6	0.52	0.1	0.04781	0.00216	0.02301	0.00114	0.15170	0.01017	89.7	104.0	146.7	7.2	143.4	9.0	-2.4
zr 7	170.1	97.2	3.5	0.59	0.1	0.04643	0.00231	0.02365	0.00096	0.15143	0.00974	19.9	115.2	150.7	6.1	143.2	8.7	-5.2
zr 8	164.1	91.7	3.3	0.57	0.2	0.04968	0.00093	0.02296	0.00096	0.15723	0.00721	179.9	43.4	146.3	6.0	148.3	6.4	1.4
zr 9	294.1	185.0	6.0	0.65	0.4	0.04683	0.00280	0.02332	0.00094	0.15059	0.01086	40.7	137.2	148.6	5.9	142.4	9.6	-4.4
zr 10	133.3	70.2	2.7	0.54	0.1	0.04977	0.00135	0.02375	0.00092	0.16301	0.00771	184.3	61.8	151.3	5.7	153.3	6.7	1.4
zr 11	343.9	206.5	6.7	0.62	0.3	0.04911	0.00091	0.02239	0.00108	0.15162	0.00782	152.9	43.0	142.8	6.8	143.3	6.9	0.4
zr 12	135.2	78.0	2.7	0.59	0.3	0.04771	0.00711	0.02299	0.00137	0.15123	0.02428	84.9	320.2	146.5	8.6	143.0	21.6	-2.4
zr 13	318.3	172.9	6.4	0.56	0.0	0.04824	0.00082	0.02334	0.00091	0.15524	0.00664	111.1	39.8	148.7	5.7	146.5	5.8	-1.6
zr 14	157.0	99.8	3.1	0.65	0.2	0.04971	0.00303	0.02312	0.00107	0.15844	0.01213	181.5	136.4	147.3	6.7	149.3	10.7	1.4
zr 15	260.3	132.2	5.2	0.52	0.0	0.04931	0.00151	0.02310	0.00070	0.15706	0.00676	162.9	69.8	147.2	4.4	148.1	5.9	0.6
zr 16	2250.9	1453.3	45.7	0.66	0.2	0.04708	0.00070	0.02342	0.00078	0.15205	0.00558	53.5	34.8	149.3	5.0	143.7	4.9	-3.8
sample BH88 (n=21). Bolbanabad-Havarpan pluton. (N35° 6' 28.26" E47° 18' 48.13")																		
zr 1	318.2	191.3	6.4	0.62	0.7	0.04517	0.00424	0.02311	0.00112	0.14392	0.01522	0.0	167.3	147.3	7.1	136.5	13.6	-8.0
zr 2	345.5	195.0	6.8	0.58	0.5	0.04790	0.00252	0.02275	0.00121	0.15024	0.01125	94.3	120.0	145.0	7.6	142.1	10.0	-2.0
zr 3	468.5	239.6	9.2	0.52	0.3	0.04922	0.00276	0.02265	0.00086	0.15373	0.01042	158.5	126.2	144.4	5.4	145.2	9.2	0.6
zr 4	321.4	173.7	6.2	0.55	1.0	0.04523	0.00452	0.02218	0.00084	0.13831	0.01479	0.0	183.3	141.4	5.3	131.5	13.2	-7.6
zr 5	546.0	354.1	10.7	0.67	0.7	0.04366	0.00349	0.02239	0.00084	0.13479	0.01190	0.0	56.9	142.7	5.3	128.4	10.7	-11.2
zr 6	315.9	158.0	6.2	0.51	0.0	0.05249	0.00146	0.02266	0.00101	0.16401	0.00865	306.9	62.0	144.5	6.4	154.2	7.6	6.2
zr 7	374.2	164.6	7.4	0.45	0.2	0.04865	0.00472	0.02278	0.00105	0.15280	0.01643	130.9	213.4	145.2	6.7	144.4	14.6	-0.6
zr 8	1388.9	1094.7	26.8	0.81	0.0	0.04804	0.00051	0.02229	0.00075	0.14766	0.00522	101.3	24.8	142.1	4.7	139.8	4.6	-1.6
zr 9	310.4	202.9	6.2	0.67	0.2	0.04895	0.00383	0.02292	0.00074	0.15472	0.01309	145.3	173.8	146.1	4.6	146.1	11.6	0.0
zr 10	299.8	158.2	5.9	0.54	0.2	0.04932	0.00681	0.02265	0.00096	0.15405	0.02225	163.1	294.6	144.4	6.0	145.5	19.8	0.8
zr 11	332.6	174.9	6.4	0.54	0.3	0.04924	0.00342	0.02201	0.00093	0.14944	0.01215	159.5	154.6	140.3	5.8	141.4	10.8	0.8
zr 12	420.1	221.5	8.5	0.54	0.0	0.05100	0.00182	0.02326	0.00083	0.16355	0.00830	240.9	80.4	148.2	5.2	153.8	7.3	3.6
zr 13	645.8	445.1	12.7	0.71	0.4	0.04677	0.00520	0.02263	0.00085	0.14595	0.01712	37.5	246.4	144.3	5.4	138.3	15.3	-4.4
zr 14	752.7	495.5	14.7	0.68	0.3	0.04875	0.00147	0.02245	0.00104	0.15091	0.00835	135.7	69.2	143.1	6.5	142.7	7.4	-0.2
zr 15	428.6	209.9	8.3	0.50	0.1	0.05178	0.00347	0.02233	0.00125	0.15944	0.01394	275.9	146.4	142.4	7.9	150.2	12.3	5.2
zr 16	630.8	401.9	12.5	0.65	0.4	0.04760	0.00226	0.02277	0.00112	0.14946	0.01022	79.7	109.0	145.1	7.0	141.4	9.0	-2.6
zr 17	531.5	368.7	10.5	0.71	0.0	0.05019	0.00131	0.02288	0.00080	0.15831	0.00694	203.9	59.4	145.8	5.1	149.2	6.1	2.2
zr 18	801.0	498.7	15.7	0.64	0.6	0.04627	0.00227	0.02256	0.00069	0.14391	0.00834	11.9	113.8	143.8	4.4	136.5	7.4	-5.4
zr 19	734.6	508.9	14.5	0.71	0.1	0.04723	0.00277	0.02274	0.00102	0.14805	0.01094	60.7	134.2	144.9	6.4	140.2	9.7	-3.4
zr 20	337.7	193.1	6.7	0.59	0.1	0.05134	0.00094	0.02300	0.00086	0.16279	0.00680	256.1	41.8	146.6	5.4	153.1	5.9	4.2
zr 21	272.2	157.7	5.3	0.59	0.0	0.05221	0.00051	0.02229	0.00102	0.16047	0.00750	294.7	22.0	142.1	6.4	151.1	6.6	6.0

**d (%)=100 (1–206/238 age/207/235 age); *f206%=(common 206Pb/total 206Pb)×100. Data are uncorrected for common lead. All errors are at the 95% confidence interval